5-31-2015

Piezoelectric scaffolds for osteochondral defect repair

Sita Mahalakshmi Damaraju
New Jersey Institute of Technology

Copyright Warning & Restrictions

The copyright law of the United States (Title 17, United States Code) governs the making of photocopies or other reproductions of copyrighted material.

Under certain conditions specified in the law, libraries and archives are authorized to furnish a photocopy or other reproduction. One of these specified conditions is that the photocopy or reproduction is not to be "used for any purpose other than private study, scholarship, or research." If a, user makes a request for, or later uses, a photocopy or reproduction for purposes in excess of "fair use" that user may be liable for copyright infringement,

This institution reserves the right to refuse to accept a copying order if, in its judgment, fulfillment of the order would involve violation of copyright law.

Please Note: The author retains the copyright while the New Jersey Institute of Technology reserves the right to distribute this thesis or dissertation

Printing note: If you do not wish to print this page, then select "Pages from: first page # to: last page #" on the print dialog screen

ABSTRACT

PIEZOELECTRIC SCAFFOLDS FOR OSTEOCHONDRAL DEFECT REPAIR

by
Sita Mahalakshmi Damaraju

Osteoarthritis is one of the most prevalent causes of disability affecting nearly 27 million Americans. Osteoarthritis is caused when extensive damage occurs to the articular cartilage later spreading to the underlying subchondral bone, resulting in osteochondral defects. The current clinical therapies aim at regenerating the hyaline cartilage, but instead fibrocartilage forms at the osteochondral defect site, which is inferior in structure and function and fails to integrate with the surrounding tissue. A biomimetic scaffold, which can provide cues similar to the native extracellular matrix, may facilitate osteochondral defect repair. Articular cartilage and bone extracellular matrix have been shown to produce electrical potentials when subjected to mechanical loading. The electrical behavior of cartilage and bone may provide signals for tissue repair and remodeling during injury and homeostasis. Therefore, a piezoelectric scaffold, which is able to generate electrical charge in response to deformation, is investigated in this study for its potential to support hyaline cartilage and bone tissue formation in combination with human mesenchymal stem cells (MSCs). The scaffold is composed of the synthetic polymer, poly(vinylidene fluoride-co-trifluoroethylene) (PVDF-TrFE), a biocompatible, piezoelectric polymer. It is hypothesized that piezoelectric scaffolds will promote chondrogenic (cartilage) and osteogenic (bone) differentiation of MSCs. PVDF-TrFE is electrospun to form a fibrous, three-dimensional scaffold (as-spun). PVDF-TrFE scaffolds are further annealed to enhance piezoelectric properties (annealed). The chondrogenic and osteogenic differentiation of MSCs is

evaluated on both as-spun and annealed PVDF-TrFE scaffolds in a perfused compression bioreactor system to simulate physiological loading. Electrospun polycaprolactone (PCL) is used as a non-piezoelectric control. Under physiological loading conditions, annealed PVDF-TrFE scaffolds have a higher voltage output compared to as-spun PVDF-TrFE scaffold. In bioreactor cultures, MSC chondrogenic differentiation is promoted on as-spun PVDF-TrFE and osteogenic differentiation is enhanced on annealed PVDF-TrFE scaffolds when compared to PCL control. These results suggest that MSCs differentiation behavior can be impacted by the differences in voltage output from the as-spun and annealed PVDF-TrFE, indicating a role for electromechanical stimulus on MSC differentiation. Therefore, piezoelectric scaffolds have the potential to support cartilage and bone growth for osteochondral defect repair.

PIEZOELECTRIC SCAFFOLDS FOR OSTEOCHONDRAL DEFECT REPAIR

by
Sita Mahalakshmi Damaraju

A Dissertation
Submitted to the Faculty of
New Jersey Institute of Technology
and Rutgers, The State University of New Jersey
in Partial Fulfillment of the Requirements for the Degree of
Doctor of Philosophy in Biomedical Engineering

Joint Program in Biomedical Engineering

May 2015

APPROVAL PAGE

PIEZOELECTRIC SCAFFOLDS FOR OSTEOCHONDRAL DEFECT REPAIR

Sita Mahalakshmi Damaraju

Dr. Treena Livingston Arinzeh, Dissertation Advisor — Date
Professor of Biomedical Engineering, NJIT

Dr. Michael Jaffe, Committee Member — Date
Research Professor of Biomedical Engineering, NJIT

Dr. Boris Khusid, Committee Member — Date
Professor of Chemical, Biological and Pharmaceutical Engineering, NJIT

Dr. J. Christopher Fritton, Committee Member — Date
Assistant Professor of Orthopaedics, Rutgers New Jersey Medical School

---

Dr. Pranela Rameshwar, Committee Member — Date
Professor of Medicine, Rutgers New Jersey Medical School

BIOGRAPHICAL SKETCH

Author: Sita Mahalakshmi Damaraju

Degree: Doctor of Philosophy

Date: May 2015

Undergraduate and Graduate Education:

- Doctor of Philosophy in Biomedical Engineering,
  New Jersey Institute of Technology, Newark, NJ, 2015

- Bachelor of Science in Biological Engineering,
  University of Georgia, Athens, GA 2007

Major: Biomedical Engineering

Presentations and Publications

Publications

S. M. Damaraju, Y. Shen, A. Eshghinejad, J. Li, B. Khusid, M. Jaffe, T. L. Arinzeh. Piezoelectric Scaffolds for Osteochondral Defect Repair. In preparation (2015).

S. M. Damaraju, C. Reformina, M. Jaffe, T. L. Arinzeh. Chondrogenic Differentiation of human Mesenchymal Stem Cells on fibrous PVDF-TrFE Scaffolds. In preparation (2015).

K. Guiro, S. M. Damaraju & T. L. Arinzeh. New Bone Grafting Technologies Using Stem Cells. In: L. Cato, J. Tao, editors. Bone Graft Substitutes and Bone Regenerative Engineering. West Conshohocken, PA : ASTM International; p 287-298, second edition, (2014).

S. M. Damaraju, S. Wu, M. Jaffe, T. L. Arinzeh. Structural Changes in PVDF Fibers due to Electrospinning and its Effect on Biological Function. *Biomedical Materials* **8**, 1-11 (2013).

Presentations

S. M. Damaraju, Y. Shen, B. Khusid, M. Jaffe, T. L. Arinzeh. Piezoelectric Scaffolds for Cartilage Tissue Engineering. Tissue Engineering and Regenerative Medicine International Society World Congress Meeting. Boston, MA. Submitted (2015)

Y-S. Lee, S. M. Damaraju, S. Wu, M. Bunge, T. L. Arinzeh. Piezoelectric Fibrous Scaffolds for Schwann Cell Induced Spinal Cord Repair. Biomedical Engineering Society Annual Meeting, San Antonio, TX. Podium Presentation (2014).

S. M. Damaraju, M. Jaffe, T. L. Arinzeh. Effect of Piezoelectric Scaffolds on the Osteogenic Differentiation of Mesenchymal Stem Cells. Orthopaedic Research Society Annual meeting, New Orleans, LA. Poster Presentation (2014).

S. M. Damaraju, S. Wu, M. Jaffe, T. L. Arinzeh The Osteogenic Differentiation of Mesenchymal Stem Cells on Piezoelectric Scaffolds. Biomedical Engineering Society Annual Meeting, Hartford, CT. Poster Presentation (2011).

Through many years of miscomprehension from others, I came to know that the life of a devotee of science is inevitably filled with unending struggle. It is for him/her to cast his/her life as an ardent offering – regarding gain and loss, success and failure, as one.

- Dr. Jagdish Chandra Bose

ACKNOWLEDGMENT

I would like to express the deepest appreciation to my advisor, Dr. Treena Livingston Arinzeh, for her support and mentorship during my graduate study. She has continually encouraged a spirit of adventure in regard to research and has been instrumental in developing me become the person I am today. Without her guidance and persistent help, this dissertation would not have been possible.

I would like to thank my committee members, Dr. Michael Jaffe and Dr. Boris Khusid from NJIT and Dr. Pranela Rameshwar and Dr. J. Christopher Fritton from Rutgers, for providing valuable advice and constant support for my work. I would like to thank Dr George Collins for being a supportive mentor especially guiding me to think with clarity. Thank you to the department of Biomedical Engineering at NJIT for their support and assistance during my research. I would like to thank National Science Foundation (NSF) sponsored STEM teaching fellowship (C2PRISM) and NSF Grant 1006510 for providing the financial support throughout my entire graduate experience.

I would like to thank my lab mates: Dr. Shobana Shanmugasundaram, Dr. Gloria Portocarrero-Huang, Khadidiatou Guiro, Amirhossein Rajabi Zamani, Svetlana Dukleska Schussler, Roseline Menezes, Atekamohdarabi Khader, and Siliang Wu. I thank you all for your support, encouragement and advice throughout my time as a graduate student. Without you all, I would not have made it this far.

I would like to thank my dearest friends, Vinita Saluja, Dr. Atul Saluja and their daughter, Ahana Saluja, for being so supportive and keeping me sane during my time as a graduate student. My deepest gratitude and appreciation to my parents, Venkata Krishna Rao Damaraju and Meenakshi Rayasam and my younger brother, Venkata Pavan Kumar

Damaraju who encouraged my rebellious ways and showed endless love and support during at all times. Lastly, I thank my best friend and better half, Rangan Gangavaram, for his unconditional love, patience and support especially during my endless weekend trips to lab. Without you, I would not have dared following my ambitions and you made me realize that anything is possible with love. For this, I am ever grateful to you, and I look forward to spending more exciting years ahead together.

TABLE OF CONTENTS

TABLE OF CONTENTS
(Continued)

TABLE OF CONTENTS
(Continued)

TABLE OF CONTENTS
(Continued)

LIST OF TABLES

LIST OF FIGURES

LIST OF FIGURES
(Continued)

LIST OF FIGURES
(Continued)

LIST OF FIGURES
(Continued)

LIST OF FIGURES
(Continued)

LIST OF FIGURES
(Continued)

LIST OF FIGURES
(Continued)

LIST OF FIGURES
(Continued)

LIST OF FIGURES
(Continued)

Figure **Page**

LIST OF FIGURES
(Continued)

Figure **Page**

CHAPTER 1

INTRODUCTION

1.1 Clinical Application

Osteoarthritis is the most prevalent cause of disability affecting nearly 27 million Americans [1], and its diagnoses are only expected to increase in the coming years. Osteoarthritis affects the patients' quality of life by limiting physical movement, causing constant pain and affecting psychological well-being. The incidence is the highest in the older adult population (>= 60 years) and is diagnosed more in women (4-5 in 1000 women) than in men (2-3 in 1000 men) [1]. Apart from its painful symptoms, osteoarthritis represents a significant financial burden on society where in 2009 alone knee and hip replacements cost $42.3 billion [1].

Osteoarthritis is caused when extensive damage occurs to the articular cartilage, which later spreads to the underlying subchondral bone causing cystic lesions and is also known as osteochondral defects (Figure 1.1). If left untreated, osteochondral damage spreads to adjacent synovial joint lining and supporting connective tissues. It occurs from an imbalance between anabolic and catabolic activities of chondrocytes and other cells present within synovial joint. The characteristic structural changes in osteoarthritis include the progressive loss of articular cartilage, subchondral bone cysts and formation of new bone at the joint margins (osteophytes) [2]. The tidemark, separating cartilage and underlying bone, begins to disappear and calcified cartilage becomes more prominent [3]. Damaged cartilage contains increased amounts of collagen types I and X and increased synthesis of proteoglycans, characteristic of immature cartilage formation [2, 4] There is

increased chondrocyte apoptosis which further hampers repair, and as a result, the compressive stiffness of cartilage decreases; therefore, affecting, metabolic activities and its electromechanical behavior [2].

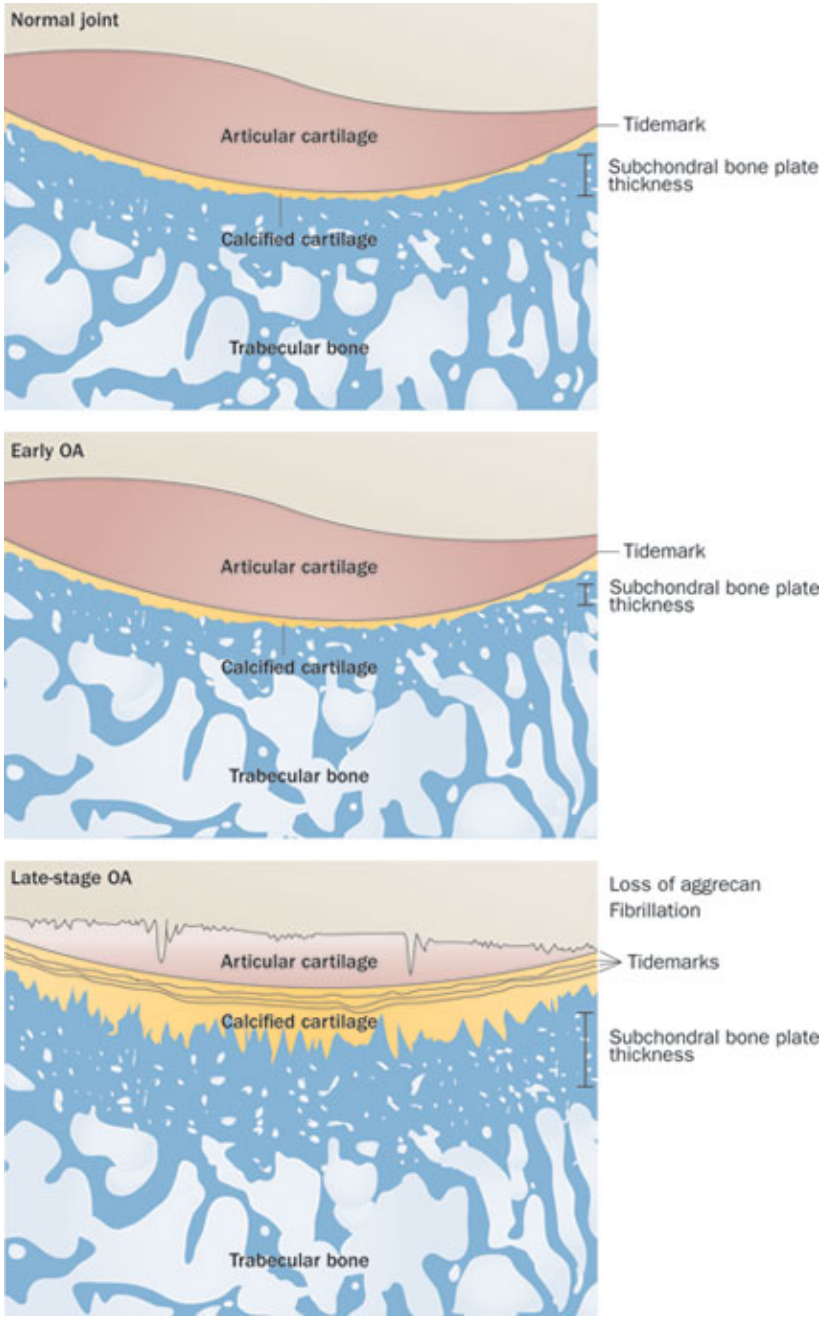

Figure 1.1 Stages of progressive joint osteoarthritis.
Source [4].

Osteochondral defects occurrence is most commonly reported for knee joints (femoral-tibial joints) but it can affect any joint in the body. For instance, lesions of the talus contribute to ankle fractures and sprains [5]. Pain and stiffness of the affected joint is the most commonly reported symptom. Some factors attributing to osteoarthritis are obesity, aging, repetitive trauma of joints especially in athletes, and genetic disposition [1, 5]. Current clinical therapy options include microfracturing, osteoarticular transfer and autologous chondrocyte transplantation (ACT). However, none of these therapies have been able to restore a normal cartilaginous surface. ACT is the only cell based FDA approved treatment for cartilage repair but has limited success. The chondrocytes have limited proliferation capacity and lose their phenotype during *in vitro* expansion; thus posing an issue to achieve adequate number of cells for transplantation [6]. Long-term studies have shown that cartilage formed with ACT is fibrocartilage, which is inferior in physiological and biomechanical properties when compared to healthy hyaline cartilage tissue [7]. None of the current treatment options have been able to completely restore an osteochondral defect, especially articular cartilage component. Therefore, there is urgency for alternative therapeutic options for addressing this clinical need.

1.2 Cartilage

Cartilage is a flexible tissue, providing support in various areas of the body. There are three main types of cartilage: fibrocartilage, elastic cartilage and hyaline cartilage. Hyaline cartilage is the most abundant and is found in articular cartilage, coating the foremost region of an osteochondral defect [5]. Cartilage tissue consists of water, collagens (60% of dry weight), proteoglycans (5-10%) and a few minor proteins [5, 8].

Additionally, it is an avascular tissue lacking blood supply, nerves and lymphatic vessels interspersed with single cell type, the chondrocytes [9]. Chondrocyte synthesizes collagens and proteoglycans, which form the extracellular matrix (ECM) for articular cartilage.

The collagens provide structural and elastic strength. Of the collagens, collagen type II, a homotrimer composed of α1 (II) chain is the most abundantly produced (80% of collagens) in articular cartilage [8]. The remaining collagens include collagen types III, V, VI, IX, XI, XII which are believed to play a role in the intermolecular interaction and modulation of collagen type II [5, 8]. Aggrecan is a proteoglycan composed of many sulfated glycosaminoglycans (GAGs) such as chondroitin sulfates and keratin sulfates, which have high density of negative charges on its surface [5]. These negative charges attract water, which gets absorbed and retained into the mesh made up of aggrecan, GAGs and collagens. This property renders articular cartilage its ability to resist high compressive forces while increasing flexibility during movement [8].

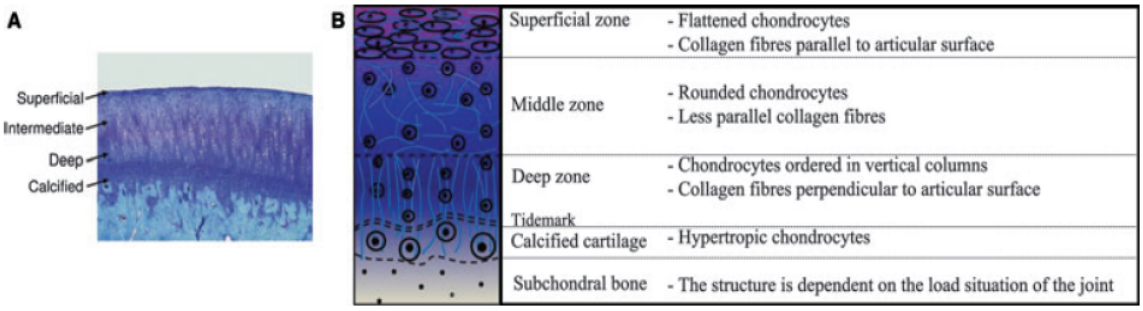

Figure 1.2 A) Osteochondral tissue showing different zones of cartilage B) Features of different zones of cartilage tissue.
Source [10].

The articular cartilage is separated into different zones where each zone has different concentrations of collagens and GAGs thus becoming one of the most complex

and challenging tissue to repair (Figure 1.2). The four zones are (1) superficial zone, (2) middle zone, (3) deep zone and (4) calcified zone. The superficial zone has the smallest collagen fiber diameter consisting of tightly packed collagen fibers arranged in parallel to the articular surface and flattened chondrocytes lying tangential to these collagen fibers [10]. The superficial zone features enable smooth, frictionless movement of joints while resisting compressive forces. The middle zone, also the largest zone, has abundant proteoglycans and obliquely arranged collagen fibers interspersed with chondrocytes having rounded morphology [5, 8, 10]. These properties cause the middle zone to have a high compressive modulus, which facilitates recovery from impact. In the deep zone, the cells and collagen fibers are oriented perpendicularly to the articular cartilage's surface and are anchored in the underlying subchondral bone [5]. The deep zone has the least number of chondrocytes and proteoglycans but has a much higher compressive modulus than the middle zone. The bottom most part of the deep zone has a thin line known as tidemark, indicating the transition from the deep zone to calcified zone. The calcified zone plays an important role as an interface between cartilage and bone for maintaining joint function [5].

Articular cartilage provides multiple biophysical cues to chondrocytes in its unique environment where cartilage has electrically charged tissue components and depth dependent mechanical properties. It has been previously demonstrated that flow of free electrolytes (Na^+, K^+, Cl^-) in surrounding interstitial water past the fixed negatively charges on proteoglycans influences the electrochemical behavior of cartilage [11]. These free flowing ions affect the water content, cartilage swelling behavior but also ion transport through interstitium, resulting in electrical potentials and current [2]. This

phenomenon is known as streaming potentials. Cartilage becomes electrically polarized under compressive loads and produces electrical potentials due to the flow of charged ions across negatively charged proteoglycans in and out of the ECM [2, 9, 12]. Conversely, application of electrical potential or current to cartilage can produce deformation in the tissue [2]. Based on these observations, ECM of cartilage is considered a mechanical signal transducer where joint loading results in multiple biophysical signals.

1.3 Subchondral Bone

Bone is a hard tissue composed of 35% of collagen, mostly collagen type I and 65% of an inorganic calcium salt, mostly hydroxyapatite. Its main function is to provide structural support required for movement. Bone continually remodels which is a dynamic process coordinated by cells such as osteoblasts (bone-producing cells) and osteoclasts (bone resorbing cells), hormones and enzymes [13]. Once an osteoblast has matured and becomes encased in its own secreted ECM, it is called an osteocyte, a terminally differentiated bone cell. Bone contains a vast vasculature network providing nutrients and assists in crosstalk with other tissues [14]. Bone continually takes up, stores and releases calcium into the blood to maintain homeostasis [13]. Unlike cartilage, bone has the ability to regenerate and self-repair to some extent. However, a person's age, activity level and type of mechanical loading significantly influences bone remodeling and self-repair.

The area underneath cartilage's calcified zone is the subchondral bone that provides an anchor for collagen fibers from the deep zone of the cartilage. The

subchondral bone is composed of bony lamella and underneath is the trabeculae [5]. The trabecula is extensively vascularized and contains nutrients for both itself and the overlying articular cartilage [14]. It has been well established that there exists a crosstalk between the joint cartilage and subchondral bone through some channels where biochemical signals are exchanged throughout the two tissues [14]. The subchondral bone plays a critical role in biomechanical function of the joint where it absorbs shocks and heals micro-fractures while maintaining joint shape due to its larger surface area and lower modulus of elasticity than cartilage [5]. The subchondral bone plate has non-uniform thickness and density; as a result, the actual mechanical strength varies at different points of this tissue [5]. Therefore, it remains challenging to repair the subchondral bone layer.

Similar to cartilage, bone is known to produce electrical potentials under compressive loads and is called a piezoelectric tissue. Piezoelectricity is a phenomenon where a material is capable of converting mechanical strain into electrical potential and the reverse is also true where the application of electrical potential can cause stress-induced deformation in the material. Bone piezoelectric phenomenon has been attributed to collagen, which exists in an highly organized fiber bundle and is tightly packed against one another [13]. Electrical potentials were recorded from dry bone, demineralized dry bone but not from decollagenated dry bone samples indicating the importance of collagen for its electrical behavior [15]. The stress-generated electrical potentials were created by the shear loading of collagen in human femur bone specimens [13]. Furthermore, individual collagen type I fibrils have been demonstrated to be piezoelectric under shear deformation using piezo force microscopy (PFM) technique [16]. Ahn et al. have

hypothesized that bone's electrical behavior may be resulting from a combination of streaming potential and its inherent piezoelectric behavior. Streaming potential in bone arises when bone is loaded and interstitial fluid within bone gets squeezed out of its pores and interacts with the fixed charges of hydroxyapatite and collagen molecules producing surface charges [17]. Piezoelectric collagen may further contribute to the magnitude of surface charges resulting in electrical potential during compression loading [17].

It has been speculated that bone piezoelectric properties affects repair and remodeling of bone tissue, and some studies have demonstrated that mechanically deformed or actively remodeling bone produces electrical current *in vivo* [15, 18]. Additionally, the amplitude of electrical potentials were shown to be dependent on the rate and magnitude of bone loading while the polarity was dependent on the direction of the deformed bone [15]. Similar to cartilage, bone is considered a mechanical transducer where joint loading results in multiple biophysical cues. Over the years bone's electrical behavior and response of bone cells to different forms of electric stimulations has been well established in many published *in vitro* studies, which has contributed to the development of electrical stimulators for healing bone fractures clinically [19].

1.4 Osteochondral Tissue Engineering

Tissue engineering is an emerging field of novel therapeutic strategies to treat damaged or diseased tissues. The conventional approach is to engineer natural or synthetic materials into scaffolds and combine them with cells and/or growth factors to generate healthy tissue that will repair, replace and/or restore the diseased tissue while mimicking the original function. The study of both bone and cartilage tissue engineering has

contributed immensely to the understanding of the individual tissue structures, mechanical properties and biology. Osteochondral tissue engineering applies bone and cartilage tissue engineering principles to the development of osteochondral constructs. Though the progress in the design and development of osteochondral constructs has come a long way, still there is a need for improvement. Some of the challenges in osteochondral tissue engineering are that the cartilage and the underlying subchondral bone have significantly different physical structures, compositions and mechanical properties that make it challenging to mimic these characteristics. Based on these features, the design criterion for osteochondral tissue engineered constructs has been defined [5, 10]. The scaffold is expected to have mechanical properties mimicking cartilage but also the underlying bone (compressive, tensile and shear), adequate porosity to allow transport of nutrients and waste removal and support host tissue integration with the scaffold, support cell survival and promote biochemical properties such as GAGs and collagen production. Many tissue engineered osteochondral constructs have been successful in achieving biochemical composition similar to that of native cartilage but have failed to achieve native mechanical properties [2]. With these parameters as guidelines, scaffolds have been designed as single phase, or bilayered materials. A single-phase scaffold is composed of the same material, which is preformed to fit a defect. Bilayered design is a composite incorporating two or more different materials to address the cartilage and bone components separately. Additionally, a third material may be incorporated as an interface between bone and cartilage layers.

In order to mimic similar physical and mechanical features of cartilage and bone, tissue engineering has encouraged the exploration of a myriad of materials sourced

naturally or developed synthetically. Some of the commonly used natural polymers for cartilage are collagen, chitosan, GAGs, alginate and poly (hydroxyalkanoates) [20]. These polymers offer flexibility to adapt different shapes, are biocompatible due to the presence of molecular domains, which guide cell attachment and growth, are biodegradable and have elastomeric properties. For instance, agarose scaffolds have been extensively used due to its hydrogel properties with the ability to retain water similar to cartilage [21]. Additionally, hydrogels support transport of cells and nutrients. The major disadvantages of using natural polymers are its limited mechanical properties, immunogenicity, purification issues and producing them in large quantities. Similarly, Synthetic polymers including but not limited to poly(lactic acid), poly(lactic-co-glycolic acid) and polycaprolactone offer wide range of chemistries, processing conditions and ability to modulate mechanical properties [10]. The fabrication can be accomplished at a larger scale and is a highly reproducible process, which is important for clinical demands. Inorganic materials such as hydroxyapatite, tricalcium phosphates (TCP) and bioglass have been widely used in bone tissue engineering [22]. These materials have demonstrated excellent osteoconductivity and osteoinductivity *in vitro* and *in vivo* studies [23, 24]. Though ceramics exhibit suitable compressive stiffness, but they are brittle and not suitable under mechanical loading conditions of an osteochondral joint. Using these materials alone or in combination with other materials, engineered scaffolds are then combined with different cell types (chondrocyte, stem cells) and/or growth factors to evaluate tissue repair *in vitro* or *in vivo* [22, 23]. Using this approach, many strategies are currently being investigated for the repair of osteochondral defects.

1.5 Cell Source

Tissue engineered constructs are often combined with a cell type to further enhance osteochondral repair but also facilitate host tissue integration. Many cell types have been proposed for cartilage and bone tissue engineering applications. For cartilage repair, the obvious choice are the chondrocytes harvested from load bearing joints but other cartilaginous tissues such as outer ear, ribs and nasal septum have also been investigated [25]. Many studies have indicated chondrocytes being conducive for regenerating functional cartilage. However, load-bearing chondrocytes are found in few numbers within cartilage and other sources, which is not optimal for clinical demands. Furthermore, chondrocytes tend to lose its phenotype and dedifferentiate *in vitro* cultures and during expansion further limiting its usage [26]. Additionally, chondrocytes-harvesting procedure utilizes harsh reagents, which may further impact chondrocyte behavior.

Due to aforementioned complications with chondrocyte harvest and usage, mesenchymal stem cells (MSCs) have become a promising cell source due to their ability to self-renew, and differentiate into various cell types including osteoblasts and chondrocytes [27]. MSCs can also be obtained from different tissue sources such as adipose tissue, umbilical cord, periosteum and dental pulp [28, 29]. Of these, bone marrow derived MSCs are extensively studied for bone and cartilage repair [30]. MSCs have been well characterized for their immunophenotype, multipotent capabilities and their proliferative capacity [31-33]. These progenitor cells have been cultured up to 15 passages as well as cryopreserved and still have the capacity to differentiate and proliferate with no indications for phenotype loss or aging [34-36]. MSCs have the

potential to be valuable as a readily available and abundant source of cells in the tissue engineering and regenerative medicine fields. Furthermore, studies have demonstrated that the use of allogeneic MSCs can successfully repair bone and cartilage tissues in many animal models without provoking an adverse immune response[37-39]. Similar to chondrocytes, MSC usage does come with a caveat especially for cartilage tissue engineering. MSCs have been successful in expressing enhanced mature cartilage markers, but studies also indicate that MSCs continue to differentiate towards hypertrophy and end with bone formation. This observation indicates its natural pathway of endochondral ossification process [27]. Therefore, MSCs may need additional stimulation to control its differentiation especially to chondrocytes and retain this phenotype in *in vitro* culture but also *in vivo*.

1.6 Growth Factors

Growth factors have become an essential part of osteochondral tissue engineering. In osteochondral environment, the growth factors are naturally produced by the body and can regulate cell proliferation and differentiation while maintaining tissue homeostasis. These growth factors can be delivered in culture medium or via scaffolds [40, 41]. In cartilage tissue engineering, growth factors commonly used include transforming growth factor- β (TGF-β), insulin growth factor (IGF), basic fibroblast growth factor (bFGF), and bone morphogenic proteins (BMPs) [42]. Of these, TGF- β1 and TGF- β3, has been the most investigated for MSC chondrogenesis and for maintaining chondrocyte phenotype *in vitro* cultures. Use of TGF- β has been shown to enhance collagen type II gene expression while down regulating collagen type I expression [43]. Similarly BMP-2,

4 and 7 are known to play a critical role in bone-healing by stimulating MSCs differentiation towards an osteoblast [44]. A detailed review on growth factors during chondrogenesis and osteogenesis have been described elsewhere [41, 43].

1.7 Mechanical and Electrical Stimulus

Increasing experimental evidence has supported the application of mechanical stimulus and its importance in regulating chondrogenesis and osteogenesis in early development, adult skeletal tissue maintenance and repair [45]. Bioreactors are designed to facilitate three-dimensional tissue growth by allowing mass transfer of nutrients and waste removal while providing controlled physical and chemical cues to cells that mimic *in vivo* conditions. Bioreactor studies have established that compression and shear forces are the two dominant physical cues that effect cartilage and bone tissues [5]. Many studies have utilized bioreactor systems to apply compressive loads on pellets, cell-laden scaffolds or bone and cartilage explants as *in vitro* model to understand cartilage and bone repair mechanisms [46, 47]. Dynamic compression at parameters ranging from of 0.01-3Hz at 0-15% strain, duration of signal (intermittent and continuous) and culture period from 48 hours up to 8 weeks have been the most explored and shown to have an effect on the production of collagen and proteoglycan [48]. Mechanically stimulated MSCs also have been shown to exhibit chondrocyte like characteristics as determined by gene expression in short term cultures when compared to statically cultured MSCs [49]. Direct perfusion bioreactors allow the control of cell culture medium flow rate, which applies fluid shear forces to the tissue constructs while increasing transfer to waste and nutrient during culture. Direct perfusion has been used for cartilage and bone tissue engineering shown to

enhance cell density in the scaffolds center, cell proliferation and differentiation of MSCs towards chondrogenesis or osteogenesis [5]. Current studies are focused on identifying the optimal mechanical stimulation parameters and the single bioreactor design that could be effective for the osteochondral tissue repair.

Electrical stimulus has also been shown to influence bone and cartilage repair due to aforementioned native tissues' electrochemical properties. Many electrical stimulus devices are clinically available for bone repair and is discussed in detail elsewhere [50]. Two modes of electrical stimulation are most commonly studied *in vitro* (1) direct current, in which field is directly applied to cells usually in a custom built chamber via agar salt bridges in culture and (2) capacitive coupling where a homogenous electric field is created between two parallel layers of metal plates that are separated by a small distance [2]. Direct current application of 5mA has shown to differentiate MSCs into chondrocytes and enhanced proliferation and formation of cartilage [2]. Brighton et al. have shown that the application 20 mV/cm via capacitvely coupling enhanced osteogenic or chondrogenic matrix proteins gene expression in osteoblasts and chondrocytes *in vitro* cultures [51, 52]. Electrical stimulus was shown to increase extracellular calcium influx via voltage gated calcium channels and an increase in activated cytoskeletal calmodulin in both electrically stimulated osteoblasts and chondrocyte. The current studies are focused on understanding the mechanisms behind electrical stimulus and optimal conditions for osteochondral tissue repair.

1.8 Thesis Motivation

Poly (vinylidene fluoride) (PVDF) and its copolymer, synthesized using PVDF and trifluoroethylene (PVDF-TrFE), are attractive for biomimetic osteochondral tissue engineering applications due to its piezoelectric properties, which can be exploited in cell cultures under mechanical and electrical stimulus. Unprocessed PVDF exists in a non-piezoelectric phase, which needs to be mechanically stretched under electrical poling to transform into piezoelectric β-phase. PVDF-TrFE, however, exists in an all-trans polar crystalline polymer consisting of β-phase and does not require any physical modifications. PVDF is a FDA approved polymer for biomedical application in sutures [53]. PVDF-TrFE has been well characterized for its piezoelectric properties in field of sensors and transducers [54]. Recent studies have demonstrated biocompatibility and established multiple tissue engineering applications using PVDF-TrFE as a scaffold. For instance, composite of PVDF-TrFE and barium titanate membranes were able to induce cell proliferation and neo bone formation when implanted under tibiae of male rabbits by day 21 [55]. Aligned, electrospun PVDF-TrFE scaffolds have been shown to support the differentiation of neural stem cells into a neuron-like phenotype [56]. Additionally, PVDF-TrFE based pressure sensor are being investigated for catheter applications [57].

In order to mimic the structure of the natural extracellular matrix, PVDF-TrFE was fabricated into a fibrous scaffold using the electrospinning technique. The micron to nanoscale fiber is a beneficial structural feature for cell adhesion and growth due to its large surface-to-volume and high aspect ratios resulting from the smallness of the diameters [58]. Therefore, PVDF-TrFE was chosen for use in this study for its well-

known piezoelectric characteristics, which is a property found in native cartilage and bone extracellular matrix and offers ease in processing into scaffolds.

1.9 Objectives

The goal of this research was to evaluate piezoelectric PVDF-TrFE polymer as a scaffold to induce MSCs differentiation to form bone and cartilage tissues *in vitro* for its potential application for osteochondral defect repair. PDVF-TrFE fibrous scaffolds were fabricated to mimic the extracellular matrix physical structure and were compared to a non-piezoelectric control. This project sought to characterize the material properties of the electrospun PVDF-TrFE and, for the first time, demonstrate MSC differentiation on PVDF-TrFE scaffolds and characterize the piezoelectric effect. This study hypothesizes that piezoelectric scaffolds will promote chondrogenic and osteogenic differentiation of MSCs. Specific aims are listed as followed:

1. To fabricate and characterize electrospun PVDF-TrFE scaffolds.
2. To evaluate the chondrogenic and osteogenic differentiation of human mesenchymal stem cells (MSCs) on fibrous piezoelectric scaffolds using a perfused compression bioreactor system.

CHAPTER 2

FABRICATION AND CHARACERIZATION OF PIEZOELECTRIC PVDF-TRFE SCAFFOLDS

2.1 Introduction

Tissue engineering offers an alternative approach by combining a biomaterial with cells for the repair of damaged tissues. The biomaterial is designed to mimic the native tissue physical structure but also provides chemical cues for the desired cell function. The electrospinning technique has been widely applied for scaffold development for bone and cartilage tissue engineering applications [59]. Electrospinning is a dynamic process where an electric field is applied to an ejecting polymer solution resulting in the formation of fibers, which are collected as a non-woven fibrous mat on a grounded plate. Electrospun scaffolds can mimic the fibrous extracellular matrix and provide a large surface area, which has been shown to influence cell attachment and protein adsorption [60]. Depending on the application, scaffolds properties such as porosity, fiber size and orientation can be customized by modifying the electrospinning process parameters and polymer concentration.

Smart biomaterials such as piezoelectric scaffolds are interesting due to its ability to generate charge in response to minute deformations, where the generated charge has been shown to influence cells behavior [61]. A commonly used piezoelectric polymer, poly(vinylidene fluoride) (PVDF), and its copolymer, poly(vinylidene fluoride – trifluoroethylene) (PVDF-TrFE) has been known to exhibit superior piezoelectric properties among other polymers. PVDF is a semi crystalline polymer that can exist in four crystal phases, α, β, γ and δ; of these, β-phase is the most sought after piezoelectric

phase [62]. In PVDF, the non-piezoelectric, α-phase is most readily formed during crystallization from melt below 160^{o}C. Its polymer chains conformation is arranged in trans-gauche-trans-gauche (TGTG), where net dipole moment is zero due to its antiparallel arrangement of fluoride atoms along the carbon backbone. The β-phase can be achieved by mechanical stretching followed by electric field poling of the α-phase [62]. However, copolymerization of PVDF with TrFE results in a copolymer that readily crystallizes from melt into the β-phase crystal, consisting of polymer chains arranged in all trans (TTTT) conformation, which results in net dipole moment (Figure 2.1) [63]. More importantly, PVDF-TrFE does not require additional mechanical stretching and electrical poling to achieve piezoelectric properties, and PVDF-TrFE exhibits much higher crystallinity than PVDF. The electrical property of PVDF-TrFE depends on the molar content of VDF and TrFE affects the crystal structure and crystallinity [63]. Additionally, PVDF-TrFE allows ease in processing into scaffolds for potential tissue engineering applications. Previous studies have reported the fabrication of electrospun PVDF and PVDF-TrFE fibers based nanogenerators and characterized its piezoelectric properties [64]. These studies have reported voltage outputs ranging from 100 mV to 1 V from PVDF-TrFE fibers based sensors when subjected to different compressive pressures [64, 65]. Thus making them suitable for self-power generators for energy harvesting applications.

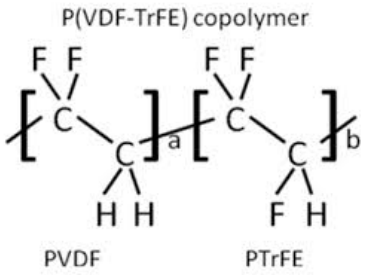

Figure 2.1 Chemical Structure of poly(vinylidene fluoride – trifluoroethylene) (PVDF-TrFE).
Source [63].

Bone and cartilage have been known to display electrical behavior when subjected to compressive deformations [2, 15]. Therefore, the application of piezoelectric PVDF-TrFE polymers as a scaffold may allow to mimic bone and cartilage extracellular matrix, which provides electrical signals relevant for biological activity. PVDF-TrFE biocompatibility is well established and has been shown to influence differentiation of neural stem cells into neurons [66]. Additionally, PVDF-TrFE/barium titanate composite films were shown to support bone formation in a calvarial defect in murine model [67]. In this chapter, PVDF-TrFE scaffolds were fabricated by electrospinning and as-spun PVDF-TrFE scaffolds were heat-treated to achieve annealed PVDF-TrFE scaffolds. Both the scaffolds were characterized for the formation of β-phase, crystallinity and piezoelectric properties. Additionally, human mesenchymal stem cells (MSCs) differentiation towards cartilage (chondrogenic) and bone (osteogenic) lineages on these scaffolds was examined to establish that the scaffolds are supportive of these lineages. Studies were performed in standard culture conditions. As a non-piezoelectric control, electrospun polycaprolactone (PCL) scaffolds were fabricated, characterized and used in

cell studies. It is hypothesized that piezoelectric scaffolds will enhance the differentiation of MSCs along chondrogenic and osteogenic lineages over PCL.

2.2 Methods

2.2.1 Scaffold Fabrication

Fabrication of fibrous scaffolds was accomplished using electrospinning technique. The electrospinning setup consisted of solution of 25 wt./vol.% poly (vinylidene difluoride – trifluoroethylene) (65/35, PVDF-TrFE, Solvay Solexis, NJ) solution in methyl ethyl ketone (Fisher Scientific, NJ). The polymer solution was transferred to a 10 mL syringe (BD, Fisher Scientific) fitted with a stainless steel needle. The syringe was placed on a syringe pump (Harvard Apparatus, MA) with a set flow rate of 15 mL/hr and a high voltage power supply (Gamma High Voltage Research, USA) was used to apply 25-28 kV to the needle. The electrospun fibers were collected on a grounded stainless steel plate placed at 35 cm distance away from the tip of the needle. The fibers were spun at room temperature (~ 20 - 23^{o}C) with 15-20% humidity for 15 minutes for thin scaffolds with ~100 - 300 μm thickness or 90 minutes for thicker scaffolds with ~3 - 4 mm. The scaffolds were placed under vacuum for at least 48 hours before further processing. The scaffolds used without further processing were labeled as-spun PVDF-TrFE scaffolds. The annealed PVDF-TrFE scaffolds were achieved by placing the as-spun scaffolds in the oven at 135^{o}C for 96 hours followed by ice water quenching for few seconds. The scaffolds were allowed to dry completely before being used further tests. As a non-piezoelectric scaffold, polycaprolactone (PCL, MW 80000, Sigma Aldrich, USA)

scaffolds were fabricated with 15 wt./wt.% PCL in methylene chloride (Fisher Scientific, USA).

2.2.2 Scaffold Morphology

Fiber morphology, fiber diameter and inter-fiber space were characterized using scanning electron microscopy (SEM, LEO 1530 Gemini, Germany). Briefly, samples were sputter coated with gold palladium and viewed using an accelerating voltage of 3-5 kV and a working distance of 4 - 8 mm. Image J software (National Institutes of Health, MD) was used for all measurements from SEM images using previously reported protocols [68]. Briefly, diameters of at least 80 fibers, 16 each from five samples per group, were measured. Porosity of dry samples was calculated using the following formula [69]:

$$\text{Porosity } (\%) = (1 - \frac{\rho_{mat}}{\rho_{raw}}) \times 100 \qquad (1)$$

where ρ_{mat} is the density of the scaffold, which was determined by dividing the mass of the scaffolds by the total volume of scaffold. The raw density, ρ_{raw}, for PVDF-TrFE and PCL is 1.78 and 1.145 gcm^{-3}, respectively. Results are reported as mean ± standard deviation.

2.2.3 Tensile Mechanical Properties

Tensile tests were performed using Instron 3342 single column system (Instron, MA) to determine Young's modulus and Ultimate tensile stress for all electrospun scaffold groups. The scaffolds were cut into 70 x 10 mm strips with a testing area of 40 x 10 mm. For each scaffold group, n = ten samples were tested at a rate of 40 mm/min. Each sample's thickness was measured at three locations along the length of the strip (at the two ends and in the center) and then was averaged to obtain final thickness. All scaffolds

were sterilized with 100% ethanol (Fisher Scientific) for 20 minutes and later rinsed with PBS prior to the mechanical testing. Results are reported as mean ± standard deviation.

2.2.4 Compression Mechanical Properties

Unconfined compression tests were performed using dynamic mechanical testing device (DMTA-4, Rheometric Scientific, NJ) system to determine compressive Young's modulus. The scaffolds were punched in to cylinders with 6 mm in diameter and 3 mm in height. For each scaffold group, n = ten samples were tested at a strain rate of 0.001 % per sec. All the scaffolds were sterilized with 100% ethanol (Fisher Scientific) for 20 mins and later rinsed with PBS prior to the mechanical testing. Results are reported as mean ± standard deviation.

2.2.5 Water Contact Angle Measurements

Wettability of the three scaffold groups was performed using sessile drop water contact measurement using a goniometer built in house. The scaffolds (6 mm diameter) were mounted on to a glass slide with the help of double-sided tape. The water (5 mL) was dropped on the scaffold and the contact angle was recorded (n = 20 per scaffold). Results are reported as mean ± standard deviation.

2.2.6 Thermal Properties

Differential scanning calorimetric (DSC; Mettler Toledo Polymer, USA) was used to determine the temperature at which permanent piezoelectricity transitions to induced piezoelectricity also called Curie temperature (T_c), melting temperature (T_m) and Heat of Fusion (ΔH_f) for all samples. The samples underwent a heat-cool-heat temperature cycle program with a heating and cooling rate of 10°C per minute from –70°C to +200°C under

nitrogen purge. The DSC data presented were representative of three independent runs. The crystallinity (X_c) of the samples was calculated using the following equation:

$$X_c(\%) = \frac{H_{fs}}{H_{ft}} \times 100 \qquad (2)$$

where H_{fs} is the measured heat of fusion for melting of sample, and H_{ft} is the heat of fusion for 100% crystalline PVDF-TrFE, which is 45 Jg^{-1} [66]. Results are reported as mean ± standard deviation.

2.2.7 Fourier Transform Infrared Spectroscopy (FTIR)

Fourier transform infrared spectroscopy (FTIR) analysis was performed for as-spun and annealed PVDF-TrFE electrospun scaffolds (Perkin Elmer FTIR-ATR 100 series, USA), and the data presented are representative of three independent samples and runs. The samples were scanned from 400 to 1500 cm^{-1} with a resolution of 4 cm^{-1} and total of 40 scans. Previously described procedures were used to determine the relative fraction of β-phase present in each sample [65]. Using characteristic absorption bands of α and β phases at 532 cm^{-1} and 846 cm^{-1}, respectively, and assuming these absorption bands follow Beer-Lambert law with absorption coefficients of K_α = 6.1 x 10^4 and K_β = 7.7 x 10^4 cm^2/mol, the fraction of β-phase can be calculated using the following equation:

$$F(\beta) = \frac{X_\beta}{X_\alpha + X_\beta} = \frac{A_\beta}{1.26A_\alpha + A_\beta} \qquad (3)$$

where X_α and X_β are the crystalline mass fractions of the α and β phases and A_α and A_β correspond to absorption bands at 532 cm^{-1} and 846 cm^{-1}, respectively. Results are reported as mean ± standard deviation.

2.2.8 X-ray Diffraction Analysis (XRD)

X-ray diffraction (XRD) was performed for as-spun and annealed PVDF-TrFE electrospun samples using an X'pert Pro Diffractrometer (Philips PW3050/60, Netherlands). The samples were irradiated with monochromatized Cu Ka (l= 0.154 nm) X-ray source with a step size (2q) of 0.02 and scan step time (s) of 1.0. The operating voltage and current used were 45 kV and 40 mA, respectively. The samples were scanned in the 2q range of 15 to 45 degrees.

2.2.9 Piezo Force Microscopy (PFM)

Piezo force microscope (PFM) was used to evaluate piezoelectric property of an individual fiber for all three groups. Briefly, few fibers were electrospun on sputter coated glass slides with gold palladium. The topography of the fibers was examined using an Asylum Research MFP-3D AFM and Olympus ac 240TS cantilever in tapping mode. The piezoresponse was examined using high voltage PFM module of MFP-3D AFM and AC 240TM cantilever mode of a tetrahedral silicon tip coated with platinum/titanium for conductivity. The piezoresponse was imaged by applying ac driving voltage ranging from 1.1 to 8.4V without a dc bias. Polarization was switched by applying a sequence of dc bias and forming a triangle wave. Between each voltage step (~100 steps total), the dc bias was stepped back to zero. [70]

2.2.10 Force Sensors

The scaffolds ranging approximately ~100 - 200 μm thick scaffolds were sandwiched between conducting copper tapes, which were attached to electrodes. The electrodes were connected to an oscilloscope (Tektronix DPO4000B, Beaverton, OR) for recording the voltage output. The sensor was mounted on Texture Analyzer (TA-XT2, Hamilton, MA)

right under the compression platen. In order to avoid over loading texture analyzer and to protect sensor, a PDMS film (3 cm x 1.5 cm x 1.5 mm thick) was used as a spacer on the sensor. Each sensor was tested at 1, 5 and 10 Hz (sinusoidal waveform) under approximately 10, 15 and 20% deformations (based on total height of sensor plus spacer).

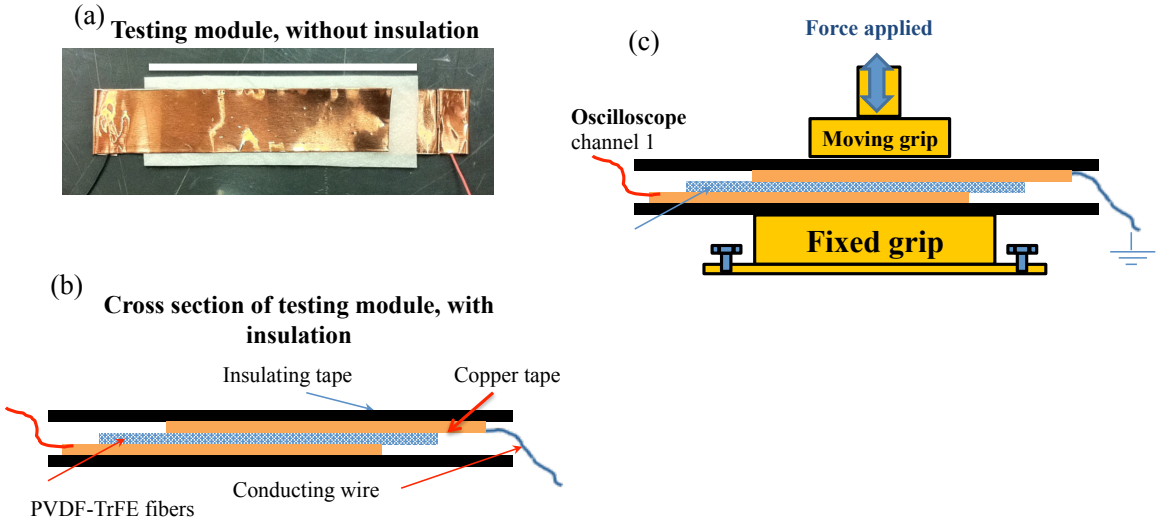

Figure 2.2 Force transducers testing setup (a) force transducer (scale bar = 63.5 mm), (b) cross-section of force transducer and (c) schematic of the testing device setup with force transducer.

2.2.11 Scaffold Sterilization

All scaffolds were cut into 6 mm diameter disks using a biopsy punch (Miltek, PA). The scaffolds were sterilized with 100% ethanol (Fisher Scientific) for 20 mins and later rinsed four times with PBS. Prior to cell seeding, scaffolds were transferred to a non-adherent, 96-well polypropylene plate and were kept hydrated in PBS (Fisher Scientific).

2.2.12 Human Mesenchymal Stem Cells (MSCs) Isolation and Culture

Human MSCs were isolated from commercially available whole bone marrow aspirates collected from the superior iliac crest of the pelvis of male donors of ages ranging from

18-30 (Lonza Biosciences, MD). The isolation method has been previously reported in detail [71]. The MSCs were plated on tissue culture polystyrene flasks (Nunc, NY) and maintained at 37°C and 5% CO_2 in control medium consisting of Dulbecco's Minimum Essential Medium (DMEM; Invitrogen, NY) supplemented with 10% fetal bovine serum (Hyclone, UT), and 1% antibiotic-antimycotic (Invitrogen).

2.2.13 Chondrogenic Differentiation

The cells were trypsinized at 70 - 80% confluent, washed and resuspended in serum-free chondrogenic medium. The chondrogenic medium consisted of high-glucose DMEM (Invitrogen) supplemented with 1 mM sodium pyruvate (Sigma Aldrich), 0.17 mM ascorbic acid-2-phosphate (WAKO Pure Chemicals, VA), 0.1 mM dexamethasone (Sigma Aldrich), 0.35 mM L-proline (Sigma Aldrich), 4 mM L-Glutamine (Invitrogen), 1% antibiotic-antimycotic (Invitrogen), 1% ITS + premix (BD), and 10 ng/mL TGF-b3 (ProSpecbio, NJ). MSCs were seeded at $1x10^5$ cells/cm^2 on each scaffold and plates were incubated at 37°C, 5% CO_2, and 85% RH. The media was replaced every 3-4 days and samples were incubated for up to 28 days. For assays, samples (n = five) were collected at Days 1, 14 and 28. The study was repeated with at least two different donors (male, ages 18-30).

2.2.14 Chondrogenic Gene Expression

At each time point, scaffolds (n = five) were pooled, rinsed in PBS and lysed in RLT buffer (Qiagen, USA) using a tissue homogenizer (Cole Parmer, IL). RNA was isolated using RNeasy Mini Kit (Qiagen) using manufacturer's protocol. The RNA concentration and integrity was performed using a nanodrop (Fisher Scientific) and spectrophotometric analysis was performed to test the integrity of RNA. Quantitative reverse transcriptase

polymerase chain reaction (RT-PCR) was performed using Real-Time PCR instrument (Stratagene, Mx3000P). RNA was reversed transcribed into complimentary DNA and amplified using One Step QuantiTect SYBR Green RT-PCR Kit (Qiagen) and gene specific forward/reverse primers (Qiagen) according to manufacturer's instructions. Briefly, the reverse transcription step ran for 30 min at 50°C, followed by a PCR initial activation step for 15 min at 95°C. Forty amplification cycles were performed, consisting of cDNA denaturation for 15 seconds at 94°C, annealing for 30 seconds at 55°C, and extension for 30 seconds at 72°C. A melting curve analysis was included for each reaction. Samples were assayed in triplicates and the values were first normalized to the housekeeping gene RPLPO (ribosomal protein, large, PO) in the same samples (ΔC_T) [72]. The mRNA expression of focal adhesion kinase (FAK), collagen type II, chondroadherin, SOX9, aggrecan and ribosomal large protein (RPLPO, house-keeping gene) were evaluated.

2.2.15 Cell Proliferation

Cell proliferation was determined by DNA quantification using the PicoGreen® ds DNA assay (Invitrogen). Standards were prepared with a known number of MSCs. Standards and samples were lysed in either 3M guanidine chloride (chondrogenic samples; Sigma Aldrich) or 0.1% triton X-100 (osteogenic samples; Sigma Aldrich). An aliquot of cell lysate was mixed with an equal volume of diluted PicoGreen reagent in 1X TE buffer (1:200, Invitrogen). Fluorescence intensity was measured with a microplate reader (FLX800, Biotek Instruments, VT) at 480 nm excitation and 520 nm emission. A standard curve correlated the fluorescence intensity of standards to known cell number.

Based on the standard curve, unknown samples' cell number was determined. Results are reported as mean ± standard deviation.

2.2.16 Glycosaminoglycans (GAGs) Assay

An aliquot of samples prepared for cell proliferation assay was used to quantify sulfated GAGs using Blyscan Assay kit (Biocolor, UK). The standards using chondroitin 4-sulfate were prepared at different concentrations ranging from 0.25 – 5.0 μg. An aliquot of the sample was reacted with dye reagent (1,9-dimethylmethyleneblue , DMMB) for 30 mins. The samples were centrifuged and any unbound reagent was discarded. Bound dye was mixed with dissociation reagent and quantified using spectrophotometer (Emax, Molecular Devices, CA) at 656 nm. The unknown GAGs were determined using the standard curve. Results are reported as mean ± standard deviation.

2.2.17 Osteogenic Differentiation

The cells were trypsinized at 70 - 80% confluent, and resuspended in general medium (GM) or osteogenic inductive medium (OS). GM consisted of low-glucose DMEM (Invitrogen) supplemented with 1% antibiotic-antimycotic (Invitrogen), and 10% fetal bovine serum (Hyclone). OS medium consisted of GM medium supplemented with 10 mM β-glycerophosphate (Sigma Aldrich), 50 μM L-ascorbic acid-2-phosphate (WAKO) and 100 nM of dexamethasone (Sigma Aldrich). MSCs were seeded at $3x10^4$ cells/cm^2 on each scaffold and plates were incubated at 37°C, 5% CO_2, and 85% RH. The media was replaced every 2 days and samples were incubated for up to 28 days. For assays, samples (n = five) were collected at Days 7, 14, 21 and 28. The study was repeated with at least two different donors (male, ages 18-30).

2.2.18 Alkaline Phosphatase Activity Assay

Alkaline phosphatase (AP) activity was measured by quantifying the conversion of para-nitrophenyl phosphate (Sigma Aldrich) to para-nitrophenol (p-NP). Samples were prepared by lysing cells with 0.1% Triton X-100 and incubated at 37^{o}C for 30 minutes. The absorbance was read at 405 nm with a microplate spectrophotometer (Emax, Molecular Devices). The AP activity was normalized to cell number determined from cell proliferation assay and expressed as nmol of p-NP/min/cell. Results are reported as mean ± standard deviation.

2.2.19 Mineralization Assay

Mineralization of the extracellular matrix was measured using a quantichrom calcium detection kit (Bioassay Systems, CA, USA). Briefly, the samples were homogenized and digested in 0.5 N HCL overnight at room temperature. The calcium standards were prepared at various concentrations. Samples and working solution was mixed and incubated for 3 minutes. The absorbance was read at 570 nm with a microplate spectrophotometer (Emax, Molecular Devices). Results are reported as mean ± standard deviation.

2.2.20 Immunofluorescence Staining for Confocal Imaging

The harvested samples were washed with PBS and fixed in 4% paraformaldehyde (Sigma Aldrich) overnight at 4^{o}C. The samples were permeablized with 0.1% triton-x100 for 15 minutes at room temperature. A blocking serum consisting of 5% donkey serum (Sigma Aldrich) or rabbit serum (Sigma Aldrich) in 1% bovine serum albumin (BSA, Fisher Scientific) was used to treat samples for 1 hour at room temperature to avoid nonspecific antibody binding. For chondrogenic samples, the samples were incubated in 1:1000

mouse antihuman collagen type II (EMD Millipore, USA) or rabbit antihuman collagen type I antibody (EMD Millipore) in 1% BSA overnight at 4^{o}C For osteogenic samples, the samples were incubated in 1:1000 rabbit antihuman collagen type I or rabbit antihuman osteocalcin antibody (EMD Millipore) in 1% BSA overnight at 4^{o}C. After a series of PBS washes, the samples were then incubated in 1:200 secondary antibody (donkey antimouse IgG or rabbit antigoat IgG in 1% BSA, Invitrogen) along with 1:100 rhodamine phalloidin (Invitrogen) to view actin for 1 hour at room temperature. The nucleus was stained with 4',6-diamidino-2-phenylindole (DAPI, Invitrogen).

2.2.21 Statistical Analysis

SPSS 20.0 software (SPSS Inc., IL, USA) was used for statistical analysis of all quantitative data. For each donor, statistical analysis was performed based on the number of samples collected at each time point for each assay. The results were initially tested for normality (Shapiro Wilk test) and Levene's equal variance test. Two-way Analysis of Variance (ANOVA) and the post hoc multiple comparison using Tukey's tests were applied. Probability (p) values < 0.05 were considered statistically significant.

2.3 Results

2.3.1 Scaffold Morphology

As shown in Figure 2.3, micron sized fibers were achieved using electrospinning technique for both as-spun and annealed PVDF-TrFE and PCL. The measured fiber diameters and inter-fiber space are shown in Table 2.1. Both of the PVDF-TrFE scaffolds had uniform fiber morphologies. PCL scaffolds showed a wide range of mixture of fiber

diameters ranging between 4 – 13 μm. The significant difference was not noted in fiber diameters, inter-fiber spacing and overall porosity between the three scaffold groups. Additionally, water drop contact angle measurements were performed to assess hydrophobicity and no differences were noted between the three scaffold groups.

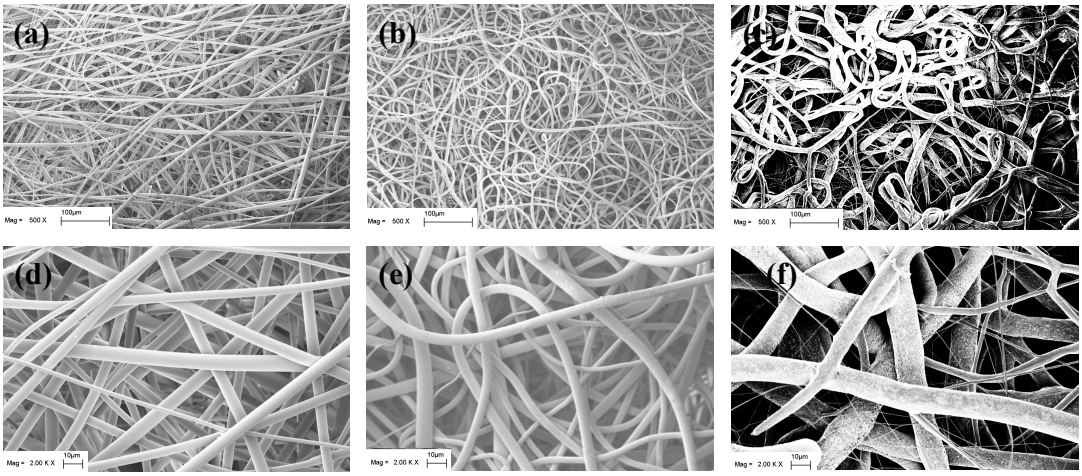

Figure 2.3 SEM images of as-spun PVDF-TrFE (a) & (d), annealed PVDF-TrFE (b) & (d) and PCL (c) & (f) at 500X and 2000X. Scale bar at 500X = 100 μm and 2000X = 10 μm.

Table 2.1 Scaffold Properties for As-spun PVDF-TrFE, Annealed PVDF-TrFE and PCL

	Fiber diameter (μm)	Inter-fiber Space (μm)	Porosity (%)	Water Contact Angle (^{o})
As-spun PVDF-TrFE	5.9 ± 2.0	81.1 ± 33.8	93	133.6 ± 2.1
Annealed PVDF-TrFE	6.9 ± 1.7	89.3 ± 28.6	92	134.3 ± 4.3
PCL	9.8 ± 3.0	62.2 ± 33.4	88	135.0 ± 3.5

2.3.2 Mechanical Properties

A summary of Young's modulus and ultimate tensile stress for all scaffold groups are reported in Table 2.2. There were no significant differences observed for Young's modulus between as-spun and annealed PVDF-TrFE and PCL groups. Annealing PVDF-TrFE did increase Young's modulus but it was not statistically significant. The ultimate tensile stress was significantly lower for PCL scaffolds compared to PVDF-TrFE

scaffolds. The compressive Young's modulus was significantly lower for as-spun PVDF-TrFE group compared to annealed PVDF-TrFE and PCL groups.

Table 2.2 Mechanical Properties for Electrospun Scaffolds

	Tensile Young's Modulus (MPa)	Ultimate Tensile Stress (MPa)	Compressive Young's Modulus (kPa)
As-spun PVDF-TrFE	4.0 ± 1.2	0.71 ± 0.08	5.6 ± 2.3[b]
Annealed PVDF-TrFE	5.3 ± 2.3	0.90 ± 0.28	10.7 ± 5.7
PCL	5.8 ± 1.0	0.48 ± 0.06[a]	16.7 ± 4.6

Values represent mean ± standard deviation
a $p<0.05$ where PCL scaffolds are significantly different PVDF-TrFE groups
b $p<0.05$ where as-spun PVDF-TrFE group is significantly different from annealed PVDF-TrFE and PCL groups.

2.3.3 Thermal Properties

The DSC was performed to determine the melting temperature (T_m) and heat of fusion of the electrospun scaffolds. Figure 2.4 shows the endothermic curves and Table 2.3 summarizes the results from DSC analysis. The crystallinity ($\%X_c$) was calculated using equation 2. PCL scaffolds had the lowest T_m as compared to both of the PVDF-TrFE scaffolds. The T_m was significantly lower for as-spun PVDF-TrFE than annealed PVDF-TrFE scaffolds. Similarly, crystallinity was significantly lower for PCL and as-spun PVDF-TrFE than annealed PVDF-TrFE scaffolds. Both PVDF-TrFE scaffolds demonstrated a curie temperature (T_c). Annealed PVDF-TrFE scaffold's T_c was significantly higher than as-spun PVDF-TrFE.

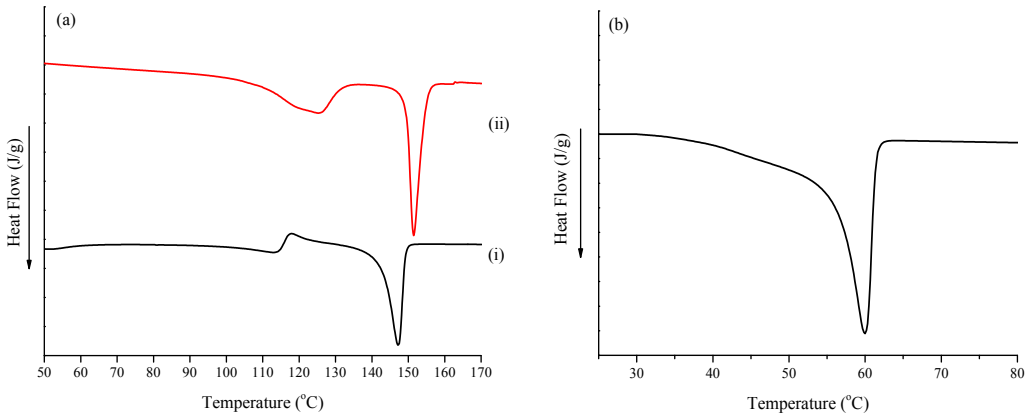

Figure 2.4 DSC spectrums for (i) as-spun PVDF-TrFE and (ii) annealed PVDF-TrFE. (b) PCL scaffolds.

Table 2.3 Thermal Properties for As-spun PVDF-TrFE, Annealed PVDF-TrFE and PCL Scaffolds

	T_c (°C)	T_m (°C)	% Crystallinity
As-spun PVDF-TrFE	113.1 ± 0.3[a]	147.4 ± 0.4[a]	44.6 ± 4.3[a]
Annealed PVDF-TrFE	125.1 ± 0.5[a]	151.5 ± 0.2[a]	63.8 ± 2.3[a]
PCL	-	60.3 ± 0.7[a]	36.5 ± 2.0[a]

Values represent mean ± standard deviation
a $p<0.05$ where all groups different

2.3.4 Fourier Transform Infrared Spectroscopy (FTIR)

FTIR spectrum (Figure 2.5) of both PVDF-TrFE scaffolds exhibited primarily β-phase peaks at 508, 846 and 1285 cm^{-1}. The α-phase peaks at 532, 612, 765, 796, 854, 870 and 970 cm^{-1} were not appreciable. The annealed PVDF-TrFE had significantly higher β-phase fraction of 75 ± 3.2% than as-spun PVDF-TrFE, 64 ± 2.8%. Similar analysis was not performed for PCL scaffolds since these peaks are specific to piezoelectric phases present in PVDF-TrFE materials, and PCL is a non-piezoelectric polymer.

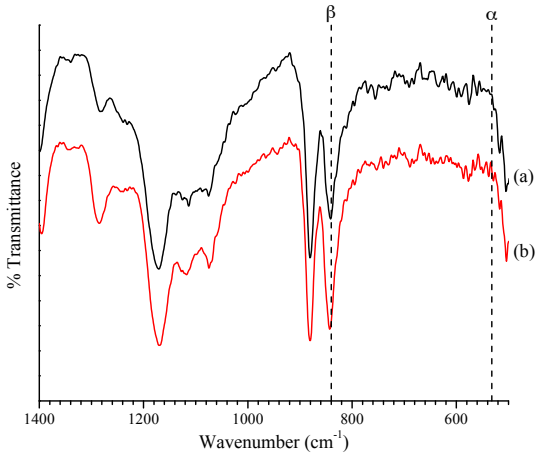

Figure 2.5 FTIR spectra of (a) as-spun PVDF-TrFE and (b) annealed PVDF-TrFE fibers.

2.3.5 X-ray Diffraction (XRD)

X-ray diffraction spectrums of both PVDF-TrFE scaffolds are shown in Figure 2.6. Both of the scaffolds spectrums consistently showed peaks characteristic of β-phase at $2\theta = 20^{o}$. The as-spun PVDF-TrFE had a small shoulder off peak at $\sim 2\theta = 18^{o}$ characteristic of α-phase, which overlapped with the β-phase peak. In annealed PVDF-TrFE scaffolds, two smaller peaks were observed at $\sim 2\theta = 37^{o}$ and 42^{o} indicating some presence of α-phase.

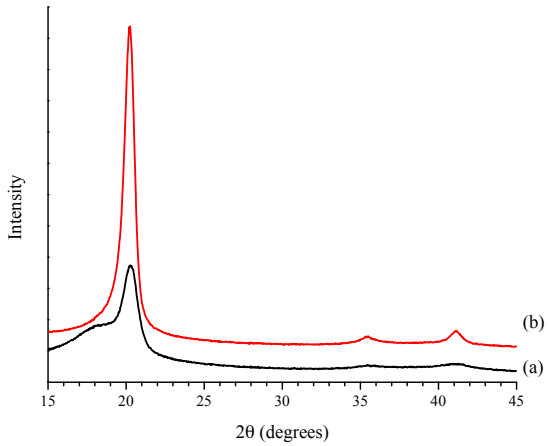

Figure 2.6 XRD spectra of (a) as-spun PVDF-TrFE and (b) annealed PVDF-TrFE fibers.

2.3.6 Piezo Force Microscopy (PFM)

A comparison of local piezoresponse loops for single point obtained from PFM for as-spun PVDF-TrFE, annealed PVDF-TrFE and PCL fibers are shown in Figure 2.7. Characteristic voltage butterfly loops were observed for both PVDF-TrFE scaffolds in the "on" state, indicating that fiber deformation occurred when voltage was applied. In the "off" state, applied voltage is stepped back to 0 V and electric interactions between AFM tip and fiber was noted. Both PVDF-TrFE fibers demonstrated amplitudes changes during "off" state indicating the inherent piezoelectric behavior of fibers. PCL fiber did not demonstrate distinct voltage butterfly loop in "on" state and only noise was detected in "off" state , thus confirming its the non-piezoelectric property.

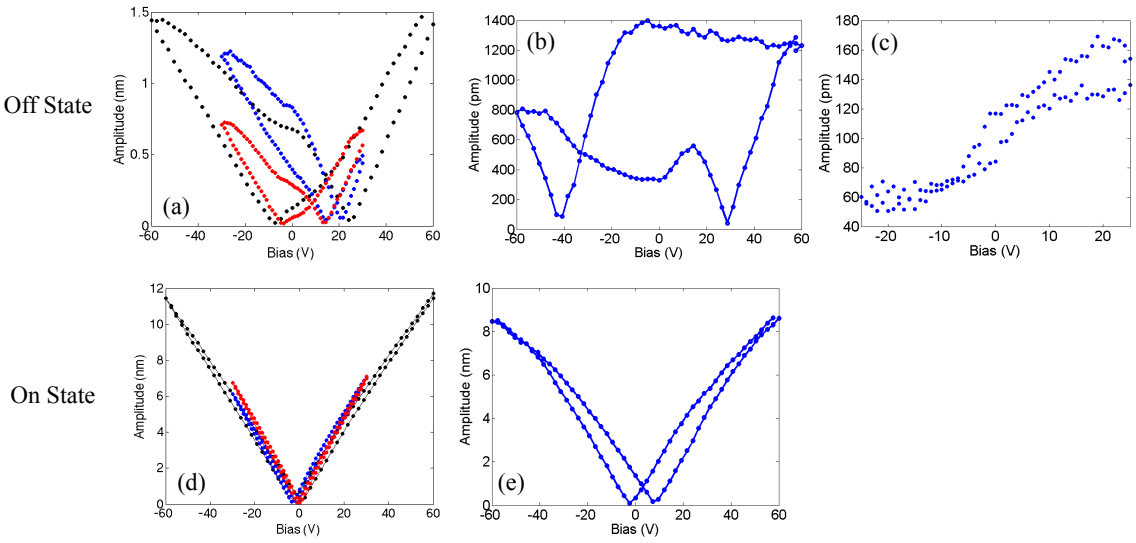

Figure 2.7 Piezo force microscopy (PFM) voltage butterfly loops for as-spun PVDF-TrFE (a, d), annealed PVDF-TrFE (b, e) and PCL fibers (c) in "on" and "off" state.

2.3.7 Force Sensors

Force sensors were fabricated with as-spun PVDF-TrFE, annealed PVDF-TrFE and PCL scaffolds for measuring electrical output under dynamic compression loads at varying frequencies. It was noted that voltage output increased with increasing deformation levels and frequencies for both PVDF-TrFE scaffolds. Annealed PVDF-TrFE scaffolds had the highest voltage output than as-spun PVDF-TrFE. PCL did not generate any electrical output. The results are summarized in Table 2.4.

Table 2.4 Electrical Output from Force Sensors

			Electrical output	
Frequency (Hz)	%Deformation	Applied Force (N)	As-spun PVDF-TrFE	Annealed PVDF-TrFE
1	10%	20	2.3 mV	117 mV
1	15%	100	6.9 mV	168 mV
1	20%	200	8.4 mV	324 mV
5	10%	20	4.4 mV	866 mV
5	15%	100	20 mV	1.5 V
5	20%	200	27.5 mV	2.9 V
10	10%	20	99 mV	2.1 V

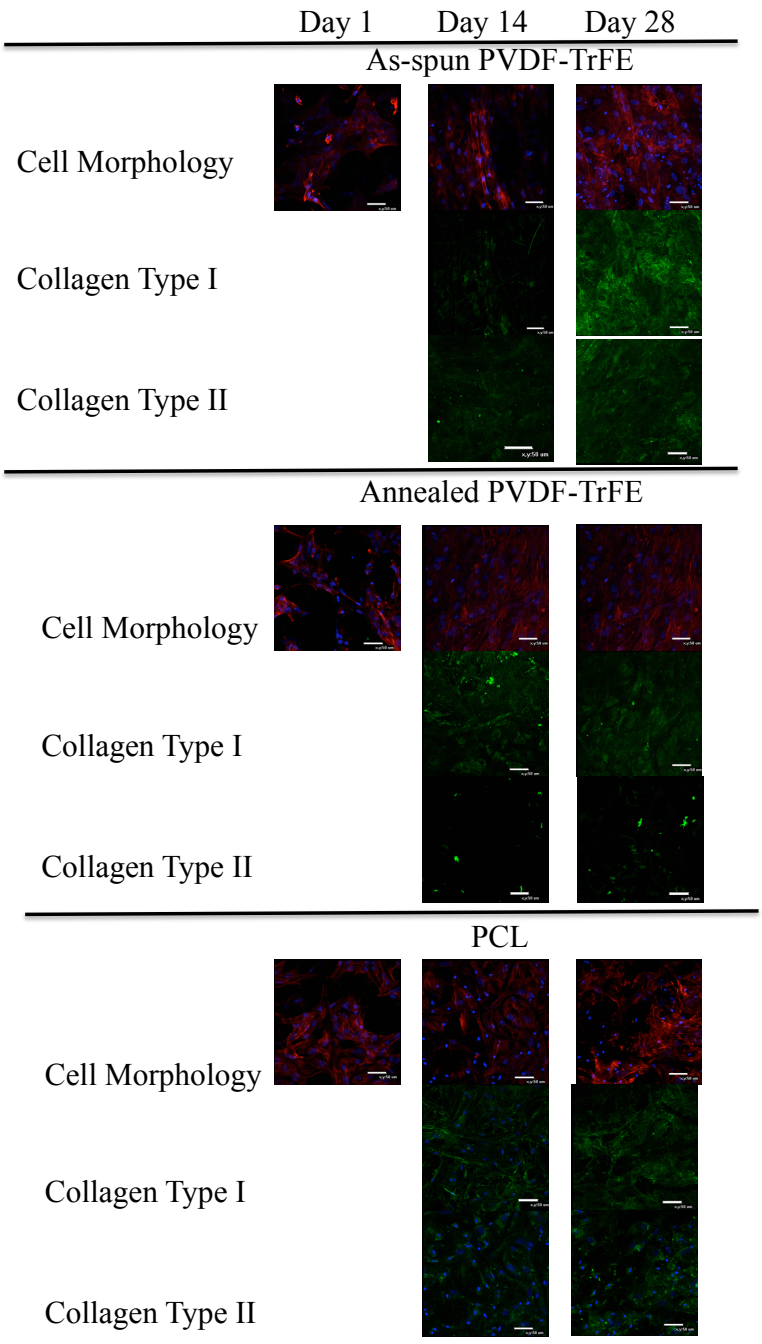

Figure 2.8 Confocal images of cells in CCM+ medium where cells were placed on as-spun PVDF-TrFE, annealed PVDF-TrFE and PCL scaffolds for up to 28 days. Cultures stained for F-actin (red), nucleus (blue), and collagen types I and II (green). Scale bar = 50 μm.

2.3.8 Cell Morphology of Chondrogenic Cultures

The confocal images confirmed cells attached to all scaffolds as evidenced by intense F-actin staining at all time points as shown in Figure 2.8. As early as day 1, cells formed aggregates on all scaffolds. Cells produced collagens type I and II as early as day 14 on all scaffolds. Cells on as-spun PVDF-TrFE appeared to produce the most collagen type II as shown by the intense staining at day 28 as compared to other groups.

2.3.9 Chondrogenic Biochemical Assays

Cell proliferation was determined over the course of 28 days in culture as shown in Figure 2.9. The results showed an increase in cell number at days 14 and 28 when compared to Day 1. At day 14, PCL was significantly different than PVDF-TrFE scaffolds. No significant differences were noted between days 14 and 28 for each scaffold group.

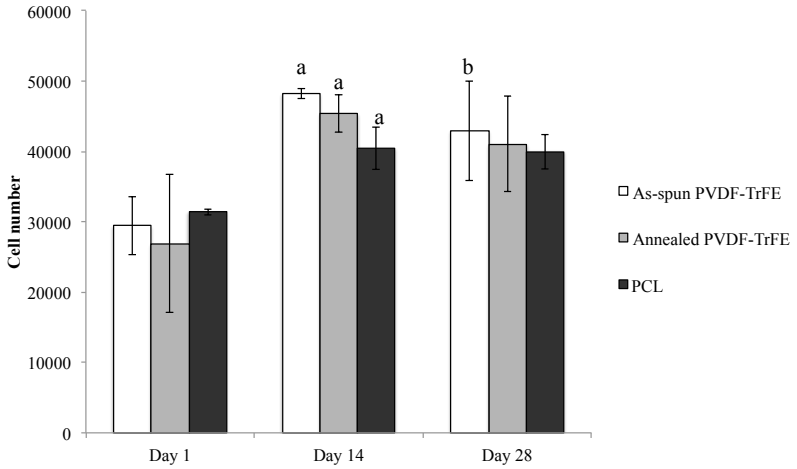

Figure 2.9 Cell proliferation shown as fold change since day 1 in CCM+ medium where cells were placed on as-spun PVDF-TrFE, annealed PVDF-TrFE and PCL scaffolds for up to 28 days. a $p<0.05$ significant difference between days 1 and 14 and b $p<0.05$ significant difference between days 1 and 28.

Glycosaminoglycan (GAGs), an early extracellular matrix marker, was determined at day 1, 14 and 28 as shown in Figure 2.10. Results are shown as total GAGs (Figure 2.10a) and normalized GAG per cell (Figure 2.10b). Results demonstrate an increase in total GAGs by day 14 and later decrease by day 28 ($p<0.05$). No significant differences were noted between as-spun and annealed PVDF-TrFE scaffolds at all time points. The cells on PCL had significantly lower amounts of total GAGs than annealed PVDF-TrFE scaffolds at day 14 ($p < 0.05$). When normalized to cell number no significant differences were detected between scaffolds and at all time points.

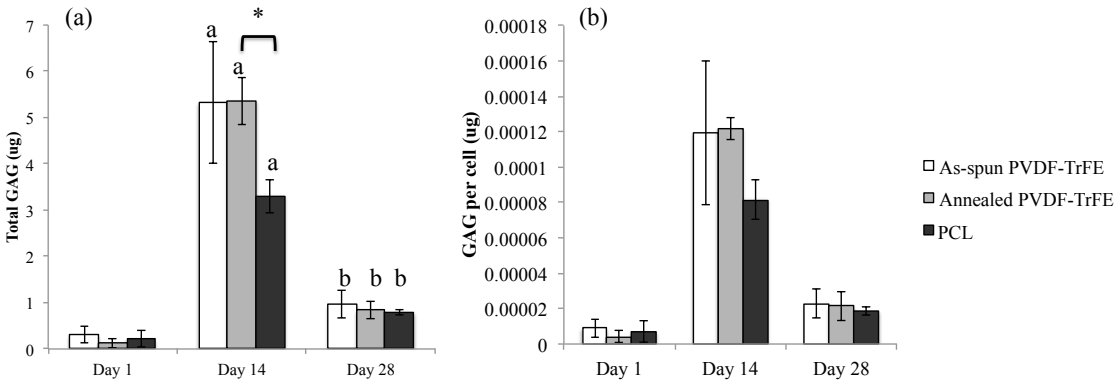

Figure 2.10 Glycosaminoglycan production (a) Total GAG per scaffold and (b) total GAGs normalized to cell number in CCM+ medium where cells were placed on as-spun PVDF-TrFE, annealed PVDF-TrFE and PCL scaffolds for up to 28 days. *$p<0.05$ significant difference between groups, a $p<0.05$ significant difference between days 1 and 14 and b $p<0.05$ significant difference between days 14 and 28 *$p<0.05$

2.3.10 Chondrogenic Gene Expression

Gene expression of chondrogenic markers was evaluated at days 1, 14 and 28 to monitor MSCs differentiation on all three scaffolds, as shown in Figure 2.11. Focal adhesion kinase (FAK), an indicator of cell attachment, was expressed by cells on all three scaffolds. At day 14, cells on PCL scaffolds had significantly higher FAK expression than as-spun and annealed PVDF-TrFE scaffolds ($p<0.05$). By day 28, FAK expression

significantly increased for cells on as-spun PVDF-TrFE but remained unchanged on other scaffolds. SOX9 gene expression, which maintains chondrogenic potential, was significantly different between annealed PVDF-TrFE and PCL group at day 1 ($p<0.05$). At day 14, SOX9 expression on PCL scaffolds decreased significantly from day 1 ($p<0.05$). By day 28, cells on both as-spun and annealed PVDF-TrFE scaffolds had a significantly higher SOX9 expression than the PCL group ($p<0.05$), which was further decreased. Aggrecan expression was highest at day 1 for cells on as-spun PVDF-TrFE when compared to annealed PVDF-TrFE and PCL groups ($p<0.05$). However, at day 14 aggrecan expression significantly decreased for all groups compared to day 1 ($p<0.05$). By day 28, cells on the annealed PVDF-TrFE had the highest aggrecan expression followed by as-spun PVDF-TrFE and lowest for PCL group ($p<0.05$). Mature chondrogenic markers collagen type II and chondroadherin were significantly different for all three groups at day 28, where as-spun PVDF-TrFE scaffolds had the highest expression followed by annealed PVDF-TrFE and lowest on the PCL group.

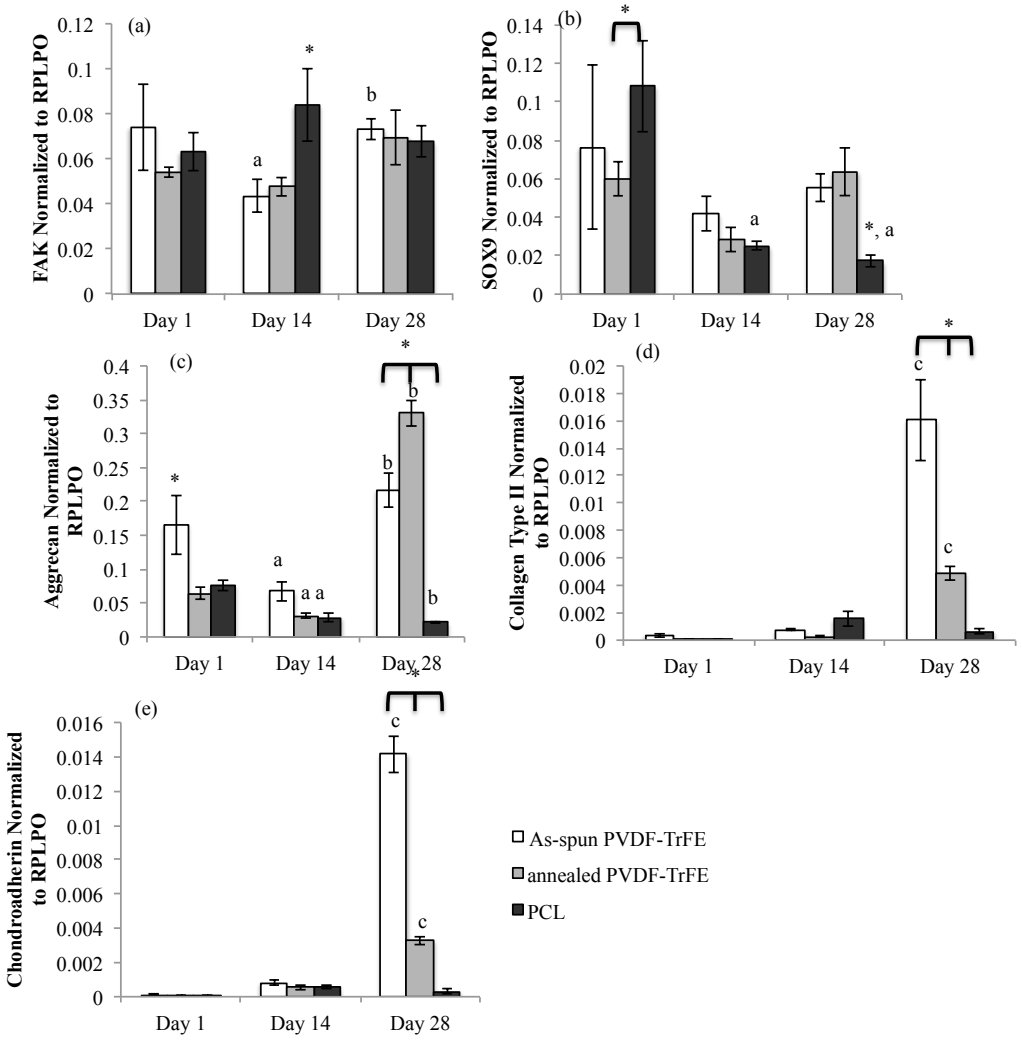

Figure 2.11 Gene expression for cells in CCM+ medium where cells were placed on as-spun PVDF-TrFE, annealed PVDF-TrFE and PCL scaffolds for up to 28 days. (a) Focal adhesion kinase (FAK) (b) SOX9 (c) aggrecan (d) collagen type II (e) chondroadherin where *$p<0.05$ significant difference between groups, a $p<0.05$ significant difference between days 1 and 14, b $p<0.05$ significant difference between days 14 and 28 and c $p<0.05$ day 28 is significantly different from days 1 and 14.

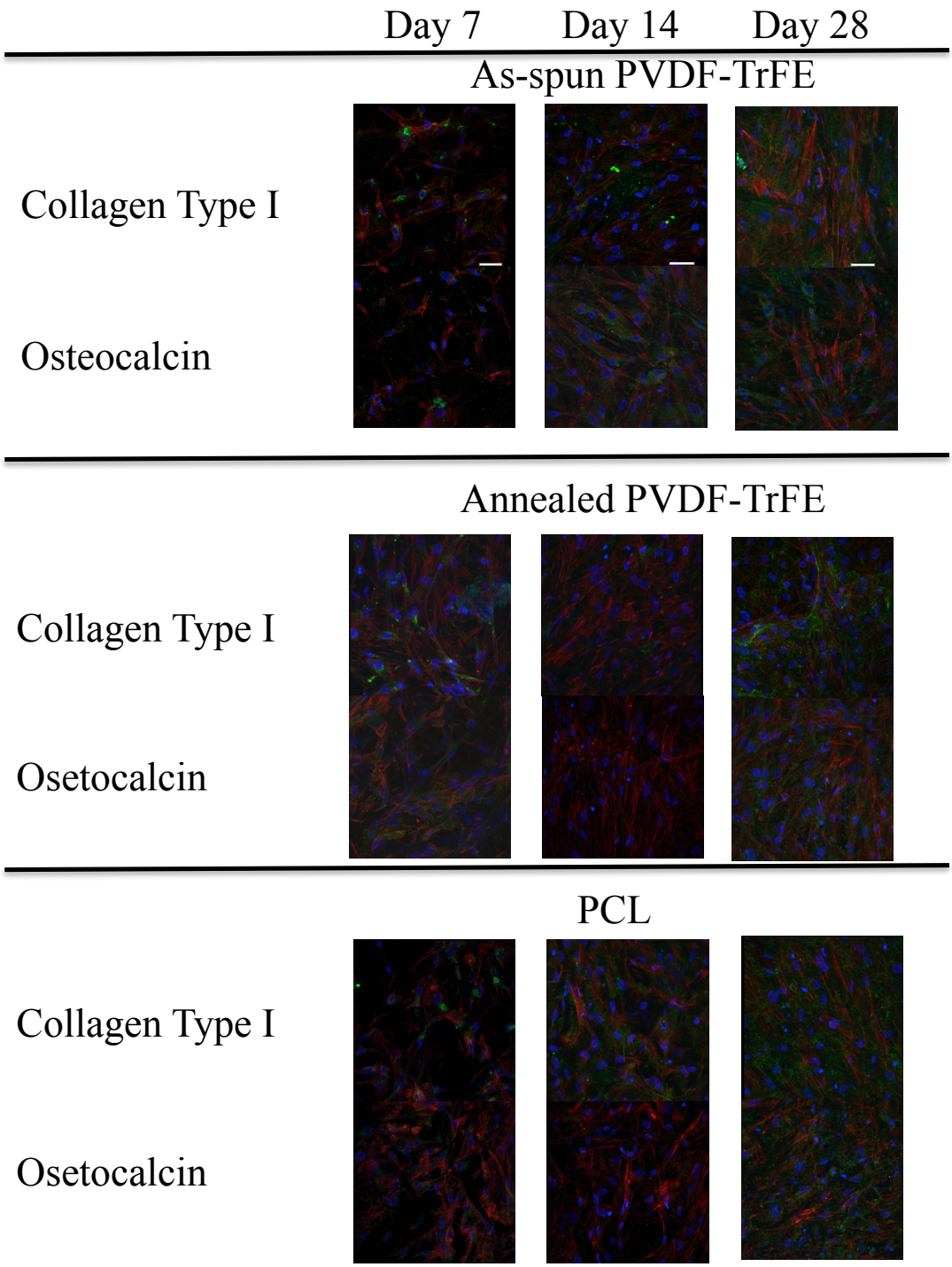

Figure 2.12 Confocal images of cells in OS medium where cells were placed on as-spun PVDF-TrFE, annealed PVDF-TrFE and PCL scaffolds for up to 28 days. Cultures stained for F-actin (red), nucleus (blue), and collagen type I or osteocalcin (green). Scale bar = 50 μm.

2.3.11 Cell Morphology of Osteogenic Cultures

Confocal images (Figure 2.12) confirmed cell attachment to all scaffolds and expression of cytoskeleton F-actin. Samples were stained for early osteogenic marker, collagen type I and osteocalcin, a mature osteogenic differentiation marker. All the scaffolds stained for collagen type I and osteocalcin from day 14 onwards.

2.3.12 Osteogenic Biochemical Assays

The osteogenic cell proliferation results, as shown in Figure 2.13, indicated an increasing trend in cell number from day 7 to 21 for all scaffolds. However, the PCL group had a significant increase in cell number at days 14 and 21 when compared to day 7 ($p<0.05$). By day 28, all scaffolds showed a slight decrease in cell number. No significant differences were observed between scaffolds at all time points.

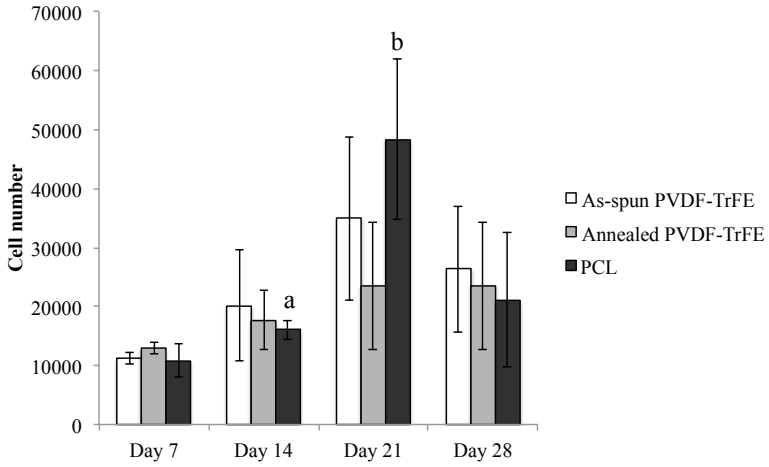

Figure 2.13 Cell number for cells in OS medium for up to 28 days. a $p<0.05$ significant difference between days 7 and 14, b $p<0.05$ significant difference between days 14 and 21.

The alkaline phosphatase activity, an early osteogenic differentiation marker, was determined at days 7, 14, 21 and 28 and normalized to cell number as shown in Figure

2.14. Results indicated a significantly higher alkaline phosphatase activity for all scaffold groups at day 14 as compared to day 7. Significant differences were noted between as-spun and annealed PVDF-TrFE groups where the annealed group was highest. Alkaline phosphatase activity significantly decreased at days 21 and 28 as compared to day 14.

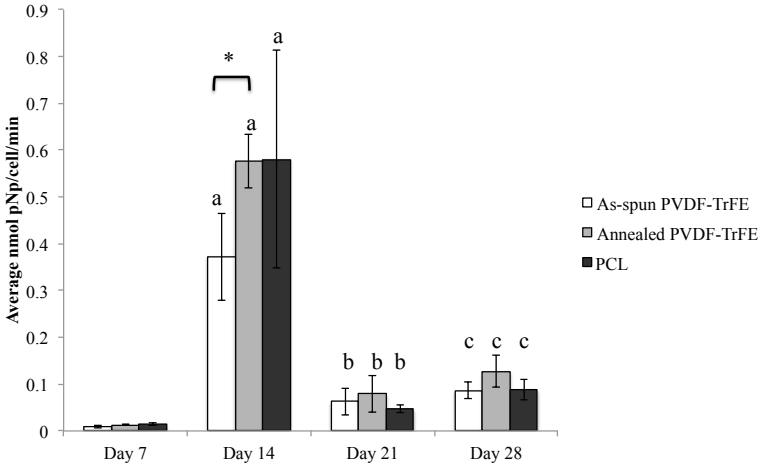

Figure 2.14 Alkaline phosphatase activity normalized to cell number on as-spun and annealed PVDF-TrFE and PCL scaffolds in OS medium for up to 28 days. *$p < 0.05$ significant difference between groups, a $p<0.05$ significant difference between days 7 and 14, b $p<0.05$ significant difference between days 14 and 21 and c $p<0.05$ significant difference between days 14 and 28.

Calcium or mineralization of the extracellular matrix, was quantified for all scaffolds at days 7, 14, 21 and 28, as shown in Figure 2.15. A significant increase in mineralization was observed at all time points for all scaffold groups. Only at day 28, cells on as-spun PVDF-TrFE scaffolds had significantly lower calcium levels than the PCL group. At all other time points, no significant differences were observed between groups.

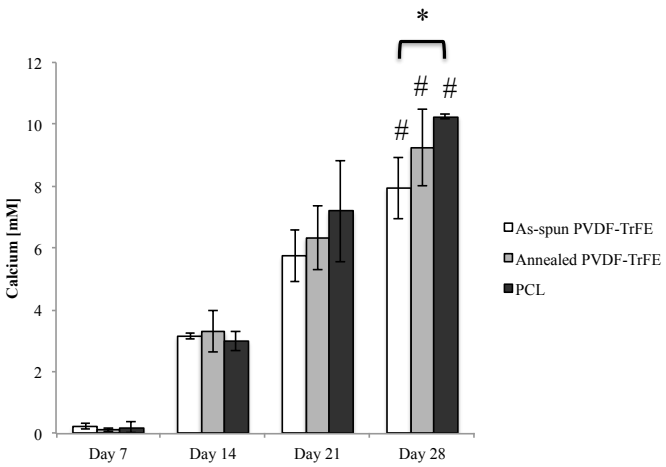

Figure 2.15 Calcium or mineralization of the extracellular matrix for cells on as-spun and annealed PVDF-TrFE and PCL scaffolds in OS medium for up to 28 days. *$p < 0.05$ significant difference between groups, # $p<0.05$ significant difference between all time points.

2.4 Discussion

The aim of this study was to characterize the material properties of the PVDF-TrFE scaffolds and assess MSCs differentiation potential along chondrogenic and osteogenic lineages on these scaffolds. Additionally, PCL scaffold was evaluated as a non-piezoelectric control in biological studies. Studies confirmed that PVDF-TrFE scaffolds contained the piezoelectric β-phase, but a significant increase in crystallinity and relative β-phase fraction occurred due to annealing. All the scaffolds were supportive of osteogenic and chondrogenic differentiation, however, chondrogenic differentiation was enhanced on PVDF-TrFE scaffolds as indicated by increased GAG production and expression of chondrogenic markers i.e. aggrecan, collagen type II and chondroadherin. Some differences were noted for osteogenic differentiation where cells on annealed PVDF-TrFE scaffolds had a higher alkaline phosphatase activity over as-spun PVDF-

TrFE but no differences in biochemical markers were detected between piezoelectric materials and non-piezoelectric control for this lineage in static culture conditions.

Electrospinning parameters such as applied voltage, solvent and polymer concentration have an impact on fiber uniformity and size. In this study, 15% wt/wt PCL was chosen as the polymer concentration with methylene chloride as the solvent for achieving scaffolds with a similar fiber diameter range as 25% wt/vol PVDF-TrFE scaffolds. Although PVDF-TrFE scaffolds have relatively uniform fiber diameters, PCL scaffolds consisted wider range of fiber sizes as noted by the large standard deviation. One reason could be the differences in boiling points between the solvents used. Methyl ethyl ketone (MEK, 79.6^{o}C) has a higher boiling point than methylene chloride (39^{o}C). As a result, MEK evaporates much faster during electrospinning than methylene chloride. Similar findings have been previously reported where mixture of nano and micron size fiber diameters where achieved for PCL scaffolds [73]. This phenomenon is common during electrospinning where an ejecting polymer solution becomes highly charged and experiences electrostatic forces, which causes repulsion of charges on its surface aids in elongating the fiber [62]. Additionally, polymer concentration affects the viscoelastic forces by hampering fiber elongation. Therefore, this polymer jet becomes highly unstable, and undergoes whipping and bending motion, which results in nano and micron fiber diameters.

Annealing is commonly used with PVDF-TrFE films to enhance degree of crystallinity, which directly influences the electrical behavior of PVDF-TrFE. In this study, 135^{o}C was chosen as the annealing temperature, which was between Curie temperature (T_c = 113^{o}C) and melting temperature (T_m = 147.4^{o}C) of electrospun as-spun

PVDF-TrFE scaffolds. Previous work with PVDF-TrFE films has suggested that choosing annealing temperature above T_c but below T_m increases the grain size and crystallinity of orientation of β-phase while polymer chains align parallel to the substrate with polarization dipole moment perpendicular to the substrate [63, 74]. This study's findings are comparable with previous study findings and have demonstrated the significant increase in T_c, T_m and crystallinity for annealed electrospun PVDF-TrFE scaffolds compared to as-spun PVDF-TrFE scaffolds.

Force sensors were fabricated to assess electrical output when scaffolds were subjected to compressive loads, and the annealed PVDF-TrFE reported the highest electrical output ranging from 117 mV to 2.9 V. Since the scaffolds were collected in a randomly oriented manner, one can speculate that there may be cancellation of net dipole moments, which are hypothesized to be perpendicularly oriented to polymer fiber from electrospinning [65] and may not produce voltage output . However, when annealed scaffolds were subjected to dynamic deformations, voltage outputs were noted, which increased with applied frequency and deformation. In this study, voltage outputs from as-spun PVDF-TrFE ranged from 2.25 mV to 99 mV depending on the applied frequency and deformation. These findings were significantly higher than previously reported where as-spun PVDF-TrFE scaffolds voltage output was ~ 2.5 mV at 27 Hz [75]. More recent studies have reported higher electrical output from as-spun PVDF-TrFE scaffolds when subjected to different ranges of pressures and frequencies. For instance, Mandal et al. have demonstrated pressure sensor fabricated by electrospinning of randomly oriented PVDF-TrFE fibers with output voltage of about 400 mV when subjected to 0.2 MPa compressive stress at 5.3Hz [76]. Similarly, a pressure sensor fabricated by

electrospinning of aligned PVDF-TrFE fibers with output ranging from 0.79 – 1.3 V under 0.1-1 Pa compressive stress at 1 and 2 Hz [65]. These recent studies further confirm that application of low pressures can stimulate electrical output from PVDF-TrFE fibers. In the current study, relatively high forces were applied because the instrument settings did not allow the modification of applied forces. Therefore, a PDMS substrate was used to dampen the excessive applied force.

The differences noted in electrical properties can be attributed to composition of PVDF-TrFE, which in this study was 65/35 wt% compared to 75/25 wt% in previous studies. The electrical properties and the formation of crystal phases depend on PVDF-TrFE ratio where higher ratio results in higher electrical output and crystallinity. This may also be the reason for observing smaller α-phase peaks in annealed PVDF-TrFE scaffolds. Additionally, the current study used MEK as the solvent, which was different from prior studies where N,N-dimethylformamide (DMF) and butan-2-one was used, which may impact the β-phase formation and electrical properties. Nevertheless, PFM results further confirmed the piezoelectric behavior of both PVDF-TrFE scaffolds compared to PCL group. However, PFM analysis performed in this study was qualitative thus the calculations for piezoelectric constant, d_{33}, which quantifies the deformation of these fibers when subjected to electric field, was not made.

Interestingly, there were no significant differences observed for Young's modulus between all three scaffolds. Although annealed PVDF-TrFE had the highest ultimate tensile strength but this was not statistically significant when compared to as-spun PVDF-TrFE and PCL scaffolds. Randomly oriented electrospun fibers have anisotropic properties due to the way the fibers are collected as non-woven. Bulk tensile properties

may not be the best method for obtaining materials true Young's modulus. Mechanical testing of single fiber has been suggested as an alternative method for assessing polymer properties [77]. Nevertheless, bulk tensile method does provide an understanding of electrospun polymer strength and differences between different chemistries. A previous study of electrospun PVDF-TrFE scaffolds had higher Young's modulus than the ones reported in this study [56]. The fiber diameters achieved in this study were much larger along with larger inter-fiber space than the previous study, which may have contributed to the differences noted in Young's modulus. Electrospinning smaller fiber diameter results in a denser collection of fibers and smaller inter-fiber space, which has been to enhance mechanical properties [78, 79].

The chondrogenic differentiation of MSCs on as-spun and annealed PVDF-TrFE was enhanced over the PCL control, as indicated by biochemical and gene markers. . PCL scaffolds have been widely used for cartilage and bone tissue engineering for *in vitro* applications [73, 80-82]. In order to compare piezoelectric scaffolds with a non-piezoelectric scaffold, PCL was the best choice due to similar mechanical properties and ability to fabricate similar fiber size and morphology as PVDF-TrFE fibers. All the three scaffold groups supported MSC attachment and similar proliferation trends in both chondrogenic and osteogenic cultures over 28 days. For the chondrogenic cultures, confocal images confirm the attachment and aggregation of cells as early as day 1 indicating the early condensation of MSCs and initiation of cell-cell contact similar to early embryonic development [6, 83]. PVDF-TrFE groups both supported chondrogenic differentiation as confirmed by early GAG production, which was significantly higher than the PCL group at day 14. MSCs undergoing chondrogenic differentiation in pellet

cultures demonstrate a peak in GAG production between days 11-19 days after which GAG accumulation decreases while collagen type II production increases [84]. SOX9, a transcription factor is expressed in early chondrogenesis, which regulates and maintains chondrocyte phenotype for differentiating MSCs and later expression of collagen type II gene [84]. In this study, both PVDF-TrFE groups had higher SOX9 expression than the PCL group at days 14 and 28 indicating higher MSCs chondrogenic differentiation potential at the gene level. Furthermore, Collagen type II expression was up-regulated on as-spun PVDF-TrFE group and was significantly higher than annealed PVDF-TrFE and PCL groups. The confocal images further confirmed an increase in collagen type II production by intense protein staining at days 14 and 28 on the as-spun PVDF-TrFE scaffolds than other scaffolds, especially PCL. Additionally, chondroadherin gene expression overlaps with collagen type II expression appearing later in the process of extracellular matrix assembly [84]. In this study, chondroadherin similar to collagen type II was detected from day 14 onwards and peaking at day 28. Both the piezoelectric scaffolds demonstrated significantly higher chondroadherin expression, especially the as-spun PVDF-TrFE group, as compared to the PCL group. Although the culture conditions were performed in static conditions, these findings suggest a role of piezoelectric activity where piezoelectric fibers may be sensitive to cell-induced deformations affecting MSCs differentiation behavior. It is well known that differentiated cells adhere, contract, and migrate/crawl in and along substrates while deforming the matrix [85]. In *in vitro* conditions, cells can contract their matrices up to 1-3 mm [86]. At the molecular scale, matrix interaction and deformation by the cell occurs via focal adhesion complexes that integrate the extracellular matrix with the actin cytoskeleton [87]. The force that the cell

generates to deform the matrix results in signal transduction cascades leading to activation of transcription factors that affect gene expression in the cell. Engler et al. have demonstrated that MSCs are sensitive to matrix elasticity, which dictates its specific lineage. FAK gene is up regulated in early MSC condensation, down regulated in chondrocyte differentiation and later re-expressed during chondrocyte hypertrophy towards bone formation [68]. FAK gene expression results showed a higher expression on the PCL group at day 14 but this later decreased by day 28. FAK expression for cells on PVDF-TrFE scaffolds continued to increase by day 28, which may indicate these cells are further differentiated on PVDF-TrFE scaffolds. Hypertrophic genes will be examined in Chapter 3. Aggrecan gene expression was consistently higher on piezoelectric groups as compared to PCL group. Further confirming increased differentiation of MSCs on piezoelectric scaffolds than non-piezoelectric polymer, PCL.

In osteogenic cultures, no significant differences were noted for early osteogenic marker, alkaline phosphatase activity, and mineralization between piezoelectric groups and PCL group. Previous studies have shown an effect of increased β-phase fraction on osteogenic differentiation of MSCs with nano sized PVDF fibrous scaffolds [62]. Similarly in this study, alkaline phosphatase activity was significantly higher for annealed PVDF-TrFE scaffold, which had a higher β-phase fraction than as-spun PVDF-TrFE. However, no differences were observed for mineralization between all scaffolds. The differences in fiber diameters of previously reported nano scale PVDF fibers [62] versus micron scale fibers in this study could have contributed to the observed trends noted in osteogenesis. It has been well-established that cell attachment and differentiation is favored on nanofibers due to the high surface density fiber arrangement [68, 88]. When

fiber size increases, cells are not able to spread across multiple fibers and may sense large fibers as film [89], which can adversely affect osteogenesis.

Previous cell studies with piezoelectric polymers such as PVDF have primarily been performed using films due to the feasibility of fabricating a non-piezoelectric control with similar chemistry as the piezoelectric group. These studies have shown variable response to the presence or lack of piezoelectric β-phase. However, PVDF-TrFE polymers are permanently piezoelectric polymer and it is not possible to obtain a non-piezoelectric form. Therefore, PCL was chosen as a non-piezoelectric polymer as a way of identifying the piezoelectric effect on MSC differentiation. The next set of studies described in Chapter 3 will aim to demonstrate MSCs differentiation towards chondrogenic and osteogenic lineages on piezoelectric materials when stimulated under physiological loading conditions using a perfused compression bioreactor system.

CHAPTER 3

CHONDROGENIC AND OSTEOGENIC DIFFERENTIATION OF MSCS ON PVDF-TRFE SCAFFOLDS IN A PERFUSED COMPRESSION BIOREACTOR SYSTEM

3.1 Introduction

In order to repair osteochondral defects, the requirements of bone, cartilage and the bone-cartilage interface must be taken into account. As a potential scaffold, piezoelectric PVDF-TrFE offers intriguing properties due to its capability of generating electrical potentials under mechanical deformation as shown in Chapter 2, which has the potential to influence MSCs differentiation. In literature, it's been well established that bone and cartilage respond to compressive mechanical stimulus but also become electrically polarized under compressive loads [2, 11, 15]. Grodzinsky et al. demonstrated the generation of electrical potentials from circular plugs of articular cartilage when subjected to compressive loading. Similarly, electrical potentials were also observed when knee joint explants where exposed to mechanical force up to 800 N [9]. The electrical activity of cartilage has been attributed to the movement of ions within interstitial fluid under compression flows over negatively charged proteoglycan molecules resulting in the generation of an electrical current [9]. Similarly, bone's piezoelectricity was demonstrated when stress-generated electrical potentials were created by the shear loading of collagen in human femur bone specimens [13]. Furthermore, individual collagen type I fibrils have been demonstrated to be piezoelectric under shear deformation using piezo force microscopy (PFM) technique [16]. It has been speculated that bone piezoelectric properties may affect repair and remodeling of bone

tissue, and some studies have demonstrated that mechanically deformed or actively remodeling bone produces electrical current *in vivo* [15, 18]. Additionally, electrical stimulus on osteoblasts and chondrocytes *in vitro* cultures has been shown to enhance osteogenic or chondrogenic matrix protein gene expression. Application of alternating electrical fields of 20 mV/cm up-regulated aggrecan and type II collagen gene expression in chondrocytes [90], and human MSCs were shown to differentiate into osteoblasts, while expressing enhanced levels of alkaline phosphatase and collagen type I [91].

Previous studies with PVDF-TrFE have been with films where PVDF-TrFE combined with barium titanate was investigated for bone regeneration *in vitro* with osteoblasts [92] and *in vivo* rat calvarial bone defects [67]. These studies confirmed biological compatibility and increased bone regeneration. However, a three dimensional environment is essential for facilitating cell growth and tissue formation if it is to be clinically relevant. In this study, PVDF-TrFE scaffolds were prepared by electrospinning and MSC differentiation towards chondrogenic and osteogenic lineages on these scaffolds was examined using a cyclic compression with continuous perfusion bioreactor system. By applying cyclic compression in culture, we can examine cell behavior when the PVDF-TrFE scaffolds are deformed and therefore, activating the piezoelectric activity of the scaffold. Comparisons were made between as-spun PVDF-TrFE, annealed PVDF-TrFE and PCL (non-piezoelectric control). We hypothesize that piezoelectric scaffold undergoing dynamic compression will enhance chondrogenesis and osteogenesis compared to PCL group.

3.2 Materials and Methods

3.2.1 Scaffold Fabrication

Fabrication of fibrous scaffolds was accomplished using electrospinning technique. The electrospinning setup consisted of solution of 25 wt./vol.% poly (vinylidene difluoride – trifluoroethylene) (65/35, PVDF-TrFE, Solvay Solexis, NJ) solution in methyl ethyl ketone (Fisher Scientific, NJ). The polymer solution was transferred to a 10 mL syringe (BD, Fisher Scientific) fitted with a stainless steel needle. The syringe was placed on a syringe pump (Harvard Apparatus, MA) with a set flow rate of 15 mL/hr and a high voltage power supply (Gamma High Voltage Research, USA) was used to apply 25-28 kV to the needle. The electrospun fibers were collected on a grounded stainless steel plate placed at 35 cm distance away from the tip of the needle. The fibers were spun at room temperature (~ 20 - 23^{o}C) with 15-20% humidity for 90 minutes for thicker scaffolds with ~3 - 4 mm. The scaffolds were placed under vacuum for at least 48 hours before further processing. The scaffolds used without further processing were labeled as-spun PVDF-TrFE scaffolds. The annealed PVDF-TrFE scaffolds were achieved by placing the as-spun scaffolds in the oven at 135^{o}C for 96 hours followed by ice water quenching for few seconds. The scaffolds were allowed to dry completely before being used further tests. As a non-piezoelectric scaffold, polycaprolactone (PCL, MW 80000, Sigma Aldrich, USA) scaffolds were fabricated with 15 wt./wt.% PCL in methylene chloride (Fisher Scientific, USA).

3.2.2 Scaffold Sterilization

All scaffolds were cut into 6 mm diameter disks using a biopsy punch (Miltek, PA, USA). The thickness of scaffold with ~ 3 mm were chosen for biological studies. The scaffolds were sterilized with 100% ethanol (Fisher Scientific, USA) for 20 mins and later air dried in sterile hood overnight. Each scaffold was transferred to sterile 5 mL polypropylene test tubes (BD) for cell seeding.

3.2.3 Human Mesenchymal Stem Cells (MSCs) Isolation and Culture

Human MSCs were isolated from commercially available whole bone marrow aspirates collected from the superior iliac crest of the pelvis of male donors of ages ranging from 18-30 (Lonza Biosciences, MD). The isolation method has been previously reported [71] The MSCs (P3 or P4) were plated on tissue culture polystyrene flasks (Nunc, NY, USA) and maintained at 37°C and 5% CO_2 in control medium consisting of Dulbecco's Minimum Essential Medium (DMEM; Invitrogen, NY, USA) supplemented with 10% fetal bovine serum (Hyclone, UT, USA), and 1% antibiotic-antimycotic (Invitrogen).

3.2.4 Bioreactor Systems Overview

Two different bioreactor systems were used in these studies. One of the systems was capable of dynamic compressive loading and simultaneous perfusion (Cartigen 9-X, Instron TERM, MA) through nine different wells and holds up to 9 different samples. Cartigen 9-X bioreactor chamber is connected to a load cell (FUTEK, CA) that is connected to a control box and laptop computer with software program (TGT). The second system is capable of only perfusion through nine different wells (Perfusion Series; Instron TERM, MA) and can also hold up to 9 different samples. In both the systems,

perfusion was achieved using Masterflex peristaltic pump systems (Masterflex L/S; Cole Parmer).

3.2.5 Cell Seeding and Bioreactor Conditions

The cells were trypsinized at 70 - 80% confluent, washed, counted using a hemocytometer and resuspended in control medium. After counting, 2.0 x 10^6 cells per mL cell suspension was prepared, and 500 μL of cell suspension was added to each scaffold in a test tube. Using a 21G sterile needle (Fisher Scientific) and 10 mL sterile syringe, vacuum was applied on sealed test tubes until cell suspension penetrated the scaffold and air bubbles were at minimum [93]. The test tubes were lightly capped and incubated at 37°C and 5% CO_2 for at least 3 hours to allow cell attachment.

For Day 0 cell count and imaging, samples (n = five per scaffold group) were harvested after 3 hours incubation period and prepared for cell count or imaging. Otherwise, scaffolds were transferred to bioreactor for differentiation studies. The samples for dynamic compressive loading (n = nine) were placed in its system, and the continuous perfusion flow rate in each was controlled at a rate of 0.5 mL/min and was applied for the duration of the experiment of 28 days. Next day (Day 1), the loading protocol was begun and consisted of 10% dynamic compressive strain (of scaffolds height) using a sinusoidal waveform at 1 Hz for 3 hours per day up to 28 days. Applied forces and platen displacement were monitored and recorded. Similarly, the samples for perfusion only (n = nine) were loaded in perfusion system, and the continuous perfusion flow rate in each was controlled at a rate of 0.5 mL/min and was applied for the duration of the experiment of 28 days. The total media volume used for each bioreactor was 200 mL and was changed once a week. The samples were collected at days 0 (n = five), 14 (n

= four) and 28 (n = five) for tissue analysis. Each scaffold was rinsed in PBS, cut into four quarters, weighed and separated for different analytical techniques. The study was repeated with at least two different donors. The bioreactor conditions were the same for chondrogenic and osteogenic differentiation studies except the cell culture medium.

3.2.6 Chondrogenic Differentiation

The chondrogenic medium consisted of high-glucose DMEM (Invitrogen) supplemented with 1 mM sodium pyruvate (Sigma Aldrich), 0.17 mM ascorbic acid-2-phosphate (WAKO Pure Chemicals, VA, USA), 0.1 mM dexamethasone (Sigma Aldrich), 0.35 mM L-proline (Sigma Aldrich), 4 mM L-Glutamine (Invitrogen), 1% antibiotic-antimycotic (Invitrogen), 1% ITS + premix (BD), and 10 ng/mL TGF-b3 (ProSpecbio, NJ, USA).

3.2.7 Osteogenic Differentiation

Osteogenic medium consisted of control medium supplemented with 10 mM beta glycerophosphate (Sigma Aldrich), 50μM L-ascorbic acid-2-phosphate (WAKO) and 100 nM of dexamethasone (Sigma Aldrich).

3.2.8 Cell Proliferation

Cell proliferation (n = four quarters per scaffold group per time point per condition) was determined by DNA quantification using the PicoGreen® ds DNA assay (Invitrogen). Standards were prepared with a known number of MSCs. Standards and samples were lysed in either 3Mguanidine chloride (chondrogenic samples; Sigma Aldrich) or 0.1% triton X-100 (osteogenic samples; Sigma Aldrich). An aliquot of cell lysate was mixed with an equal volume of diluted PicoGreen reagent in 1X TE buffer (1:200, Invitrogen). Fluorescence intensity was measured with a microplate reader (FLX800, Biotek

Instruments, VT) at 480 nm excitation and 520 nm emission. A standard curve correlated the fluorescence intensity of standards to known cell number. Based on the standard curve, unknown samples' cell number was determined. Results are reported as mean ± standard deviation.

3.2.9 Glycosaminoglycans (GAGs) Assay

An aliquot of samples prepared for cell proliferation assay was used to quantify sulfated GAGs using Blyscan Assay kit (Biocolor, UK). The standards using chondroitin 4-sulfate were prepared at different concentrations ranging from 0.25 – 5.0 μg. An aliquot of the sample was reacted with dye reagent (1,9-dimethylmethyleneblue , DMMB) for 30 minutes. The samples were centrifuged and any unbound reagent was discarded. Bound dye was mixed with dissociation reagent and quantified using spectrophotometer (Emax, Molecular Devices, CA) at 656 nm. The unknown GAGs were determined using the standard curve. Results are reported as mean ± standard deviation.

3.2.10 Collagen Types I and II ELISA

Solubilized collagen types I and II were quantified using separate ELISA kits (Chondrex, WA, USA). Prior to assay, collagens were solubilized in samples according to the manufacturers protocol. Briefly, the samples were homogenized and digested with 3M guanidine chloride to remove GAGs overnight on shaker at 4^{o}C. Next day the samples were treated in acetic acid overnight in fridge to remove guanidine chloride. The samples were further digested at 10 mg/mL pepsin on shaker at 4^{o}C for up to 6 days to solubilize collagens. For collagens quantification, the supernatant was diluted at 1:40 or 1:10 with dilution buffer. In the sample mixture, the collagen proteins were captured by polyclonal anti-human collagen types I or II antibodies and detected by the biotinylated counterparts

and streptavidin peroxidase. OPD and H_2O_2 were added to the mixture, and sulfuric acid was then added after 30 min to stop the reaction. The spectrophotometric absorbance of the mixture was measured at 490 nm. Results are reported as mean ± standard deviation.

3.2.11 Alkaline Phosphatase Activity Assay

Alkaline phosphatase (AP) activity was measured by quantifying the conversion of para-nitrophenyl phosphate (Sigma Aldrich) to para-nitrophenol (p-NP). Samples were prepared by lysing cells with 0.1% Triton X-100 and incubated at 37^{o}C for 30 minutes. The absorbance was read at 405 nm with a microplate spectrophotometer (Emax, Molecular Devices, CA, USA). The AP activity was normalized to cell number determined from cell proliferation assay and expressed as nmol of p-Np/min/cell. Results are reported as mean ± standard deviation.

3.2.12 Mineralization Assay

Mineralization of the extracellular matrix was measured using a quantichrom calcium detection kit (Bioassay Systems, CA, USA). Briefly, the samples were homogenized and digested in 0.5 N HCL overnight at room temperature. The calcium standards were prepared at various concentrations. Samples and working solution was mixed and incubated for 3 minutes. The absorbance was read at 570 nm with a microplate spectrophotometer (Emax, Molecular Devices). Results are reported as mean ± standard deviation.

3.2.13 Tissue Mechanical Properties

Biomechanical analysis was performed using Cartigen 9X bioreactor system. Using data from the cycles of applied dynamic compression profile, dynamic modulus was

calculated as the peak-to-peak stress divided by peak-to-peak strain on days 1, 14 and day 28. Results are reported as mean ± standard deviation.

3.2.14 Gene Expression

The samples for gene expression were collected at Days 14 and 28. At each time point, scaffolds (n = five) were pooled, rinsed in PBS and homogenized in 500 μL lysis buffer (Qiagen, USA) and stored at -80^{o}C until further processing. The RNA concentration and integrity was performed using a nanodrop and spectrophotometric analysis was performed to test the integrity of RNA. Cell lysate was centrifuged through a QIAshredder homogenizer column and combined with an equal volume of 70% ethanol. RNA was isolated using RNeasy Mini Kit (Qiagen) using manufacturer's protocol. Quantitative reverse transcriptase (qRT) polymerase chain reaction (qRT-PCR) was performed using One Step QuantiTect SYBR Green RT-PCR Kit (Qiagen, USA) with Real-Time PCR instrument (Stratagene, MX4000, USA), according to manufacturer's instructions. Briefly, the reverse transcription step ran for 30 min at 50^{o}C, followed by a PCR initial activation step for 15 min at 95^{o}C. Forty amplification cycles were performed, consisting of cDNA denaturation for 15 s at 94^{o}C, annealing for 30 s at 55^{o}C, and extension for 30 s at 72^{o}C. QuantiTect Assay primers (Qiagen, USA) were used for analyzing chondrogenic differentiation by assessing SOX9, aggrecan, collagen types I, II, IX and X and chondroadherin gene expression. For osteogenesis differentiation, collagen type I, RUNX2, alkaline phosphatase, osteocalcin and osteopontin were analyzed. Samples were assayed in triplicates and the values were first normalized to the housekeeping gene RPLPO (ribosomal protein, large, PO) in the same samples (ΔC_T).

Fold change was determined by normalizing dynamic groups to perfusion only groups using $2^{-\Delta\Delta C_T}$ [94].

3.2.15 Immunofluorescence Staining for Confocal Imaging

The harvested samples were washed with PBS and fixed in 4% paraformaldehyde overnight at 4°C. The samples were then permeablized with 0.1% triton-x100 for 15 minutes at room temperature. As a negative control, scaffolds without cells were immunostained along with harvested samples to ensure lack of any non-specific staining. A blocking serum consisting of 5% donkey serum or rabbit serum in 1% bovine serum albumin (BSA) was used to treat samples for 1 hour at room temperature to avoid nonspecific antibody binding. For cartilage tissue, the samples were incubated in 1:1000 mouse antihuman collagen type II antibody in 1% BSA overnight at 4°C For bone tissue, the samples were incubated in 1:1000 rabbit antihuman collagen type I or rabbit antihuman osteocalcin antibody in 1% BSA overnight at 4°C. After a series of PBS washes, the samples were then incubated in 1:200 secondary antibody (donkey antimouse IgG or rabbit antigoat IgG in1% BSA, Invitrogen) along with 1:100 rhodamine phalloidin (Invitrogen) to view actin for 1 hour at room temperature. The nucleus was stained with 4',6-diamidino-2-phenylindole (DAPI; Invitrogen).

3.2.16 Statistical Analysis

SPSS 20.0 software (SPSS Inc., IL, USA) was used for statistical analysis of all quantitative data. Results are expressed as mean ± standard deviation. The results were initially tested for normality (Shapiro Wilk test) and Levene's equal variance test. Two-way Analysis of Variance (ANOVA) and the post hoc multiple comparison using

Tukey's tests were applied. Probability (p) values < 0.05 were considered statistically significant.

3.3 Results

3.3.1 Day 0 Cell Attachment

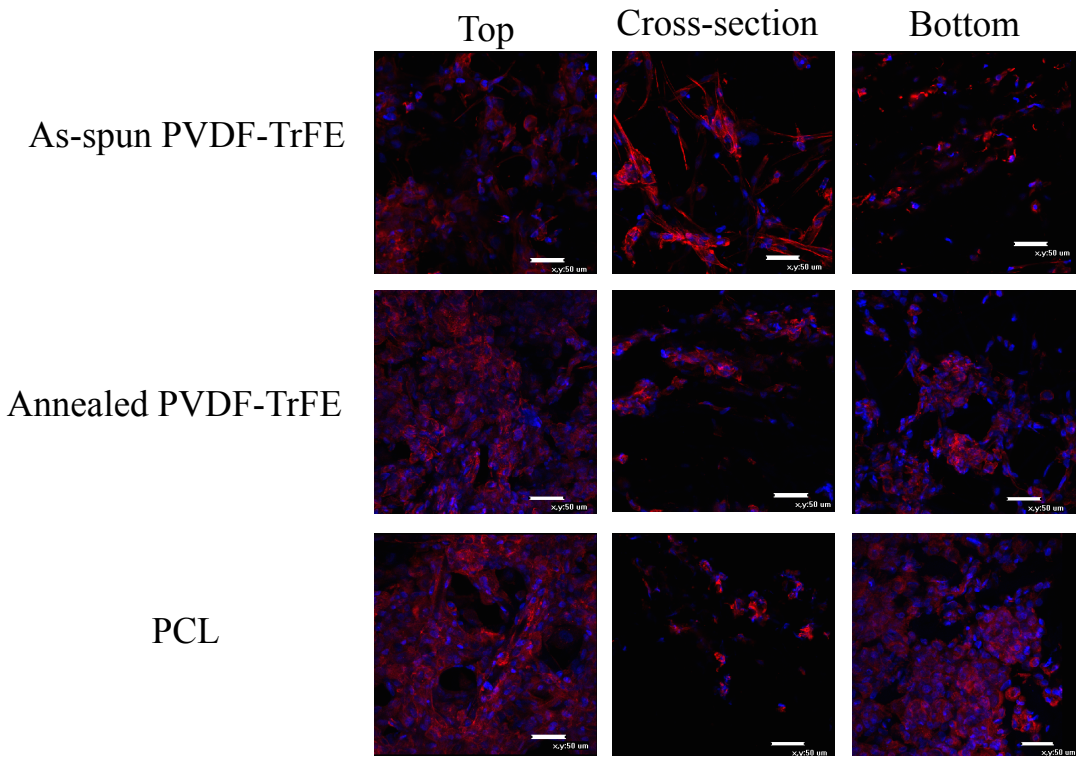

Figure 3.1 Confocal images of cells attached to scaffolds on day 0. Cultures stained for F-actin (red) and nucleus (blue). Scale bar = 50 μm.

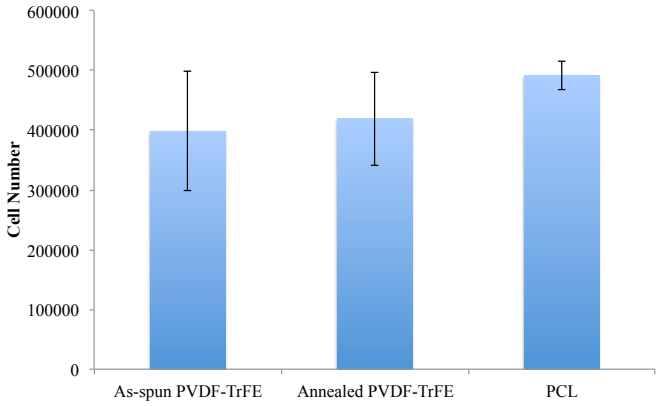

Figure 3.2 The number of cells attached to as-spun PVDF-TrFE, annealed PVDF-TrFE and PCL scaffolds at day 0.

The confocal images confirmed the attachment of cells to all scaffolds as evidenced by intense F-actin and nucleus staining in Figure 3.1. Additionally there was no significant difference in number of cells attached to scaffold between all the three groups as shown in Figure 3.2.

3.3.2 *In vitro* Chondrogenesis

The piezoelectric scaffolds, as-spun and annealed PVDF-TrFE, were evaluated for their ability to support and enhance chondrogenesis of human MSCs as well as compare to non-piezoelectric, PCL, as a control. MSCs were distributed throughout the fibrous constructs, which were cultured in chondrogenic induction medium over a period of 28 days. After 28 days culture, all the constructs transitioned from loose fibrous material to an elastic like, discrete mass of tissue with a shiny appearance similar to hyaline cartilage as shown in Figure 3.3. To isolate the effects of dynamic compression stimulus on MSCs differentiation, all the quantitative results presented were normalized to perfusion group for each scaffold group. The actual values from quantitative results for chondrogenic bioreactor studies are shown in Appendix A.

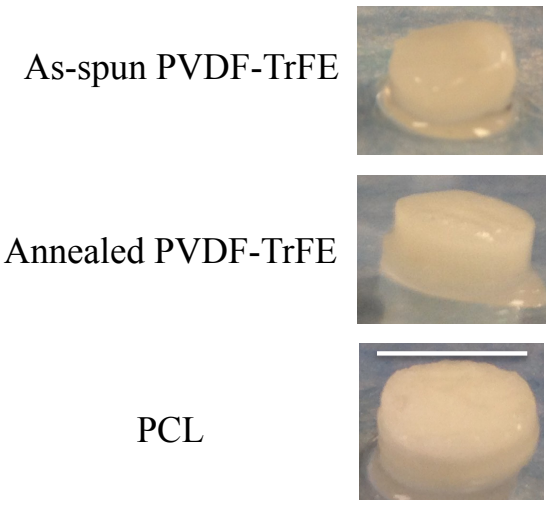

Figure 3.3 Cartilage tissue constructs at day 28 which underwent dynamic compression harvested from bioreactor. Scale bar = 6 mm.

The cell proliferation was monitored by quantifying the DNA content of the scaffolds at days 14 and 28. For all the three groups, cell proliferation was significantly influenced by culture time as shown in Figure 3.4a. Dynamic stimulus encouraged increased cell proliferation at day 14 for both as-spun and annealed PVDF-TrFE when compared to perfusion group baseline. In contrast, for PCL scaffolds' undergoing dynamic stimulus, number of cells decreased by 30% at day 14 when compared to perfusion group baseline. By day 28, cell number significantly decreased on as-spun and annealed PVDF-TrFE groups by 36% and 44% fold, respectively. Interestingly, annealed PVDF-TrFE scaffold groups demonstrated a higher number of cells at days 14 and 28 when compared to as-spun PVDF-TrFE and PCL groups.

To determine whether the piezoelectric scaffolds enhanced chondrogenesis, sulfated GAGs, collagen types II and I contents for each scaffold group was examined. The amount of GAGs, an indicator of hyaline cartilage proteoglycan, depended on culture time but also the scaffold type as shown in Figure 3.4b. At day 14, cells within annealed

PVDF-TrFE produced more total GAGs content compared with cells within as-spun PVDF-TrFE or PCL. By day 28, however, all three groups had significantly different amounts of total GAGs where as-spun PVDF-TrFE group had the highest GAGs amount. Interestingly, by day 28, all dynamic groups were well below the perfusion groups' baseline indicating the increased GAGs production in perfusion groups than dynamic.

Collagen type II, a mature hyaline cartilage marker, and collagen type I, marker for immature cartilage, production was quantified on all three constructs at days 14 and 28. As-spun PVDF-TrFE scaffolds promoted an increased collagen type II production compared to PCL and annealed PVDF-TrFE constructs as shown in Figure 3.4c. Especially, by day 28, both as-spun and annealed PVDF-TrFE constructs demonstrated significantly higher collagen type II than PCL scaffolds. Collagen type II production remained unchanged over time for PCL constructs. Enhanced production of collagen type II production in both the piezoelectric, as-spun and annealed PVDF-TrFE can be attributed to dynamic compression stimulus compared to perfusion alone. Collagen type I synthesis was consistently lower in all scaffolds undergoing dynamic compression than perfusion groups. Nevertheless, collagen type I was detected in all three scaffolds and was significantly different between days 14 and 28 for all three constructs as shown in Figure 3.4d. Annealed PVDF-TrFE scaffolds consistently demonstrated the highest collagen type I production compared to as-spun PVDF-TrFE and PCL scaffolds. Collagen type I production increased on as-spun PVDF-TrFE and PCL groups and was statistically different.

The quality of hyaline cartilage produced is assessed by noting the ratio of collagens types II to I as shown in Figure 3.4e. All three groups had significant

differences between days 14 and 28 where the ratio decreased with time. At day 14, PCL and as-spun PVDF-TrFE had the highest collagen types II/I ratio than annealed PVDF-TrFE group. Interestingly, by day 28 as-spun PVDF-TrFE continued to demonstrate significantly higher collagen types II/I ratio than PCL and annealed PVDF-TrFE groups.

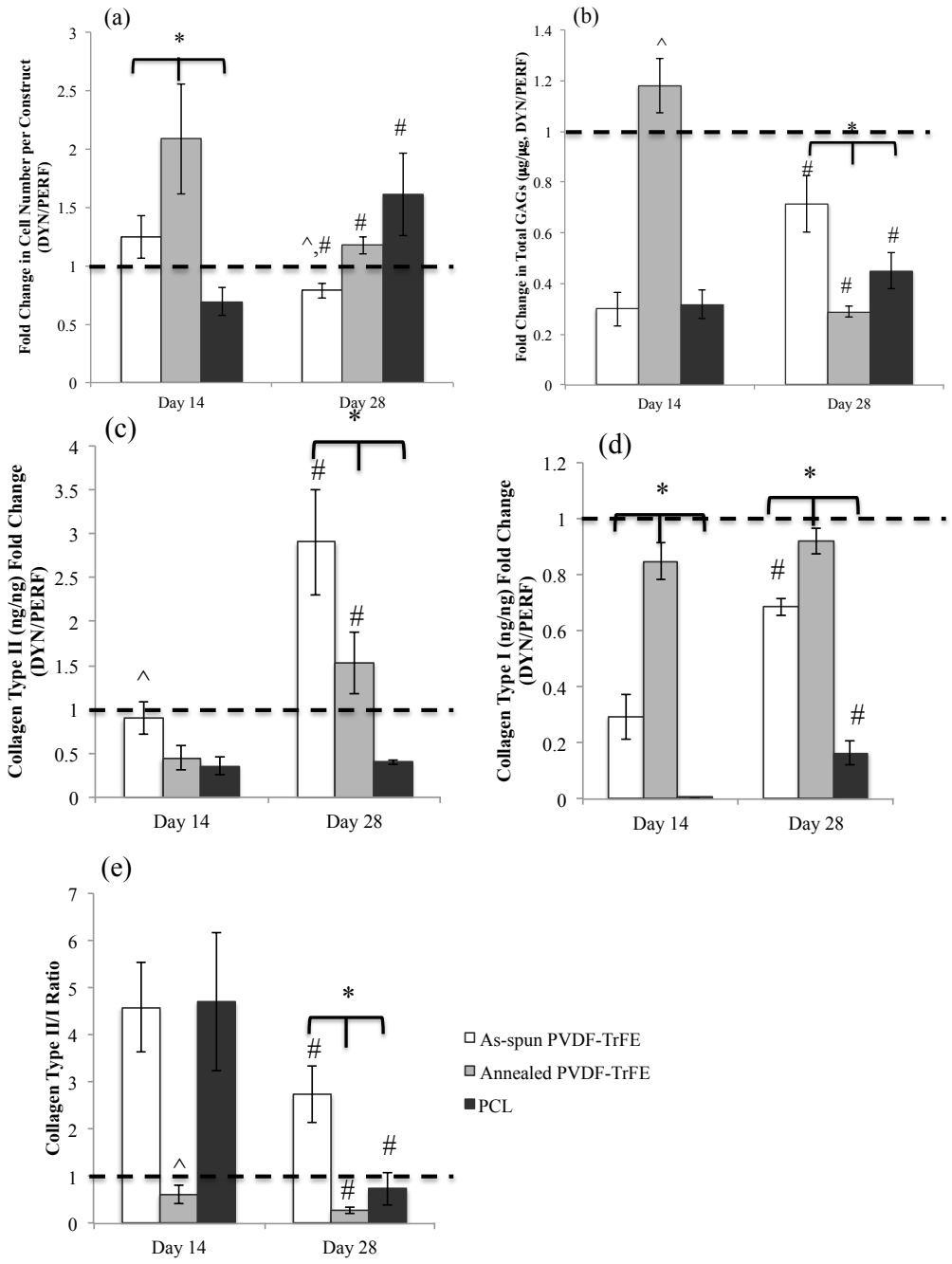

Figure 3.4 Biochemical analysis for MSCs chondrogenesis on PCL, as-spun PVDF-TrFE and annealed PVDF-TrFE scaffolds. Plots show cell number (a), total GAGs production (b), collagen type II production (c), collagen type I production (d) when normalized to perfusion only groups and collagen types II/I ratio (e) at days 14 and 28. At specific time point, significant difference between groups is noted by ^ $p<0.05$. Within a specific group, significant difference between time points is noted by # $p<0.05$. When all three groups are significantly different is noted by * $p<0.05$.

Cartilage tissue specific gene expression was evaluated to assess MSCs differentiation on all scaffolds as shown in Figure 3.5. SOX9, an early chondrogenic transcription factor, was significantly different for all three groups at day 14. The PCL group had the highest expression at both days 14 and 28 when compared to as-spun and annealed PVDF-TrFE groups. SOX9 expression on annealed PVDF-TrFE significantly decreased by day 28. Aggrecan, proteoglycan of hyaline cartilage marker, was significantly up-regulated on PCL scaffolds compared to as-spun and annealed PVDF-TrFE scaffolds at day 14. Aggrecan expression over time remained constant on all groups. At day 28, aggrecan expression was significantly different between PCL and as-spun PVDF-TrFE groups. Collagen type II expression was significantly up-regulated on annealed PVDF-TrFE group when compared to other groups. Collagen type IX, known to interact with collagen type II and found in hyaline cartilage, was significantly higher for as-spun PVDF-TrFE group at day 14 than PCL and annealed PVDF-TrFE groups. Collagen type IX expression down-regulated over time on as-spun PVDF-TrFE, but was up-regulated on annealed PVDF-TrFE constructs. There was no change in gene expression levels for PCL over time. Chondroadherin, another mature hyaline cartilage marker, expression was significantly up-regulated on annealed PVDF-TrFE group compared to PCL and as-spun PVDF-TrFE at day 14. Between time points, PCL and annealed PVDF-TrFE had significant increase in chondroadherin expression. Collagen type I expression on as-spun PVDF-TrFE constructs significantly decreased by day 28. However, collagen type I expression significantly increased on annealed PVDF-TrFE scaffolds by day 28 and remained unchanged on PCL scaffolds. Collagen type X, a

hypertrophic marker, was significantly up-regulated annealed PVDF-TrFE scaffolds by day 28.

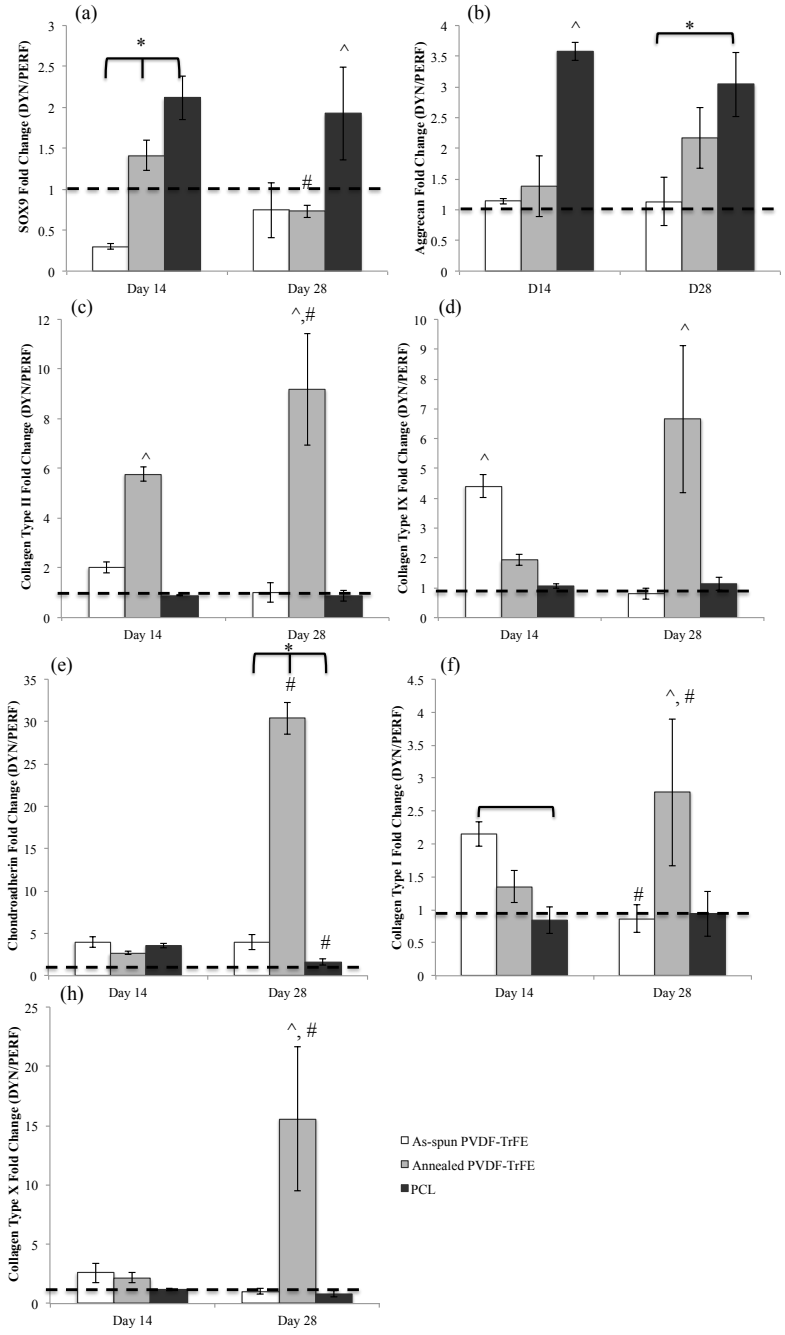

Figure 3.5 Chondrogenic gene expression for SOX9 (a), aggrecan (b), collagen type II (c), collagen type IX (d), chondroadherin (e), collagen type I (f) and collagen type X (h) for MSCs cultured on as-spun PVDF-TrFE, annealed PVDF-TrFE and PCL scaffolds at days 14 and 28. At specific time point, significant difference between groups is noted by ^ $p<0.05$. Within a specific group, significant difference between time points is noted by # $p<0.05$. When all three groups are significantly different is noted by * $p<0.05$.

Dynamic modulus of all three groups increased over time as shown in Table 3.1. PCL and annealed PVDF-TrFE groups had statistically different dynamic modulus between days 1, 14 and 28. As-spun PVDF-TrFE construct's dynamic modulus significantly increased since day 1 but remain unchanged between day 14 and 28. At day 1, all groups had statistically different dynamic modulus where annealed PVDF-TrFE demonstrated higher modulus. By day 28 PCL group had significantly higher dynamic modulus than both of the PVDF-TrFE groups.

Table 3.1 Dynamic Young's Modulus of Cartilage Tissue Constructs, which underwent dynamic compression

	As-spun PVDF-TrFE (kPa)	Annealed PVDF-TrFE (kPa)	PCL (kPa)
Day 1	$31.1 \pm 2.9^{a, \#}$	$55.2 \pm 0.73^{b,\#}$	$18.9 \pm 0.7^{b,\#}$
Day 14	77.4 ± 18.9	$102.4 \pm 1.1^{b,*}$	$97.6 \pm 1.1^{b,*}$
Day 28	$73.8 \pm 3.9^{\#}$	$82.5 \pm 0.75^{b, \#}$	$89.3 \pm 1.0^{b, \#}$

a $p<0.05$ significant difference between Day 1 and other time points of that group.
b $p<0.05$ significant difference between all time points of that group.
# $p<0.05$ significant difference between all groups at that time point.
* $p<0.05$ significant difference between annealed PVDF-TrFE and PCL at day 14.

The confocal images (Figures 3.6 – 3.8) confirmed cell attachment as evidenced by actin staining on all the scaffolds. As-spun PVDF-TrFE scaffold group showed intense staining for collagens types II & I and SOX9. Annealed PVDF-TrFE group had no detectable staining for SOX9 at days 14 and 28. Collagen type II was detectable only at day 28 and collagen type I was intensely stained on both days. On PCL scaffolds collagen type II and SOX9 was detected. Collagen type I staining was intensely stained at days 14 and 28 on PCL scaffolds, which were similar to annealed PVDF-TrFE scaffold.

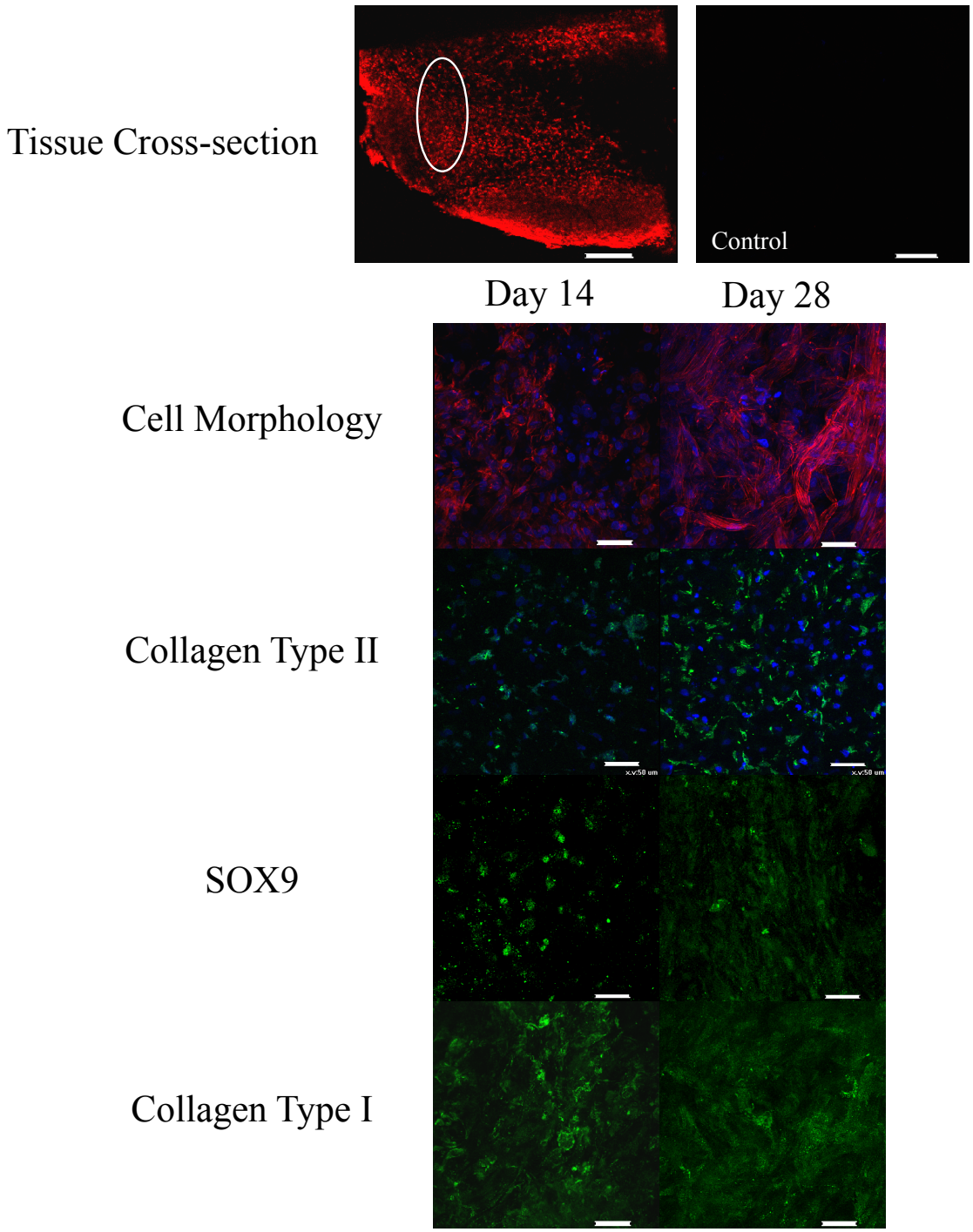

Figure 3.6 As-spun PVDF-TrFE scaffolds confocal images showing tissue cross-section (scale bar = 500 μm) and distribution of collagen type II, SOX9 and collagen type I proteins within that cross section cultured in chondrogenic media, which underwent dynamic compression at days 14 and 28. Scaffolds without cells (control) and scaffolds with cultures stained for SOX9 (green), collagen type I (green), collagen type II (green), F-actin (red) and nucleus (blue). Scale bar = 50 μm.

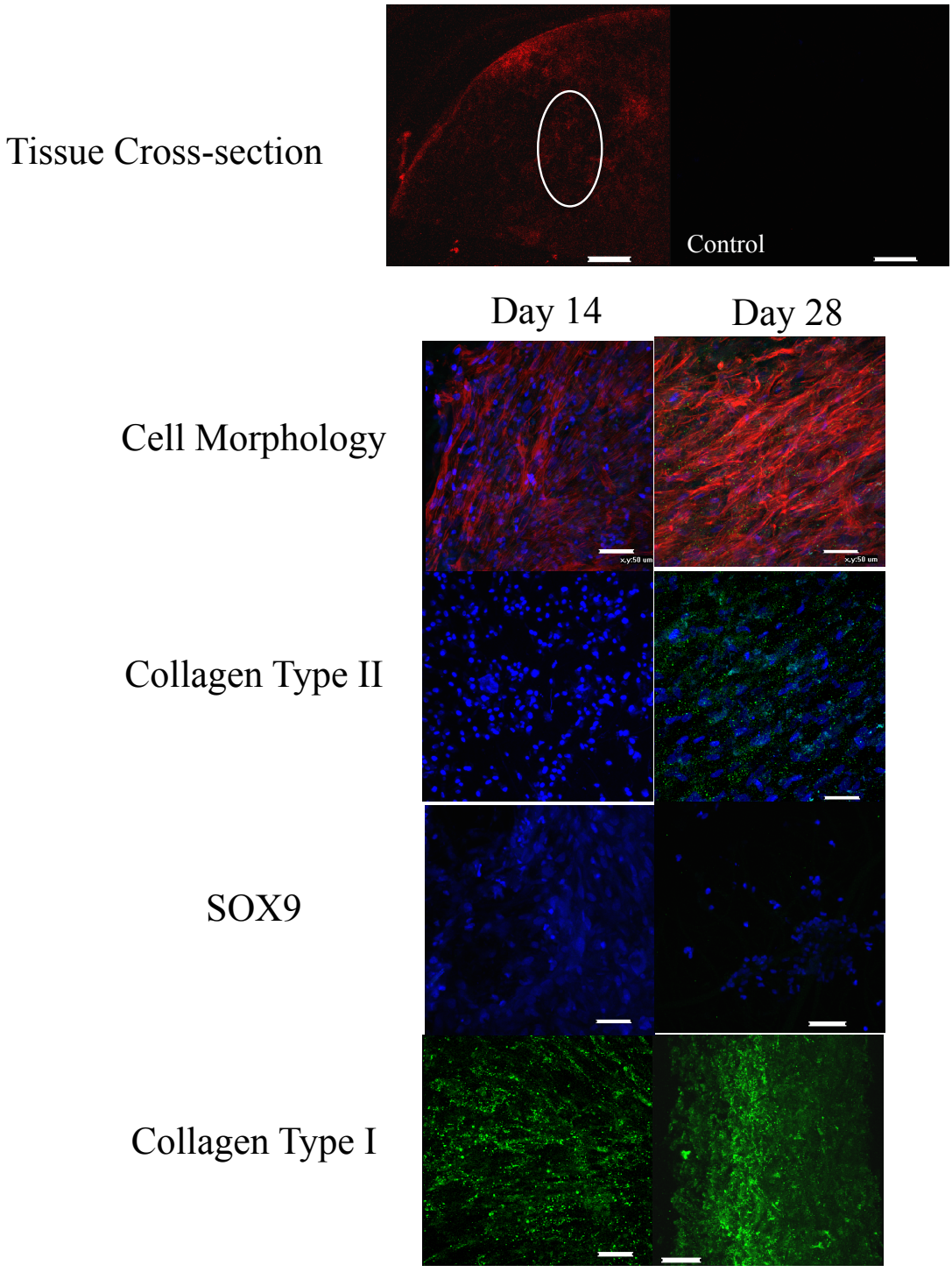

Figure 3.7 Annealed PVDF-TrFE scaffolds confocal images showing tissue cross-section (scale bar = 500 μm) and distribution of collagen type II, SOX9 and collagen type I proteins within that cross section cultured in chondrogenic media, which underwent dynamic compression at days 14 and 28. Scaffolds without cells (control) and scaffolds with cultures stained for SOX9 (green), collagen type I (green), collagen type II (green), F-actin (red) and nucleus (blue). Scale bar = 50 μm.

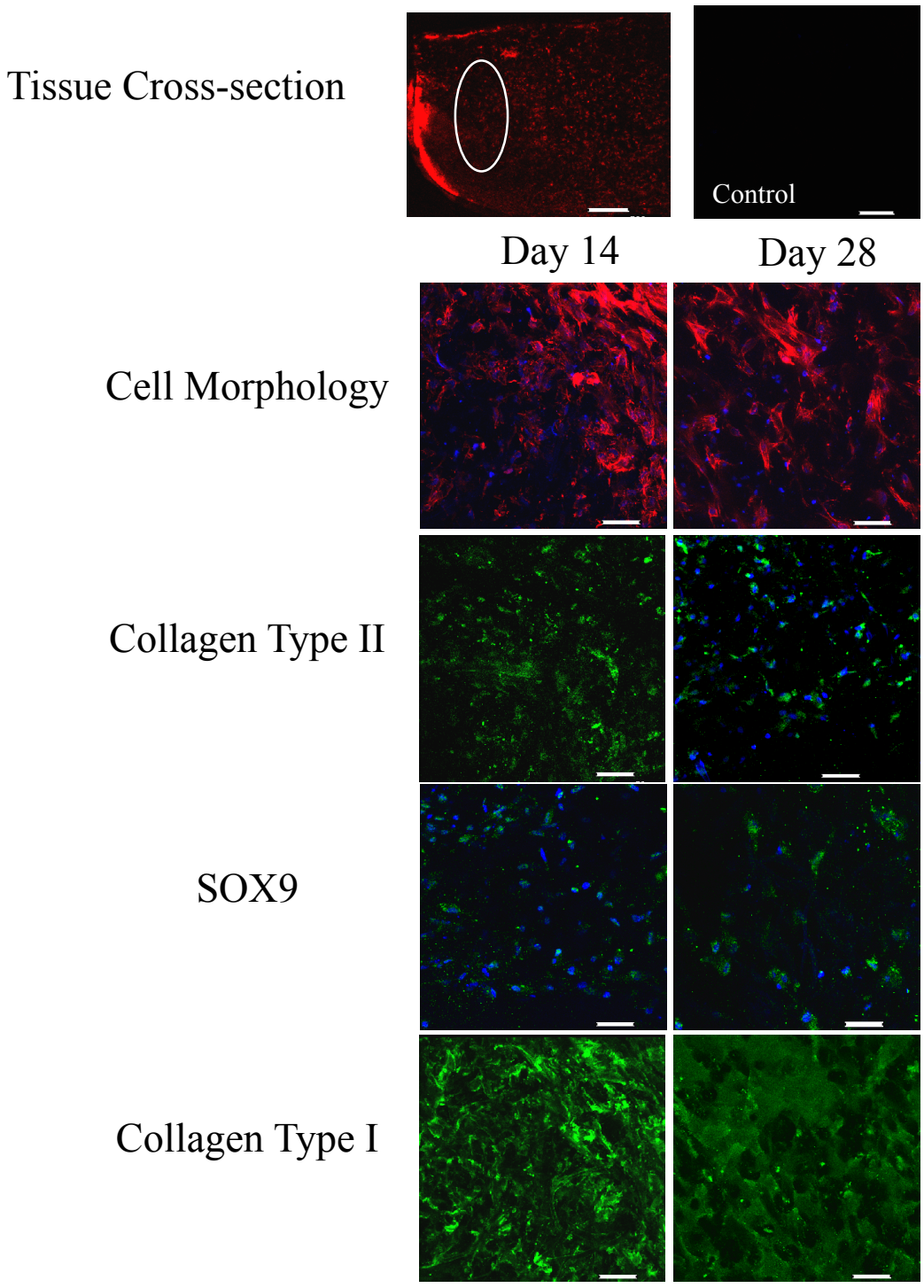

Figure 3.8 PCL scaffolds confocal images showing tissue cross-section (scale bar = 500 μm) and distribution of collagen type II, SOX9 and collagen type I proteins within that cross section cultured in chondrogenic media, which underwent dynamic compression at days 14 and 28. Scaffolds without cells (control) and scaffolds with cultures stained for SOX9 (green), collagen type I (green), collagen type II (green), F-actin (red) and nucleus (blue). Scale bar = 50 μm.

3.3.3 *In vitro* Osteogenesis

The osteogenic differentiation potential of MSCs was evaluated on the piezoelectric scaffolds, as-spun and annealed PVDF-TrFE, as well as compare to non-piezoelectric, PCL, as a control when placed in bioreactor where dynamic compression was applied with continuous perfusion and continuous perfusion only. MSCs were cultured in osteogenic induction medium over a period of 28 days. After 28 days culture, all the constructs transitioned from loose fibrous material to slightly firm, discrete mass of tissue as shown in Figure 3.9. To demonstrate the effects of dynamic compression stimulus on MSCs differentiation, all the quantitative results presented were normalized to perfusion group for each scaffold group are represented as fold change mean standard deviation. The actual values from quantitative results for chondrogenic bioreactor studies are shown in Appendix B.

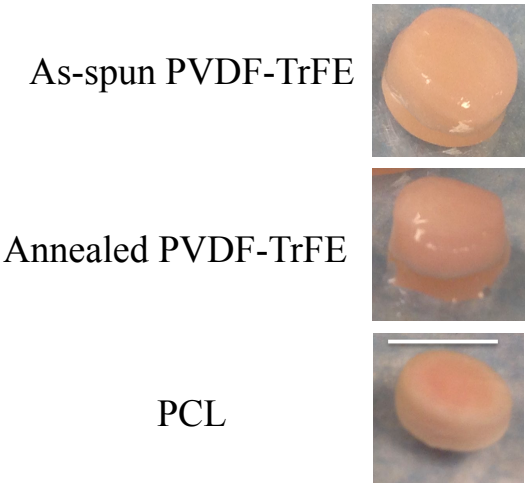

Figure 3.9 Tissue constructs in osteogenic media, which underwent dynamic compression for 28 days. Scale bar = 6 mm.

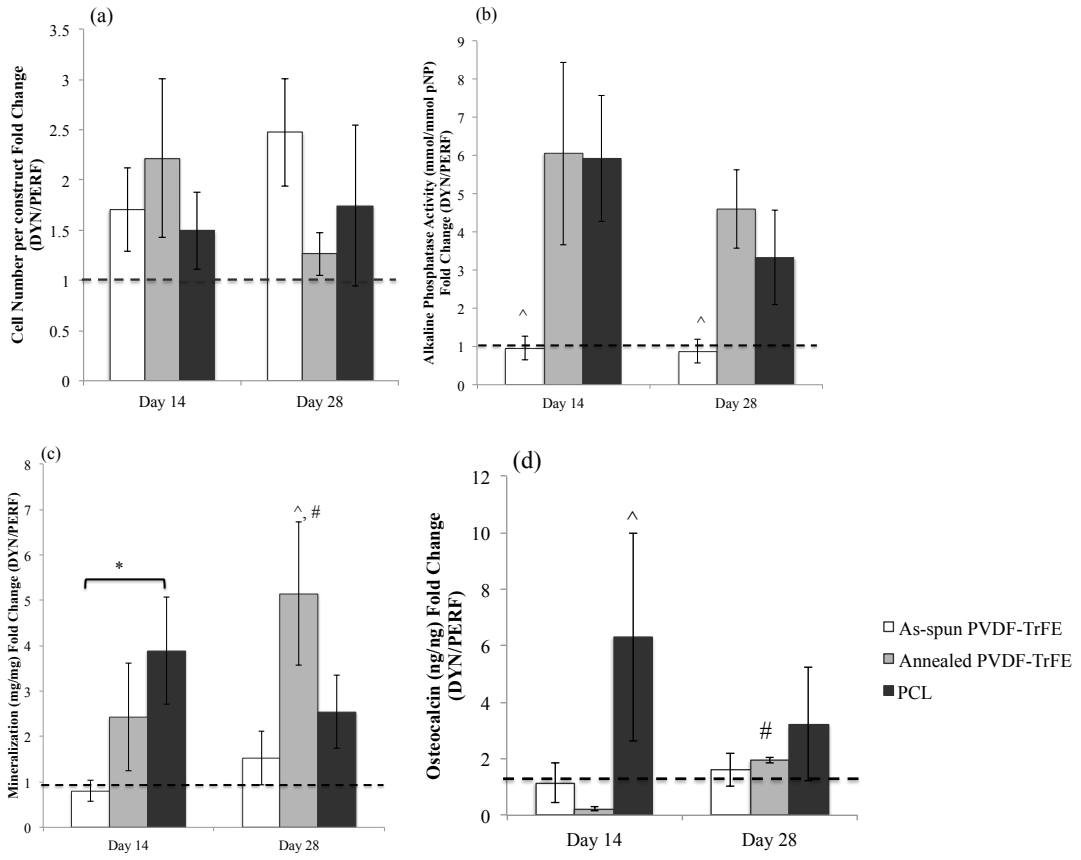

Figure 3.10 Biochemical analysis for MSCs osteogenesis on PCL, as-spun PVDF-TrFE and annealed PVDF-TrFE scaffolds. Plots show cell number (a), total alkaline phosphatase activity (b), mineralization (c) and osteocalcin (d) where dynamic group is normalized to perfusion only group at days 14 and 28. At specific time point, significant difference between groups is noted by ^ $p<0.05$. Within a specific group, significant difference between time points is noted by # $p<0.05$. When all three groups are significantly different is noted by * $p<0.05$.

The cell number in dynamic groups was higher than in perfusion only groups for all three scaffolds as shown in Figure 3.10a. There were no significant differences noted between scaffold groups and over time. To determine whether piezoelectric scaffolds enhanced osteogenesis, alkaline phosphatase (ALP), mineralization, and osteocalcin content in each group was examined and is shown in Figure 3.10b-d. ALP activity was significantly lower on as-spun PVDF-TrFE scaffolds on both days 14 and 28 compared to

annealed PVDF-TrFE and PCL groups. ALP activity on both annealed PVDF-TrFE and PCL was significantly higher by almost five-fold and two-fold at days 14 and 28, respectively, than as-spun PVDF-TrFE, and there were no statistical differences noted between annealed PVDF-TrFE and PCL.

Mineralization was quantified by assaying the calcium concentration in each group. Dynamic compression stimulus enhanced mineralization on annealed PVDF-TrFE and PCL but only slightly on as-spun PVDF-TrFE. At day 14, PCL group was significantly higher than as-spun PVDF-TrFE group. No differences were detected between annealed PVDF-TrFE group , as-spun PVDF-TrFE and PCL groups. By day 28, mineralization increased significantly on annealed PVDF-TrFE compared to other groups. Osteocalcin, a protein produced from mature bone cells, was significantly higher on PCL scaffolds at day 14 compared to both as-spun and annealed PVDF-TrFE groups. At day 28, annealed PVDF-TrFE had higher osteocalcin production but was not statistically different from other groups.

Gene expression (Figure 3.11) characteristic for bone formation and maturation was predominantly expressed for annealed PVDF-TrFE scaffold groups. ALP and RUNX2, early osteogenic markers, was significantly up regulated on annealed PVDF-TrFE group compared to as-spun PVDF-TrFE and PCL scaffold groups at day 28. Collagen type I expression was down regulated in all dynamic groups compared to perfusion groups. At day 14, collagen type I was significantly lower on annealed PVDF-TrFE scaffolds. Osteopontin, a mature bone marker, expression was highest on PCL scaffolds at day 14. However, by day 28, annealed PVDF-TrFE groups had significantly higher osteopontin expression while expression on PCL significantly decreased. There

was no change in osteopontin expression on as-spun PVDF-TrFE over time. Osteocalcin expression was significantly higher on annealed PVDF-TrFE at day 28.

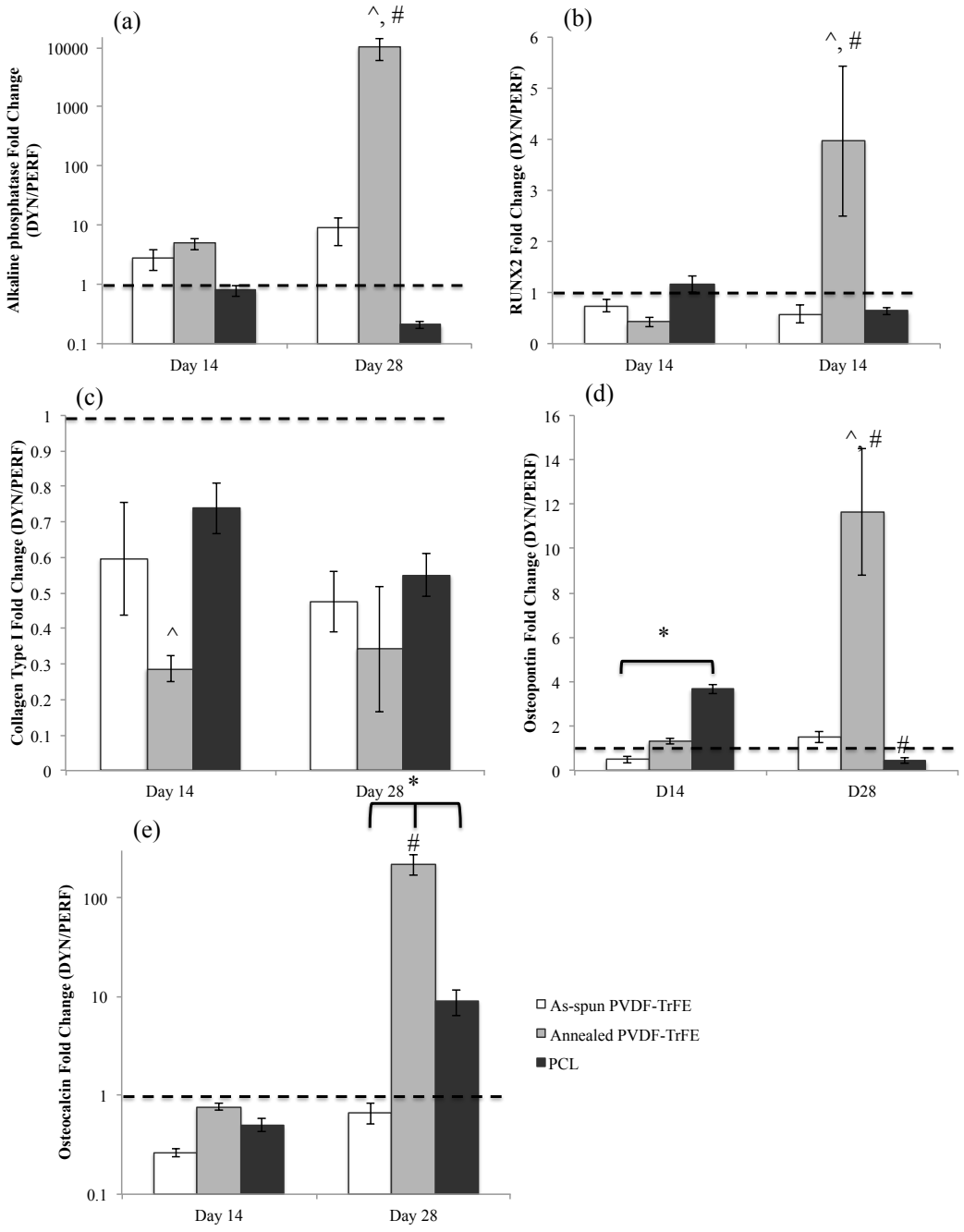

Figure 3.11 Gene expression analysis for MSCs osteogenesis on PCL, as-spun PVDF-TrFE and annealed PVDF-TrFE scaffolds. Plots show alkaline phosphatase (a), Runx2 (b), collagen type I (c), osteopontin (d) and osteocalcin (e) where dynamic group is normalized to perfusion only group at days 14 and 28. At specific time point, significant difference between groups is noted by ^ $p<0.05$. Within a specific group, significant difference between time points is noted by # $p<0.05$. When all three groups are significantly different is noted by * $p<0.05$.

Confocal images were taken at different areas of the tissue cross-section to compare collagen type I and osteocalcin detection between all groups at day 28 as shown in Figures 3.12 - 3.14. The cell attachment was confirmed by intense actin cytoskeleton staining on all scaffolds. As-spun PVDF-TrFE scaffolds stained for both collagen type I and osteocalcin in all the three areas. The center section had sparse staining for both collagen type I and osteocalcin. Annealed PVDF-TrFE scaffolds, however, demonstrated intense staining for collagen type I and osteocalcin on all the sections. PCL scaffolds had intense staining collagen type I and osteocalcin on the edge and top sections of the construct. However, in center section, there was not much detectable staining for both proteins.

Dynamic Young's modulus of all three groups increased over time as shown in Table 3.1. Annealed PVDF-TrFE groups had significantly different dynamic modulus between days 1, 14 and 28. As-spun PVDF-TrFE construct's dynamic modulus significantly increased since day 1 but remain unchanged between day 14 and 28. PCL group's dynamic modulus significantly increased by day 28. At day 14, as-spun PVDF-TrFE had the highest modulus than other groups. By day 28 as-spun PVDF-TrFE and PCL group had significantly higher dynamic modulus than annealed PVDF-TrFE groups.

Table 3.2 Dynamic Young's Modulus of Bone Tissue Constructs, which underwent Dynamic Compression

	As-spun PVDF-TrFE (kPa)	Annealed PVDF-TrFE (kPa)	PCL (kPa)
Day 1	50.7 ± 4.8^{a}	57.3 ± 6.5^{b}	76.4 ± 7.7
Day 14	$145.7 \pm 2.5^{\#}$	$130.4 \pm 5.9^{b,\#}$	$88.1 \pm 24.2^{\#}$
Day 28	156.1 ± 16.1	$109.0 \pm 11.6^{b,*}$	210 ± 61.8^{c}

a $p<0.05$ significant difference between Day 1 and other time points of that group.
b $p<0.05$ significant difference between all time points of that group.
c $p<0.05$ significant difference between day 28 and other time points of that group.
# $p<0.05$ significant difference between all groups at that time point.
* $p<0.05$ significant difference between annealed PVDF-TrFE and other groups at day 28.

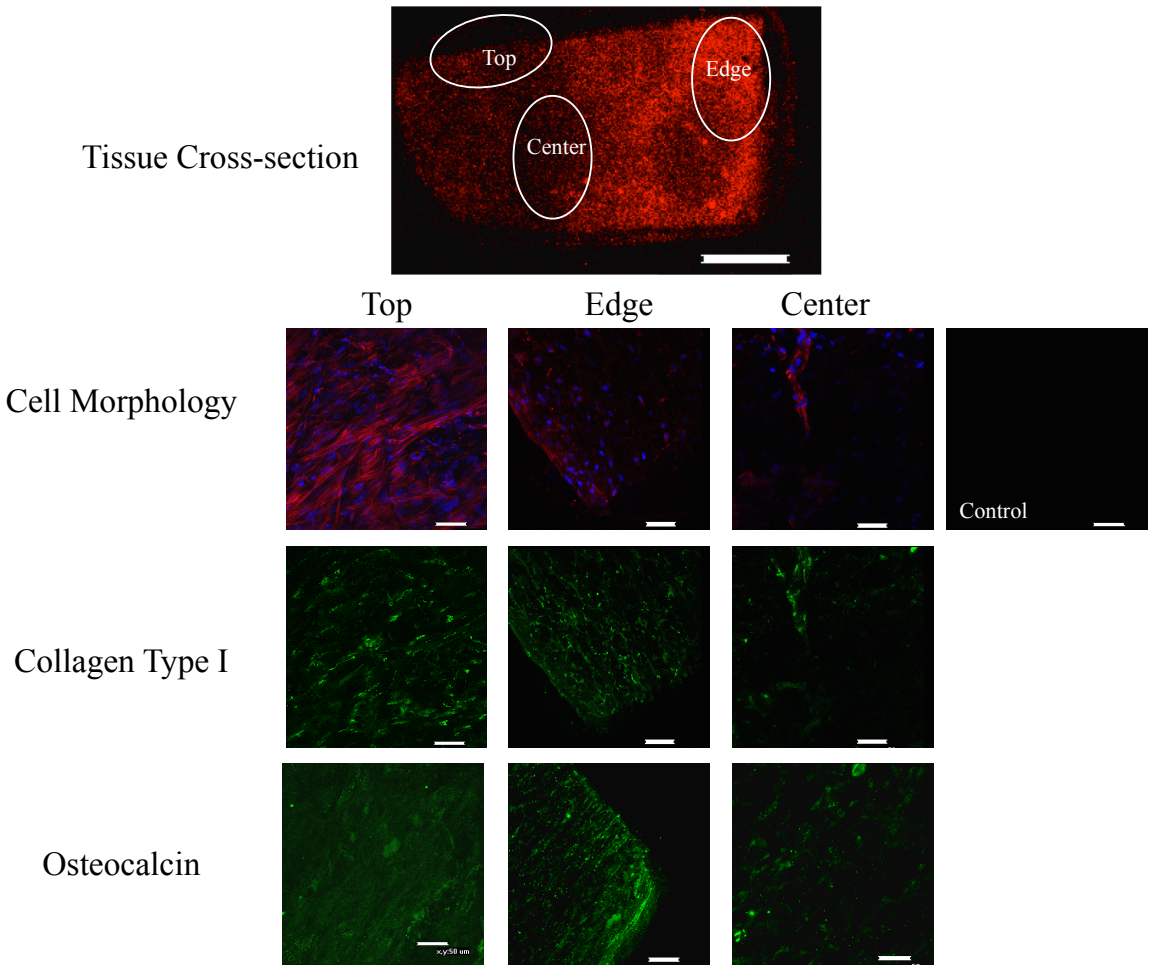

Figure 3.12 As-spun PVDF-TrFE scaffolds confocal images showing tissue cross-section (scale bar = 500 μm) and distribution of collagen type I and osteocalcin proteins within that cross section cultured in osteogenic media, which underwent dynamic compression at day 28. Scaffolds without cells (control) and scaffolds with cultures stained for collagen type I (green), osteocalcin (green), F-actin (red) and nucleus (blue). Scale bar = 50 μm.

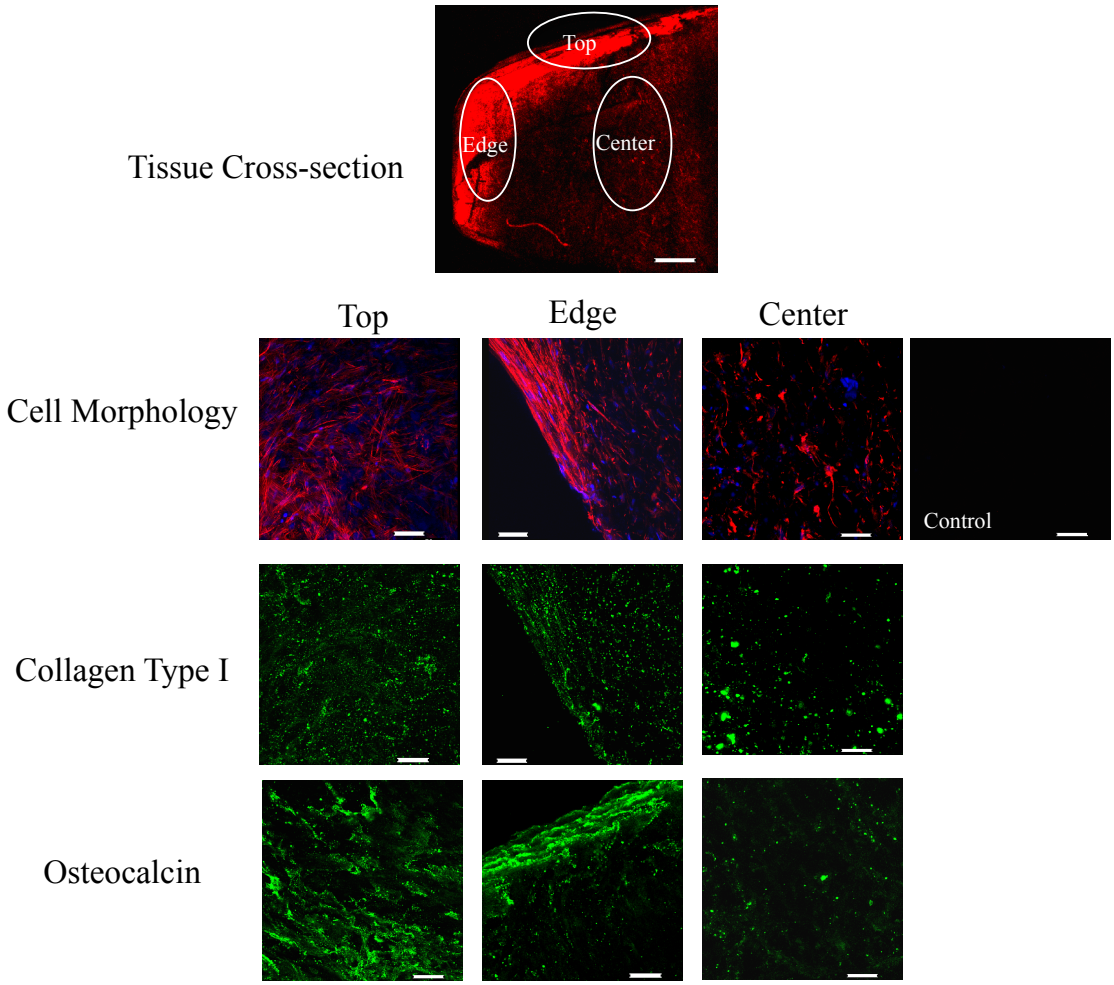

Figure 3.13 Annealed PVDF-TrFE scaffolds confocal images showing tissue cross-section (scale bar = 500 μm) and distribution of collagen type I and osteocalcin proteins within that cross section cultured in osteogenic media, which underwent dynamic compression at day 28. Scaffolds without cells (control) and scaffolds with cultures stained for collagen type I (green), osteocalcin (green), F-actin (red) and nucleus (blue). Scale bar = 50 μm.

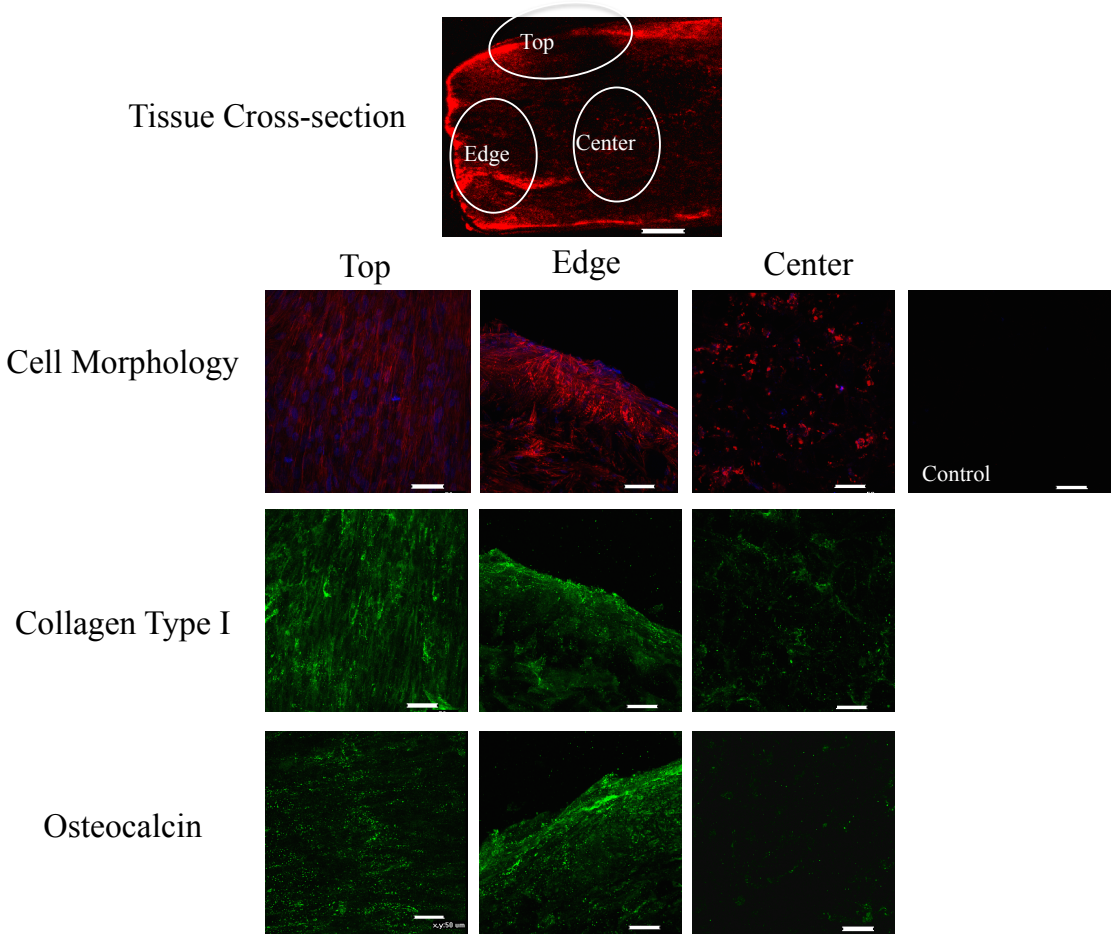

Figure 3.14 PCL scaffolds confocal images showing tissue cross-section (scale bar = 500 μm) and distribution of collagen type I and osteocalcin proteins within that cross section cultured in osteogenic media, which underwent dynamic compression at day 28. Scaffolds without cells (control) and scaffolds with cultures stained for collagen type I (green), osteocalcin (green), F-actin (red) and nucleus (blue). Scale bar = 50 μm.

3.4 Discussion

The goal of the bioreactor studies was to apply physiologically relevant mechanical stimulus to piezoelectric scaffolds and assess its effects on MSCs differentiation towards chondrogenesis and osteogenesis *in vitro*. In these studies, PCL served as a non-piezoelectric scaffold. It was hypothesized that piezoelectric scaffolds will enhance chondrogenesis and osteogenesis. The results confirmed an increased chondrogenic differentiation of MSCs on as-spun PVDF-TrFE scaffolds as determined from GAG, collagen type II and gene expression compared to PCL group. Additionally, annealed PVDF-TrFE scaffolds demonstrated an enhanced MSCs mineralization and gene expression in osteogenic cultures compared to PCL group. To our knowledge, the present work is the first report using a compression perfusion bioreactor system for stimulating piezoelectric materials.

In the chondrogenic study, as-spun PVDF-TrFE constructs favored chondrogenesis compared to other groups. This finding was supported by an increase in the collagen type II protein production that overlapped with increased collagen type IX gene expression, a characteristic of mature chondrocytes. Collagen IX is located at the surface of heterotypic collagen type II/XI fibrils and influences the assembly of these collagens. Lack of Collagen IX has been shown to result in degenerative joint lesions in mice further emphasizing its importance in stabilizing cartilage matrix [95]. During early development, MSCs condense into aggregates transforming into prechondroblasts. Within this precartilage stage, heterogeneous population of cells exists where different maturation stages of MSCs determine the production of stem cell, chondrogenic or hypertrophic markers [95]. Undifferentiated MSCs do express collagen type I and as

differentiation occurs, a switch from collagen type I to type II occurs [84]. This was observed on as-spun PVDF-TrFE constructs where collagen type I gene expression decreased over time. However, collagen type I protein was detected and was shown to increase slightly by day 28 indicating the presence of undifferentiated MSCs. Furthermore, SOX9 and collagen type II gene expression was found to be lower on as-spun PVDF-TrFE indicating a heterogeneous population of undifferentiated MSCs along with a subset population of mature chondrocyte like phenotype within the construct. The confocal images, however, does confirm the presence of SOX9 by intense staining and collagen type II protein production did increase over time in constructs. Interestingly, collagen type X expression was consistently lower on as-spun PVDF-TrFE group, indicating the maturation of MSCs into mature chondrocytes while maintaining it in pre-hypertrophic stage. Barry et al. have shown that undifferentiated MSCs do express collagen type X mRNA early in cultures that gets down regulated as MSCs differentiates into chondrocytes [84]. Annealed PVDF-TrFE scaffolds had increased cell proliferation and did not demonstrate increased production of hyaline cartilage markers. Instead, hypertrophic gene expression of collagen types X and I protein was enhanced, indicating MSCs hypertrophy and fibrocartilage tissue formation.

In bone studies, up-regulation of bone transcription factor, Runx2 in association with other bone markers ALP, osteocalcin and osteopontin provided evidence of increased MSCs differentiation towards osteogenesis especially in dynamic compression group. The application of cyclic compression with or without perfusion has been identified as a positive effect on MSCs differentiation to osteoblasts [96]. In the current study, perfusion groups did not support enhanced expression of mature bone markers as

well as dynamic compression groups. MSCs during osteogenic differentiation undergo stepwise maturational stages. At early stage, MSCs begin to express Runx2, which also controls the later expression of ALP and mature bone marker, osteopontin. In this study, cells on annealed PVDF-TrFE scaffolds did demonstrate highest Runx2 expression, which also overlapped with increased expression ALP, osteopontin, and osteocalcin gene expression. This was further supported by protein results for ALP and osteocalcin production at later time point. PCL scaffolds may have consisted of a heterogeneous population of MSCs as evidenced in large standard deviations noted in protein results but also lower gene expression of mature bone markers. The enhanced osteoblasts markers were not evident on as-spun PVDF-TrFE and PCL groups indicating that there may be an influence of inherent piezoelectric properties of annealed PVDF-TrFE in combination with dynamic stimulus influencing this maturation. From chondrogenic studies, annealed PVDF-TrFE favored hypertrophy, which may be the reason for observing enhanced MSCs osteogenesis in the bone studies.

In the present study, dynamic moduli for both piezoelectric and PCL scaffolds were lower than natural cartilage dynamic modulus [97]. These findings were similar to previously published studies using PCL [47, 98] and the most commonly used agarose gels for cartilage and bone tissue engineering [99]. Possible explanation for this difference, include the heterogeneous production of GAGs and collagen type II protein within all the constructs which was primarily restricted to the ~0.5 mm in depth from the edge of the scaffold as confirmed in confocal images. A previous study has shown an increase in mechanical properties by delaying the application of dynamic compression on cell-seeded constructs [100]. In this study, however, dynamic compression was applied

from day 1 after cell seeding. This could have resulted in reduced cell attachment over time and variable differentiation of MSCS resulting in heterogeneous production of proteins, which contribute to the mechanical properties of *in vitro* tissue.

PCL, in this study, served as a non-piezoelectric control. Though PCL has a different surface chemistry from PVDF-TrFE, PCL was chosen primarily due to its slow degradation rate and ability to fabricate fibers similar in morphology and size to PVDF-TrFE scaffolds. Additionally, its well known for its biocompatibility with many cell types and also has been FDA approved for medical applications such as wound dressings, sutures and stents. PCL chondrogenic gene expression of collagen types II and I, presented in this study, was comparable to a previously published study where similar trends of gene expression were noted on micron sized PCL fibers [101]. Multiple studies have indicated MSCs seeded on PCL scaffolds for chondrogenesis have shown to become hypertrophic phenotype in long cultures times [98, 101]. In this study, however, increased collagen type X expression was not as evident as increased collagen type I, with no change in collagen type II production. The tissue formed in PCL may be fibrocartilage as evidenced by increasing collagen type I production. On the other hand, PCL scaffolds have been shown to support MSCs osteogenesis but are often combined with hydroxyapatite and/or β-tricalcium phosphate to improve cell adhesion and mechanical strength [22, 58]. In this study, PCL did show higher osteocalcin production when compared to PVDF-TrFE scaffolds. Interestingly, mineralization and osteogenic gene expression was consistently higher on annealed PVDF-TrFE scaffolds. This may indicate an influence of localized piezoelectric activity between cell and fiber interface during its differentiation and tissue formation.

A previous study used electrospun polyurethane (PU) as a non-piezoelectric control when comparing with co-electrospun PU and PVDF for wound healing applications. The study confirmed the enhanced cell proliferation of fibroblasts and protein production due to the application of cyclic tension of PU/PVDF scaffolds [102]. PCL as the control was considered advantageous since direct comparisons can be made with a well-established polymer for bone and cartilage tissue engineering applications. The majority of the studies used PVDF films where it was feasible to fabricate piezoelectric β-phase PVDF and α-phase as a non-piezoelectric control. These studies have shown variable cell response of fibroblasts having better cell spreading on α-phase films than on β-phase films compared to non-piezoelectric films [103]. Ribeiro et al. demonstrated that poled β-phase PVDF films promoted higher osteoblast adhesion and proliferation, which was further enhanced under dynamic conditions when compared to non-poled PVDF films [104]. Osteogenic differentiation of human adipose derived stem (ASCs) cells was enhanced on pre-absorbed fibronectin on poled β-phase films compared to non-poled PVDF [105]. However, no study to date has shown MSCs differentiation on piezoelectric PVDF-TrFE scaffolds especially using a compression bioreactor for both chondrogenesis and osteogenesis making it difficult to directly compare our findings with others.

In the current study, it is evident that even with similar polymer chemistries of as-spun and annealed PVDF-TrFE, MSCs demonstrated different differentiation paths where as-spun PVDF-TrFE scaffolds enhanced chondrogenesis and annealed PVDF-TrFE scaffolds favored osteogenesis. It is speculated that this preferential differentiation choice may be attributed to the cell induced deformations of fibers in combination with cyclic

compression of the piezoelectric scaffolds, which may be producing different levels of electrical fields in culture. This reflects the complexity of this study for understanding and isolating the impact of mechanical stimulus and electrical stimulus. Electrical field measurements within bioreactor environment were not made in this study due to limitations in the experimental design. A recent study, however, has confirmed electrical signal albeit a dampened output of ~ ± 0.1 V from aligned PVDF-TrFE scaffolds at 2 Hz when placed in cell culture media [106]. The reduction of electrical signal was attributed to conductivity and ionic components of cell culture media. Annealed PVDF-TrFE may be producing higher electrical output than as-spun PVDF-TrFE to which MSCs were sensitive.

It has been well established that cells are able to respond to electrical stimulation by activation of calcium channels present within cell membranes and release of calcium from intracellular calcium repositories [107]. Extensive work by Brighton et al. have shown that electrical field causes an increase in extracellular calcium influx via voltage gated calcium channels and an increase in intracellular calcium levels can induce osteogenesis and chondrogenesis through a calcineurin/NF-AT (nuclear factor of activated T cells) signaling pathway [51, 52]. McCullen et al. have shown that ASCs exposed to alternating current electric field (AC; 1, 3 and 5 V/cm) at 1 Hz induced a dose dependent increase in calcium signaling during osteogenic differentiation. Their results showed that AC electric field of 1V/cm at 1 Hz showed a significant increase in the amount of mineralization produced relative to controls and higher electric fields [108]. Similar findings have been reported during MSCs osteogenesis where MSCS exposed to 1 V/cm at 1 Hz increased production of ALP and mineralization [109]. These studies

emphasize that varying electrical fields is directly proportional to the amount of calcium, which enter the cells through voltage gated calcium channels on its outer membrane. The cytoplasmic calcium concentrations have been shown to affect downstream signaling pathways and release of growth factors, which later impacts the differentiation of MSCs [110]. Fitzsimmons et al. showed that application of low amplitude (10^{-7} V/cm), low frequency (<100 Hz) capacitively coupled electric field led to an increase in insulin like growth factor (IGF-II) mRNA accumulation, IGF-II secretion and IGF-II receptors in an osteoblast. Other growth factors such as cyclic adenosine monophosphate (cAMP) and prostaglandin E_2 were shown to be released following electrical stimulation [51]. Similar phenomenon may be occurring in as-spun and annealed PVDF-TrFE where variable MSCs response was shown as evidenced in the current study findings.

Mechanical stimulation also impacts calcium signaling where, unlike electrical stimulus, calcium is released via intracellular repositories [51]. The main pathway involved is the activation of inositol phosphate cascade in the cell membrane. When a cell experiences mechanical strain, inositol phosphate increase resulting in release of intracellular calcium stores in endoplasmic reticulum [51]. The amount of calcium released has an effect on downstream signaling pathways. Brighton et al. have demonstrated that electrical stimulus and mechanical strain merge to the common pathway ultimately resulting in increase in activated cytoskeletal calmodulin.

In conclusion, this study has demonstrated that piezoelectric scaffolds can enhance cartilage and bone tissue formation using a compression bioreactor system. Further studies are needed for making electrical measurements within the bioreactor

setting in order to understand the induced electric field from piezoelectric scaffold and its effects on MSCs differentiation.

CHAPTER 4

DISCUSSION

Piezoelectric, three-dimensional, fibrous PVDF-TrFE scaffolds are intriguing for osteochondral tissue engineering applications due its inherent ability to produce electrical fields when subjected to cyclic compression. Endogenous electrical fields existence has been well acknowledged during embryonic development, wound healing and limb regeneration. During wound healing, for instance, steady electrical fields ranging between 1 and 2 V/cm have been estimated at the surface of wounds that exists locally for days after the injury [1]. Illingworth et al. have also reported the measurements of electrical currents of 30 A/cm^2 during the regeneration process of amputated fingertips in children, which were comparable to limbs regeneration in salamander [2]. Streaming potentials and piezoelectricity of collagen molecules has been shown to contribute to electrical behavior of bone [1, 3]. Similarly, chondrocytes within cartilage have been shown to respond to multiple biophysical cues such as mechanical signal from joint loading and streaming potentials caused by the flow of interstitial fluid over the negatively charged GAGs in its extracellular matrix [4]. Therefore, the application of piezoelectric PVDF-TrFE scaffolds provides a unique method for investigating mechanisms involved in MSCs differentiation to electrical fields generated when dynamically compressed within a bioreactor system for osteochondral tissue repair.

The results of this study demonstrated the piezoelectric properties of PVDF-TrFE scaffolds. Annealing PVDF-TrFE increased the piezoelectric β-phase in scaffolds and also impacted the electrical output when subjected to compressive deformations. Additionally, chondrogenic differentiation of MSCs was promoted on as-spun PVDF-

TrFE scaffolds and osteogenesis was promoted on annealed PVDF-TrFE scaffolds when stimulated in compression bioreactor compared to PCL control. The differences in electrical output from as-spun and annealed PVDF-TrFE scaffolds and combined with dynamic compression could be driving MSCs differentiation to either chondrogenic or osteogenic lineages. This is the first time to our knowledge, that fibrous, PVDF-TrFE scaffolds have been investigated for bone and cartilage tissue engineering applications.

Annealing is commonly used with PVDF and PVDF-TrFE films to enhance degree of crystallinity, which directly influences the electrical behavior of PVDF-TrFE. Previous work with PVDF-TrFE films has suggested that choosing annealing temperature above T_c but below T_m increases the grain size and crystallinity of orientation of β-phase while polymer chains align parallel to the film substrate with polarization dipole moment perpendicular to the substrate [5, 6]. In this study, the annealing temperature (135^{o}C) was between Curie (T_c = 113^{o}C) and melting temperatures (T_m = 147.4^{o}C) of electrospun as-spun PVDF-TrFE scaffolds, which resulted in increased crystallinity and β-phase fraction in annealed electrospun PVDF-TrFE scaffolds. More importantly, annealed PVDF-TrFE scaffolds demonstrated an increase in voltage output from applying physiologically relevant compression deformation compared to as-spun PVDF-TrFE. Electric field generated by piezoelectric scaffolds was approximated from force sensors results where as-spun PVDF-TrFE had ~112.5 mV/cm and annealed PVDF-TrFE generated ~ 5.8 V/cm electric fields when subjected to 10% strain at 1 Hz in dry conditions. PCL scaffolds did not generate voltage output under similar dynamic deformations. The forces sensor findings from this study are comparable with a previous study, where pressure sensor fabricated by electrospun, randomly oriented PVDF-TrFE fibers demonstrated output

voltage of about 400 mV when subjected to 0.2 MPa compressive stress at 5.3Hz [7]. Nevertheless, aligned electrospun fibers can result in higher voltage outputs, which may be due to the arrangement of fibers. Persano et al. fabricated pressure sensor from aligned PVDF-TrFE fibers and demonstrated output ranging from 0.79 – 1.3 V under 0.1-1 Pa at 1 and 2 Hz [8]. Electrical properties of PVDF-TrFE have been shown to depend on PVDF to TrFE ratio, solvent choice, polymer concentration and orientation of electrospun PVDF-TrFE fibers. These parameters affect the morphology, fiber diameters and affect the dipole moment orientation and size of the β-phase crystal within these fibers.

Overall, the chondrogenic bioreactor studies reinforced the importance of dynamic compression for MSCs differentiation towards chondrogenesis by increasing mature hyaline cartilage marker, collagen type II production especially on piezoelectric scaffolds. Of the piezoelectric groups compared, as-spun PVDF-TrFE enhanced chondrogenesis of MSCs as demonstrated by an increased production of collagen type II that overlapped with increased collagen type IX gene expression and demonstrated the highest collagen type II/I ratio later in culture. Previous studies have applied electrical stimulus using direct current or capacitively coupled modes to cultures of MSCs and chondrocytes seeded on tissue culture plates or suspended in agarose constructs. Nogomi et al. applied 5 μA direct current stimulation to differentiate muscle derived MSCs into chondrocytes instead it was demonstrated that differentiated chondrocytes had enhanced proliferation and cartilage formation at the cathode region with no effect on MSCs [9]. Brighton et al. demonstrated that electrical stimulus to bovine articular chondrocytes up-regulated gene expression of aggrecan and collagen type II by 3-4 fold [10]. Additionally,

chondrocytes seeded agarose gel samples were stimulated by the application of sinusoidal current density, which enhanced chondrocyte proliferation and collagen and GAGs production [11]. In this study, only annealed PVDF-TrFE scaffolds demonstrated increased cell proliferation but the expression of hyaline cartilage markers was not enhanced compared to as-spun PVDF-TrFE. In the electrical stimulus studies, the duration of the electrical stimulus varied from 30 minutes to 7 days in culture and was predominantly performed with chondrocytes therefore limiting the comparison with the current study. To date in cartilage tissue engineering, there has been some success in combining agarose-based scaffolds with chondrocytes to engineer cartilage with properties approximating those of native tissue. For instance, Hu et al. demonstrated self-assembled cartilage tissue formation when chondrocytes were seeded on agarose substratum, and this tissue-engineered cartilage contained two thirds more GAG/dry weight than native cartilage. Collagen/dry weight was one-third the level of native tissue and the mechanical stiffness reached more than one third that of native tissue [12]. Nevertheless, replicating native tissue properties remains a challenge.

In all the scaffolds groups, collagen types X and I was detected through gene expression. These results indicate the presence of heterogeneous populations within the constructs, which is a well-acknowledged limitation of MSCs as a cell source for cartilage repair. Murdoch et al. analyzed cartilage tissue formation from individual clonal populations of MSCs, and demonstrated variable differentiation capacity of individual clones [13]. Pelttari et al. compared cartilage formation potential for human MSCs and chondrocytes cultured as pellets and the study demonstrated that in MSCs pellets, premature induction of collagen types I and X genes within 1-2 days, which occurred

well before collagen type II was expressed [14]. Following this, broad range of hyaline cartilage markers together with markers for terminal differentiation and osteoblast was detected. In contrast, hypertrophy and terminal differentiation related genes were not detectable in chondrocyte pellets when subjected to similar chondrogenic culture conditions as MSCs [14]. This was indicative of MSCs undergoing endochondral ossification path with ultimately forming bone like tissue. Interestingly, in our study, as-spun PVDF-TrFE scaffolds showed down regulation of collagen type I and maintained lower expression of collagen type X compared to annealed PVDF-TrFE, suggesting that material properties combined with dynamic compression maybe influencing MSCs phenotype and reduced expression of hypertrophic marker. This was a promising finding since to date curbing MSCs differentiation towards hypertrophy has not been well controlled in scaffolds based cartilage repair *in vitro* cultures.

Application of dynamic compression enhanced MSCs osteogenic differentiation on piezoelectric annealed PVDF-TrFE scaffolds compared to PCL group and annealed PVDF-TrFE perfusion group. Our findings were comparable to Jagodzinski et al. study where MSCs seeded on demineralized bovine bone scaffolds enhanced mature bone marker, osteocalcin, production when subjected to 10% compressive strain with perfusion for three weeks when compared to perfusion only groups [15]. Piezoelectric films of PVDF and PVDF-TrFE films have been investigated for bone tissue engineering. Dynamically stimulated piezoelectric β-PVDF films demonstrated increased proliferation and differentiation of human adipose stem cells compared to static conditions and non-piezoelectric PVDF films when cultured under similar conditions of piezoelectric β-PVDF, indicating piezoelectric scaffolds can provide necessary electrical cues for bone

tissue engineering [16]. An advantage of using films is the feasibility of fabricating a non-piezoelectric control with same chemistry as the piezoelectric group. However, films lack the necessary 3D structure to facilitate tissue ingrowth and formation of organized tissue further limiting its clinical relevancy. For instance, PVDF-TrFE/barium titanate composite was shown to support in vivo bone formation and expression marker of mature bone when implanted in rat calvarial bone defects, but there was no tissue in growth within the composite and layer of fibrous tissue was formed at the composite interface [17]. Long-term use of such films for tissue repair is questionable. Nevertheless, MSCs were shown to respond favorably to annealed PVDF-TrFE scaffolds and demonstrating its osteoinductive properties for its osteogenic differentiation.

The current study did not measure electrical potentials within bioreactor cultures during tissue formation. However, we have been able to make some electrical measurements from annealed PVDF-TrFE (0.8 mV) scaffolds subjected to 40% strain at 1 Hz when placed in the phosphate buffered saline (PBS) bath. A recent study, has also confirmed the electrical signal albeit a dampened output of ~ ± 0.1 V from aligned PVDF-TrFE scaffolds at 2 Hz when placed in cell culture media [18]. We hypothesize that as-spun PVDF-TrFE will have lower electrical output due to aforementioned material properties and has lower approximated electric field of 112.5 mV/cm when compared to annealed PVDF-TrFE, which has an approximated electric field of 5.8 V. The differences in electrical output from as-spun and annealed PVDF-TrFE scaffolds combined with dynamic compression could be the driving factors for MSCs differentiation to either chondrogenic or osteogenic lineages on both the piezoelectric scaffolds. We are currently in process of optimizing the method for obtaining voltage

outputs within the bioreactor system, and this method will enable making measurements from tissue construct during culture period.

Previous electrical stimulus studies have repeatedly shown that MSCs respond to electrical stimulation by activation of calcium channels present within cell membranes [19]. Extensive studies by Cho et al. have established that varying electrical fields is directly proportional to the amount of calcium, which enter the cells through voltage gated calcium channels on its outer membrane [20]. The cytoplasmic calcium concentrations have been shown to affect downstream signaling pathways and release of growth factors, which later impacts the differentiation of MSCs towards chondrogenesis and osteogenesis [20-22]. As a future work, it will be important to investigate the calcium level changes within MSCs when as-spun and annealed PVDF-TrFE scaffolds are subjected to dynamic compression. This finding will be essential to explain the signaling pathways involved and allow us to compare to previously reported electrical stimulus studies.

In osteochondral tissue engineering, it has been suggested that scaffolds should be porous with at least 300 μm pore size and mechanically similar to native tissue in order to support tissue in growth and sustain joint loading [23]. Electrospun scaffolds offer large surface area relative to volume and nano to micron range fibers, which has been shown to be beneficial for MSCs based cartilage bone growth *in vitro* [24]. In our study, PVDF-TrFE scaffolds had an average inter-fiber spacing <200 μm. The confocal images confirmed cell infiltration, but majority of the extracellular matrix production was restricted to the periphery around the scaffold. This could be due to limited oxygen and nutrient transport throughout the scaffolds. The bioreactor also uses perfusion as a

mechanism for the transport of media throughout the scaffold in an unconfined space. So the fluid may not have entered the scaffold and may have flowed around the scaffold as the tissue developed, which could have limited the efficient transport of nutrients and oxygen in the center of the scaffold.

One of the limitations in our study was that the mechanical properties of all the three scaffold groups were found to be much lower when compared to native cartilage and bone. In our study, cell density was 1 million cells/mL, which is lower than the previously reported studies where cell density varied between 10 – 60 million cells/mL [25-27]. This could have contributed to the lower mechanical properties observed as compared to previous studies. For instance, Mauck et al. demonstrated that higher seeding cell density (60 million cells/mL) in agarose hydrogels showed >2 fold increase in mechanical properties relative to free swelling controls. In bone tissue engineering, scaffolds aim to mimic bone tissue properties where bone is a composite consisting of hydroxyapatite and collagen fibers, and for this reason, polymers are combined with ceramics to enhance mechanical properties, and have demonstrated success in bone regeneration. For instance, PCL/tricalcium phosphate (TCP) based composite demonstrated 3 times higher compressive modulus than PCL group, and human alveolar osteoblasts proliferation and expression of bone markers was enhanced [28]. Polymer based scaffolds such as clinically available PCL (Osteopore) constructs are extensively used for non-load bearing bone repair such as craniofacial applications [29]. However, the objective of our study was to evaluate the influence of piezoelectric materials on MSCs differentiation, and the addition of ceramics will further confound the effects of

scaffolds. Nevertheless, additions of ceramics to piezoelectric scaffolds may be a useful strategy when developing scaffolds for preclinical studies.

Another limitation in our study is the lack of a non-piezoelectric scaffold with same chemistry as PVDF-TrFE scaffolds. We had attempted to prepare non-piezoelectric scaffold by coating electrospun PCL fibers with PVDF solution. However, PCL scaffolds became stiff with film like morphology; thus making it unusable for bioreactor studies. Annealing PVDF-TrFE films above T_m has been shown to retain its piezoelectric activity [6]. Therefore, limiting our attempts to prepare a non-piezoelectric scaffold with PVDF-TrFE. Though PCL is not similar in chemistry, it is a non-piezoelectric polymer and is routinely used in tissue engineering. Therefore, by comparing our piezoelectric scaffolds to PCL, we were able to evaluate the potential of PVDF-TrFE scaffolds for osteochondral tissue engineering applications. Using PCL as a control, our studies indicate that piezoelectric scaffolds do enhance MSCs differentiation towards chondrogenesis and osteogenesis.

In the current study, only two donors were compared for biological studies, but in future studies, it may be important to investigate multiple donors of MSCs to account for donor variability and age group differences for clinical applications. Additionally, higher cell seeding density should be investigated to be able to compare to existing strategies in cartilage and bone tissue engineering. Though MSCs have limitations, a recent study demonstrated MSCs capability to form mechanically functional human cartilage while interfaced with demineralized bone scaffold *in vitro* by mimicking early developmental condensation process of MSCs. Engineered tissue resulted in anatomically shaped cartilage with physiologically similar zonal distribution of cells [30]. Using similar

approach, optimal cell seeding density of MSCs can be determined for achieving tissue engineered cartilage on as-spun PVDF-TrFE, which can later be interfaced with tissue engineered bone formed on annealed PVDF-TrFE scaffolds to form an engineered osteochondral tissue.

Chondrocytes as a cell source should also be investigated using PVDF-TrFE scaffolds for cartilage repair. Chondrocytes have been well established as the preferred cell source for cartilage tissue repair since they are primary cartilage cells, which generate and maintain cartilage's extracellular matrix. Multiple studies have demonstrated chondrocytes ability to express hyaline cartilage markers, not undergo hypertrophy and achieve mechanical properties similar to that of native cartilage using scaffold based cartilage tissue engineering [12, 27]. However, chondrocytes have a tendency to dedifferentiate and lose its phenotype after passaging through *in vitro* cultures thus forming undesired fibrocartilage. It will be interesting to see if the inherent electrical properties of piezoelectric scaffolds can provide additional cues and retain chondrocytes mature phenotype and stimulate functional hyaline cartilage tissue regeneration. The findings from these studies will be essential before preclinical studies.

Additionally, optimizing bioreactor conditions for cell culture media flow rate, applied compressive strain and its frequency along with growth factors administration will also need to be investigated. The compressive strain and frequency does impact MSCs differentiation towards bone or cartilage and influences gene expression profile and protein production. In our study, we chose the bioreactor based on well-published protocols, however, lowering strain and/or frequency can impact MSCs differentiation behavior. Additionally, cartilage tissue engineering studies have suggested that TGF-β3

should be discontinued later in culture, which may reduce unwanted molecules production such as collagen types I and X in chondrogenesis [31]. Similarly, delayed application of compressive strain, for instance, after 14 days of culture, has also shown to enhance MSCs chondrogenesis and tissue construct properties [27]. On the other hand, bone tissue engineering studies have emphasized the importance of media flow rate that can significantly influence cell morphology, proliferation and differentiation. For instance, Porter et al. have suggested optimizing flow rate between 0.1 – 0.2 mL/min in order to achieve enhanced bone formation *in vitro* [32]. Therefore, optimizing these bioreactor conditions is important and may result in desired hyaline cartilage and bone tissues formation *in vitro*.

Our study has demonstrated MSCs chondrogenesis on as-spun PVDF-TrFE scaffolds and osteogenesis on annealed PVDF-TrFE scaffolds compared to PCL scaffolds. Additionally, our studies revealed that annealing enhanced the presence of piezoelectric β-phase within scaffolds and had higher voltage output under physiologically relevant deformations when compared to as-spun PVDF-TrFE scaffolds. PCL scaffolds did not generate electrical output when subjected to similar deformations. MSCs differentiation behavior may have been impacted by the differences in voltage output from the as-spun and annealed PVDF-TrFE generated during dynamic compression, indicating a role of electrical stimulus for MSCs differentiation. There may be an optimal electromechanical stimulus needed for achieving native hyaline cartilage and bone tissue formation *in vitro*. Therefore, piezoelectric PVDF-TrFE is an attractive polymer due to its inherent electrical properties, which can potentially mimic the native bone and cartilage electrical behavior. These studies demonstrated the feasibility of

PVDF-TrFE as a scaffold for osteochondral tissue engineering. Further studies should focus on understanding the mechanism by which voltage output from the scaffold affects MSCs differentiation and ultimately tissue formation.

APPENDIX A

CHONDROGENESIS STUDIES RESULTS

The results shown in this appendix are the actual values from quantitative proteins assay and gene expression for MSCs cultured on as-spun PVDF-TrFE, annealed PVDF-TrFE and PCL scaffolds, which underwent perfusion and dynamic compression conditions in chondrogenic medium in bioreactor system. For statistical analysis, perfusion groups of all scaffolds were compared at all time points. Similarly, dynamic scaffolds groups were compared at all time points. SPSS 20.0 software (SPSS Inc., IL, USA) was used for statistical analysis of all quantitative data. Results are expressed as mean ± standard deviation. The results were initially tested for normality (Shapiro Wilk test) and Levene's equal variance test. Two-way Analysis of Variance (ANOVA) and the post hoc multiple comparison using Tukey's tests were applied. Probability (p) values < 0.05 were considered statistically significant.

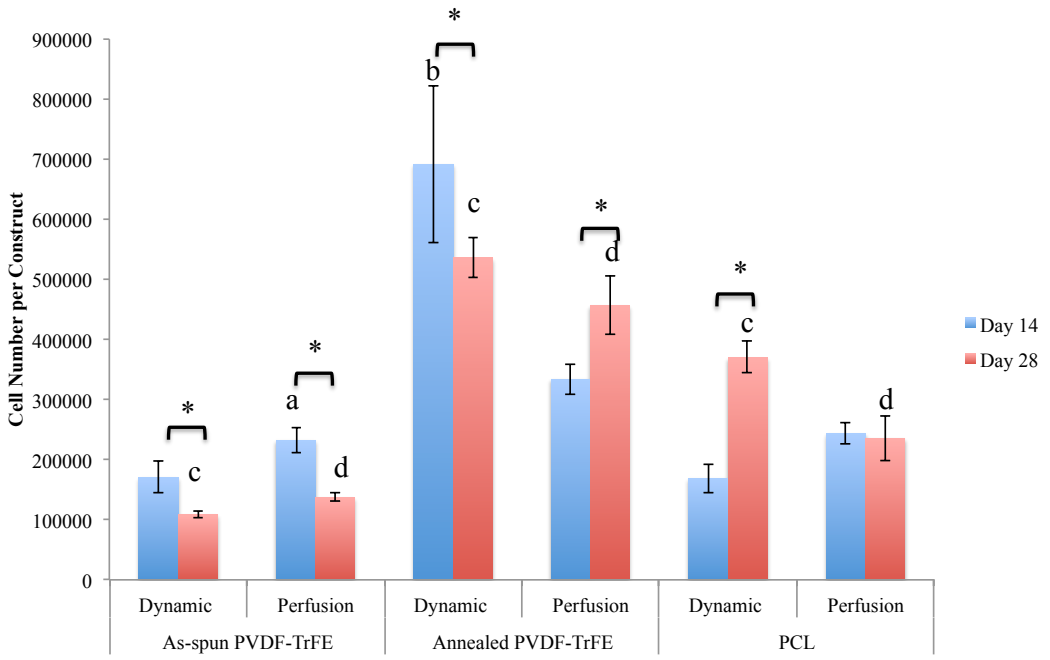

Figure A.1 Cell number on scaffolds of as-spun PVDF-TrFE, annealed PVDF-TrFE and PCL in chondrogenic cultures, which underwent dynamic compression and perfusion only in bioreactor conditions at days 12 and 28. *$p<0.05$ significant difference between day 14 and 28. a $p<0.05$ significant difference between as-spun PVDF-TrFE and annealed PVDF-TrFE in perfusion only at day 14. b $p<0.05$ significant difference between annealed dynamic and other dynamic groups at day 14. c $p<0.05$ significant difference between all dynamic groups at day 28 . d $p<0.05$ significant difference between all perfusion groups at day 28.

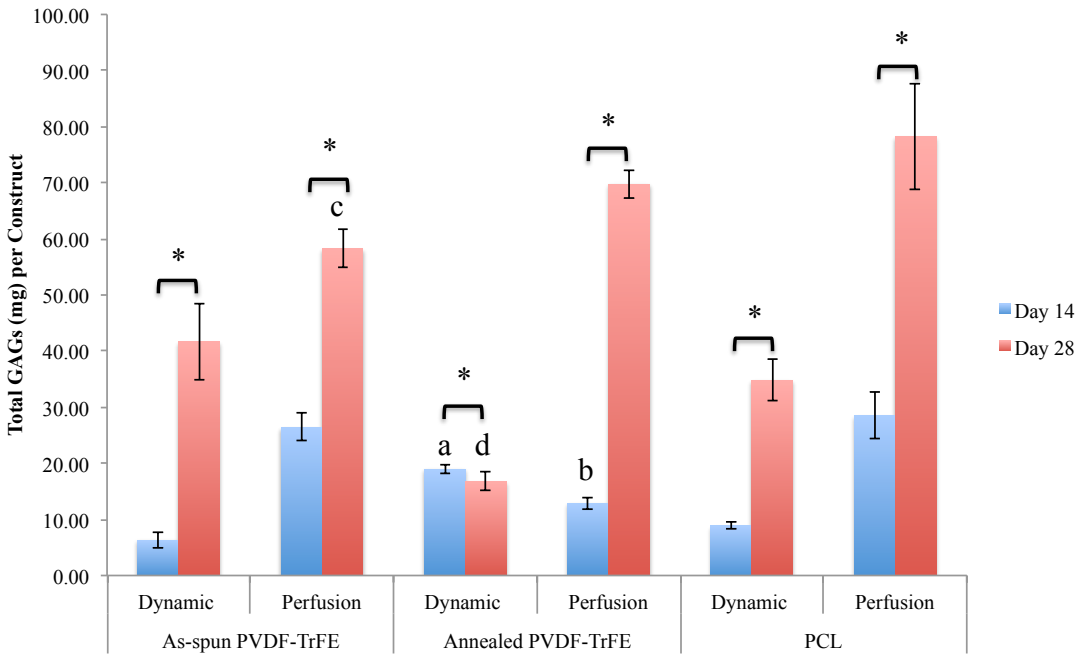

Figure A.2 Glycosaminoglycans (GAGs) production on scaffolds of as-spun PVDF-TrFE, annealed PVDF-TrFE and PCL in chondrogenic cultures, which underwent dynamic compression and perfusion only in bioreactor conditions at days 12 and 28. *$p<0.05$ significant difference between day 14 and 28. a $p<0.05$ significant difference between as-spun PVDF-TrFE dynamic and other dynamic groups at day 14. b $p<0.05$ significant difference between annealed PVDF-TrFE perfusion and other perfusion groups at day 14. c $p<0.05$ significant difference between as-spun perfusion and other perfusion groups at day 28. d $p<0.05$ significant difference between annealed PVDF-TrFE dynamic and other dynamic groups at day 28.

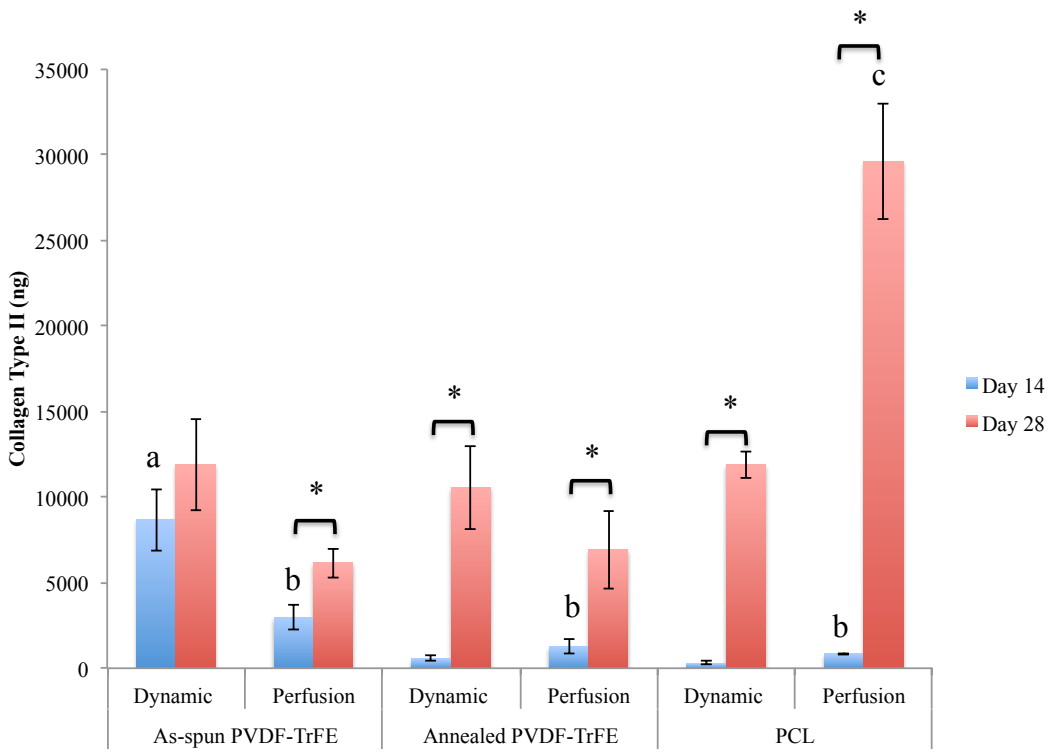

Figure A.3 Collagen type II production on scaffolds of as-spun PVDF-TrFE, annealed PVDF-TrFE and PCL in chondrogenic cultures, which underwent dynamic compression and perfusion only in bioreactor conditions at days 12 and 28. *$p<0.05$ significant difference between day 14 and 28. a $p<0.05$ significant difference between as-spun PVDF-TrFE dynamic and other dynamic groups at day 14. b $p<0.05$ significant difference between all perfusion groups at day 14. c $p<0.05$ significant difference between PCL perfusion and other perfusion groups at day 28.

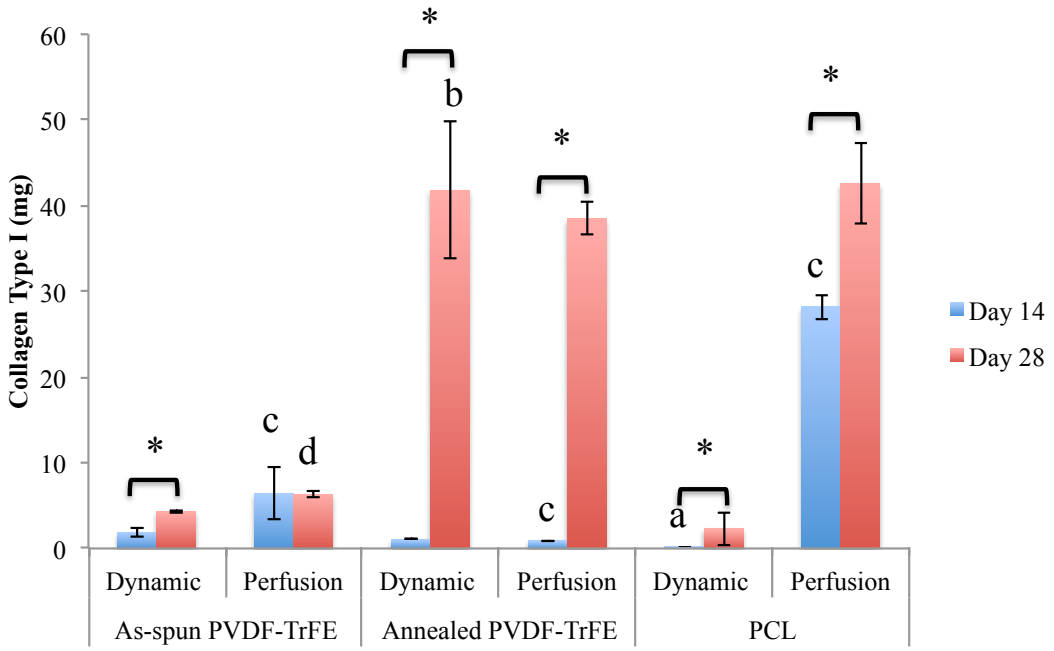

Figure A.4 Collagen type I production on scaffolds of as-spun PVDF-TrFE, annealed PVDF-TrFE and PCL in chondrogenic cultures, which underwent dynamic compression and perfusion only in bioreactor conditions at days 12 and 28. *$p<0.05$ significant difference between day 14 and 28. a $p<0.05$ significant difference between PCL dynamic and other dynamic groups at day 14. b $p<0.05$ significant difference between annealed PVDF-TrFE and other dynamic groups at day 28. c $p<0.05$ significant difference between all perfusion groups at day 28. d $p<0.05$ significant difference between as-spun PVDF-TrFE perfusion and other perfusion groups at day 28.

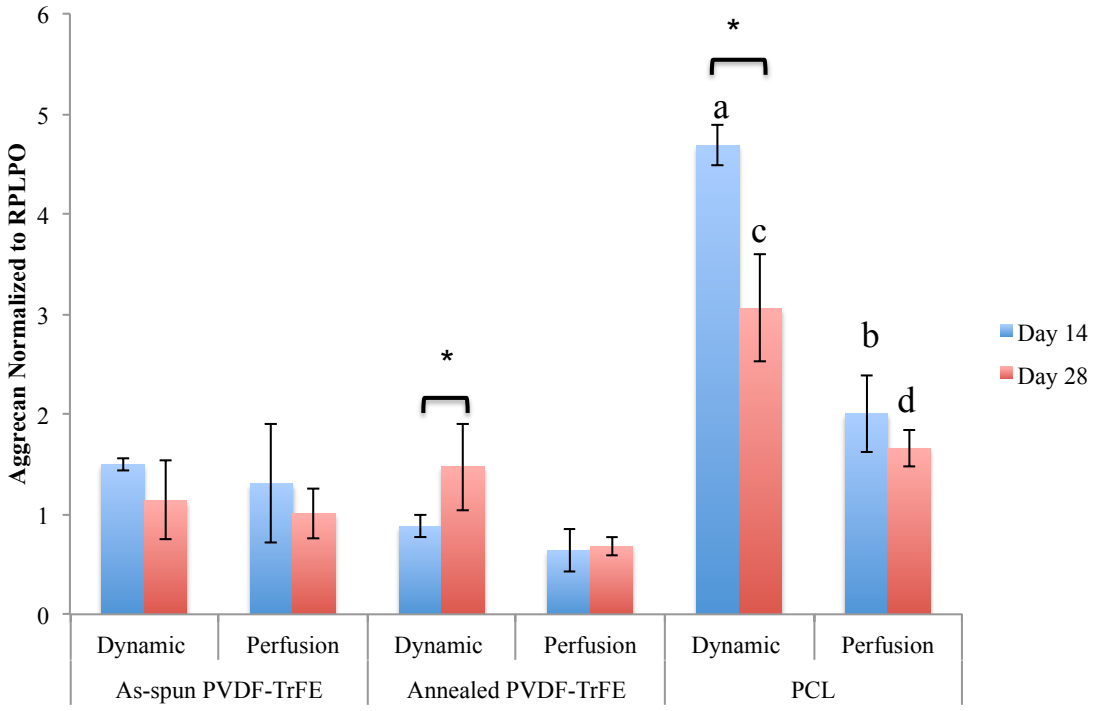

Figure A.5 Aggrecan gene expression normalized to RPLPO (housekeeping gene) on scaffolds of as-spun PVDF-TrFE, annealed PVDF-TrFE and PCL in chondrogenic cultures, which underwent dynamic compression and perfusion in bioreactor conditions at days 12 and 28. *$p<0.05$ significant difference between day 14 and 28. a $p<0.05$ significant difference between PCL dynamic and other dynamic groups at day 14. b $p<0.05$ significant difference between PCL perfusion and annealed PVDF-TrFE perfusion at day 14. d $p<0.05$ significant difference between PCL dynamic and other dynamic groups at day 28. c $p<0.05$ significant difference between PCL perfusion and annealed PVDF-TrFE perfusion at day 28.

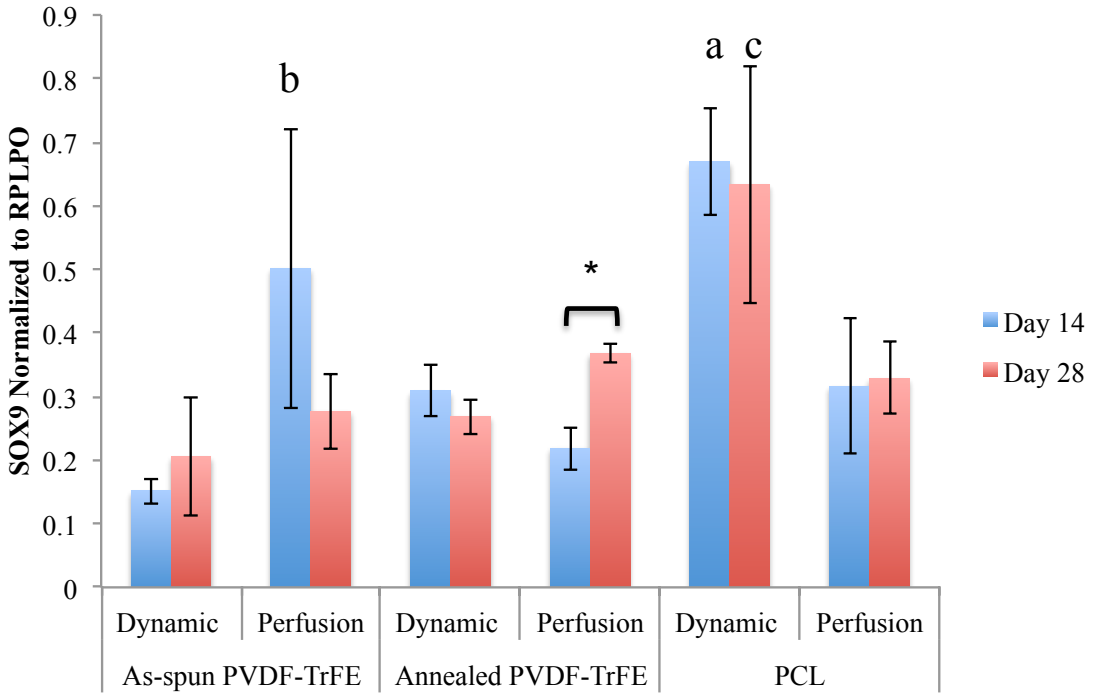

Figure A.6 SOX9 gene expression normalized to RPLPO (housekeeping gene) on scaffolds of as-spun PVDF-TrFE, annealed PVDF-TrFE and PCL in chondrogenic cultures, which underwent dynamic compression and perfusion in bioreactor conditions at days 12 and 28. *$p<0.05$ significant difference between day 14 and 28. a $p<0.05$ significant difference between PCL dynamic and other dynamic groups at day 14. b $p<0.05$ significant difference between as-spun PVDF-TrFE and annealed PVDF-TrFE in perfusion condition at day 14. c $p<0.05$ significant difference between PCL dynamic and other dynamic groups at day 28.

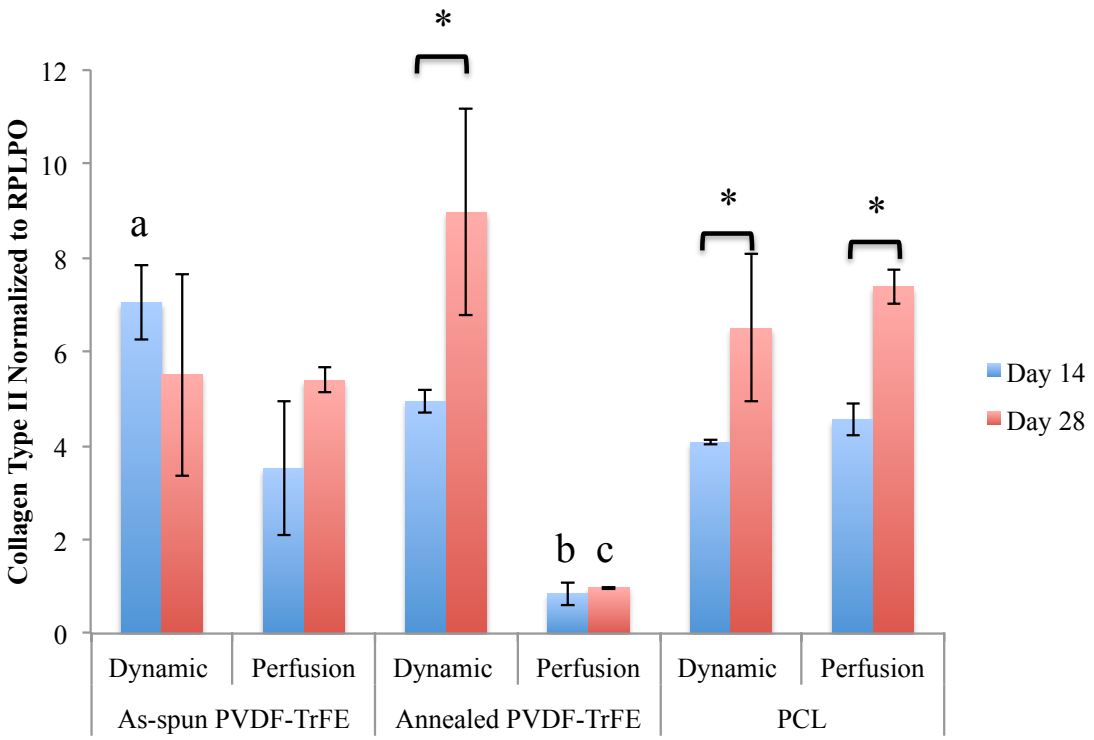

Figure A.7 Collagen type II gene expression normalized to RPLPO (housekeeping gene) on scaffolds of as-spun PVDF-TrFE, annealed PVDF-TrFE and PCL in chondrogenic cultures, which underwent dynamic compression and perfusion in bioreactor conditions at days 12 and 28. *$p<0.05$ significant difference between day 14 and 28. a $p<0.05$ significant difference between as-spun PVDF-TrFE dynamic and other dynamic groups at day 14. b $p<0.05$ significant difference between annealed PVDF-TrFE perfusion and PCL perfusion at day 14. c $p<0.05$ significant difference between annealed PVDF-TrFE perfusion and other perfusion groups at day 28.

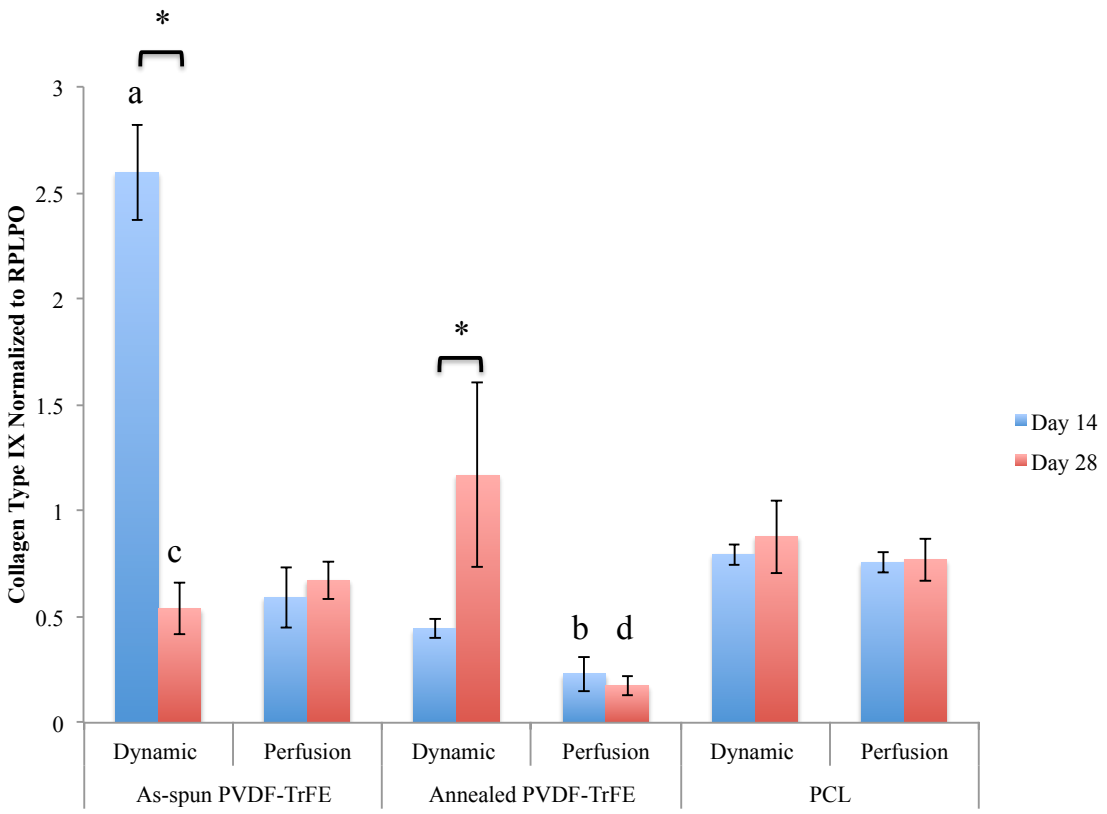

Figure A.8 Collagen type IX gene expression normalized to RPLPO (housekeeping gene) on scaffolds of as-spun PVDF-TrFE, annealed PVDF-TrFE and PCL in chondrogenic cultures, which underwent dynamic compression and perfusion in bioreactor conditions at days 12 and 28. *$p<0.05$ significant difference between day 14 and 28. a $p<0.05$ significant difference between as-spun PVDF-TrFE dynamic and other dynamic groups at day 14. b $p<0.05$ significant difference between annealed PVDF-TrFE perfusion and other perfusion groups at day 14. c $p<0.05$ significant difference between as-spun PVDF-TrFE dynamic and other dynamic groups at day 28. d $p<0.05$ significant difference between annealed PVDF-TrFE perfusion and other perfusion groups at day 28.

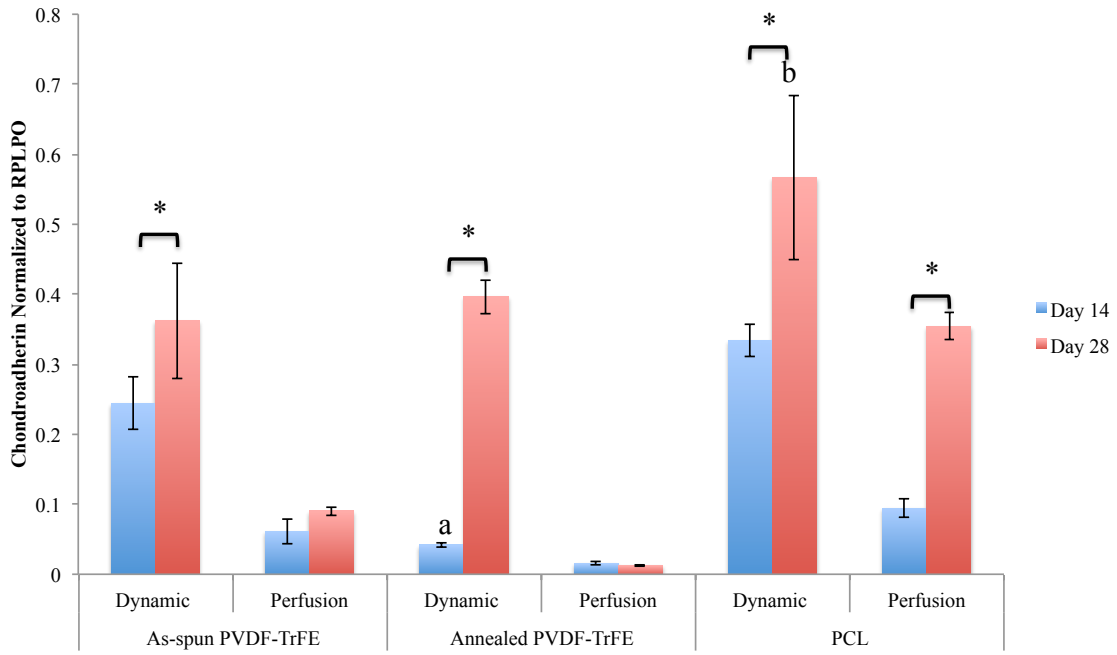

Figure A.9 Chondroadherin gene expression normalized to RPLPO (housekeeping gene) on scaffolds of as-spun PVDF-TrFE, annealed PVDF-TrFE and PCL in chondrogenic cultures, which underwent dynamic compression and perfusion in bioreactor conditions at days 12 and 28. *$p<0.05$ significant difference between day 14 and 28. a $p<0.05$ significant difference between annealed PVDF-TrFE dynamic other dynamic groups at day 14. b $p<0.05$ significant difference between PCL dynamic and annealed PVDF-TrFE dynamic at day 28.

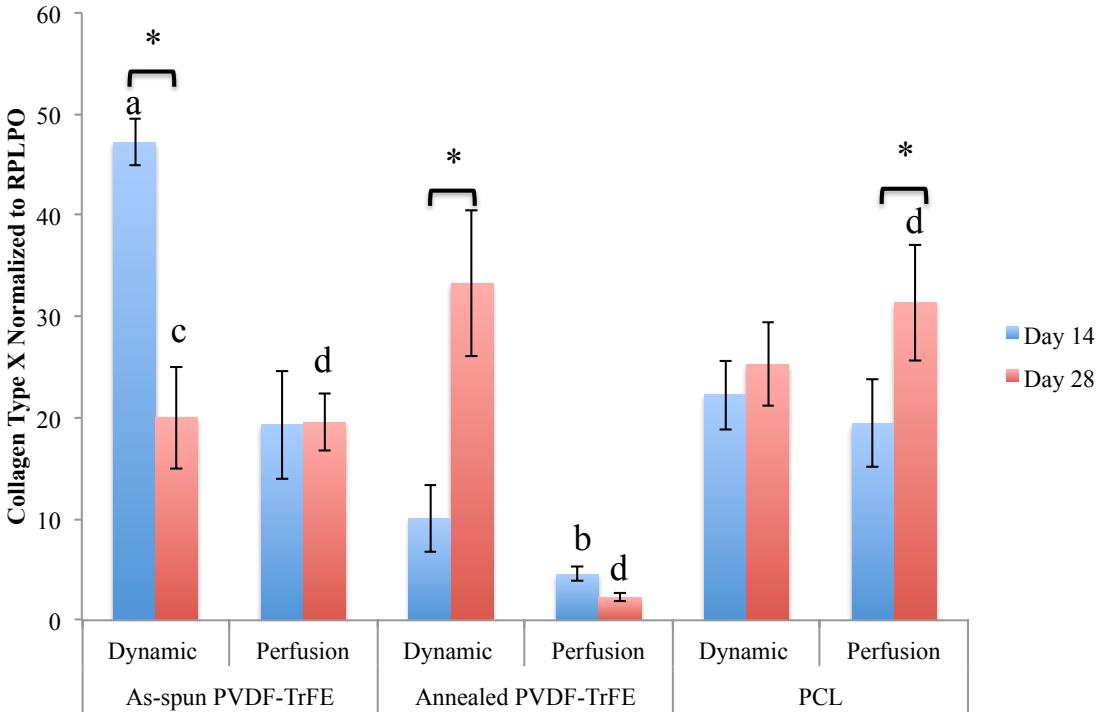

Figure A.10 Collagen type X gene expression normalized to RPLPO (housekeeping gene) on scaffolds of as-spun PVDF-TrFE, annealed PVDF-TrFE and PCL in chondrogenic cultures, which underwent dynamic compression and perfusion in bioreactor conditions at days 12 and 28. *$p<0.05$ significant difference between day 14 and 28. a $p<0.05$ significant difference between as-spun PVDF-TrFE dynamic and other dynamic groups at day 14. b $p<0.05$ significant difference between annealed PVDF-TrFE perfusion and other perfusion groups at day 14. c $p<0.05$ significant difference between as-spun PVDF-TrFE dynamic and annealed dynamic at day 28. d $p<0.05$ significant difference between all perfusion groups at day 28.

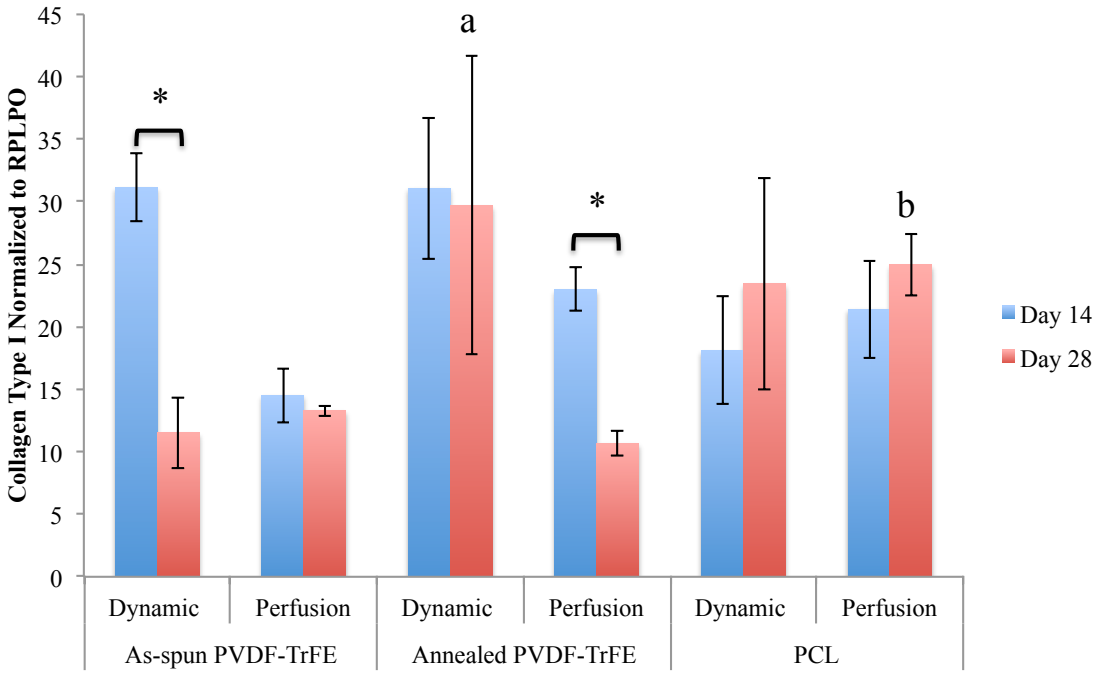

Figure A.11 Collagen type I gene expression normalized to RPLPO (housekeeping gene) on scaffolds of as-spun PVDF-TrFE, annealed PVDF-TrFE and PCL in chondrogenic cultures, which underwent dynamic compression and perfusion in bioreactor conditions at days 12 and 28. *$p<0.05$ significant difference between day 14 and 28. a $p<0.05$ significant difference between annealed PVDF-TrFE dynamic and as-spun PVDF-TrFE dynamic, at day 28. c $p<0.05$ significant difference between PCL perfusion and annealed PVDF-TrFE perfusion at day 28.

APPENDIX B

OSTEOGENESIS BIOREACTOR STUDIES RESULTS

The results shown in this appendix are the actual values from quantitative proteins assay and gene expression for MSCs cultured on as-spun PVDF-TrFE, annealed PVDF-TrFE and PCL scaffolds, which underwent perfusion and dynamic compression conditions in osteogenic medium in bioreactor system. For statistical analysis, perfusion groups of all scaffolds were compared at all time points. Similarly, dynamic scaffolds groups were compared at all time points. SPSS 20.0 software (SPSS Inc., IL, USA) was used for statistical analysis of all quantitative data. Results are expressed as mean ± standard deviation. The results were initially tested for normality (Shapiro Wilk test) and Levene's equal variance test. Two-way Analysis of Variance (ANOVA) and the post hoc multiple comparison using Tukey's tests were applied. Probability (p) values < 0.05 were considered statistically significant.

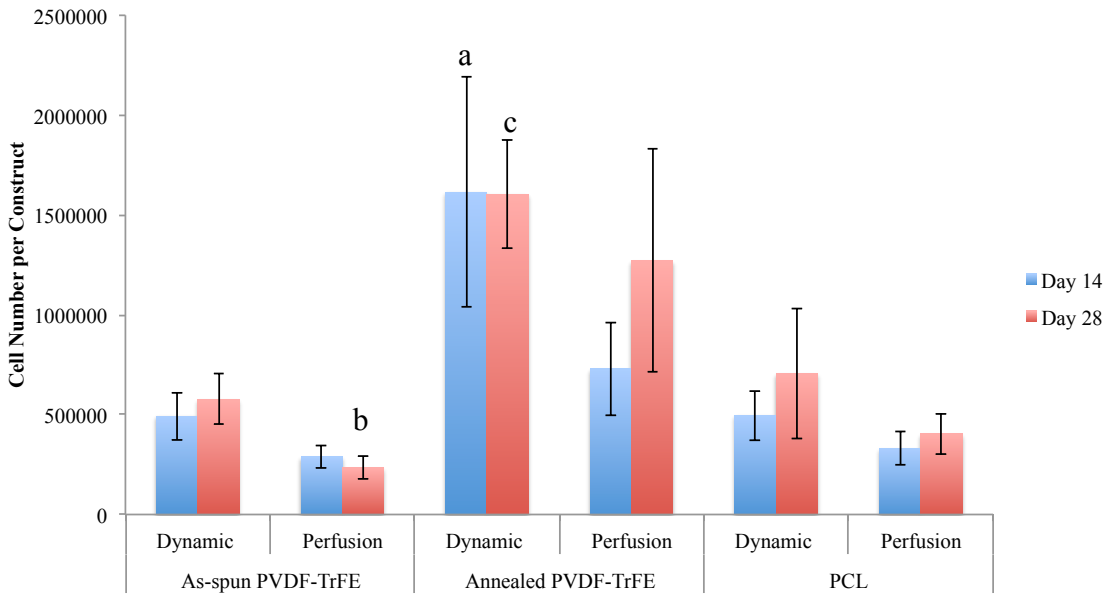

Figure B.1 Cell number on scaffolds of as-spun PVDF-TrFE, annealed PVDF-TrFE and PCL in osteogenic cultures, which underwent dynamic compression and perfusion only in bioreactor conditions at days 14 and 28. a $p<0.05$ significant difference between annealed PVDF-TrFE and other groups in dynamic at day 14. b $p<0.05$ significant difference between as-spun PVDF-TrFE and other perfusion groups at day 28. c $p<0.05$ significant difference between annealed PVDF-TrFE and other dynamic groups at day 28.

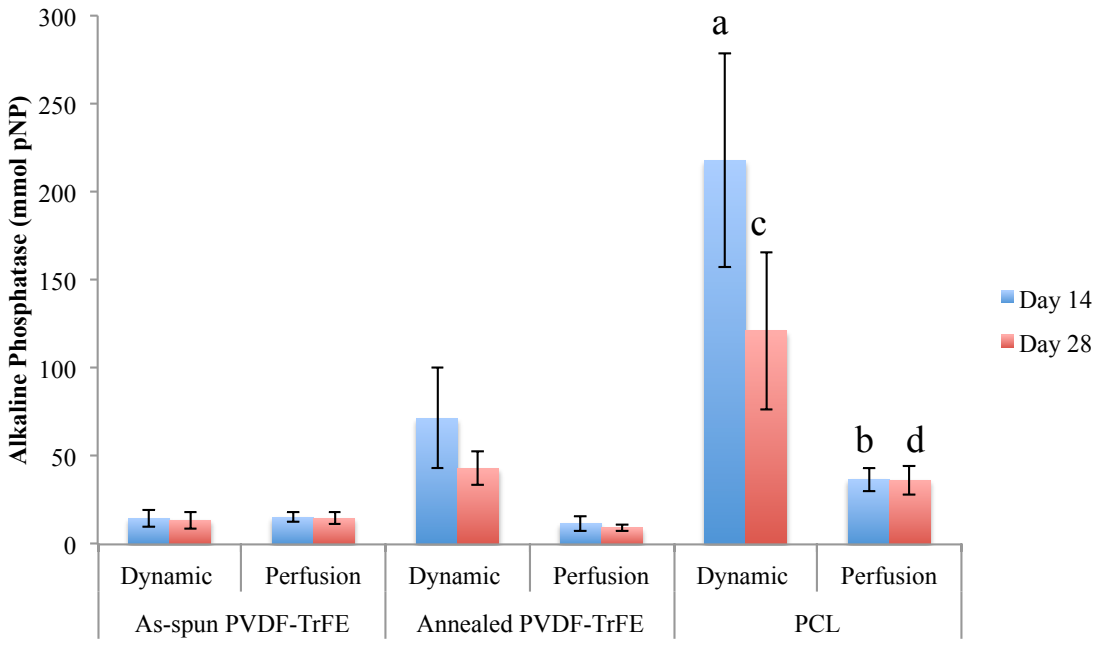

Figure B.2 Alkaline phosphatase activity on scaffolds of as-spun PVDF-TrFE, annealed PVDF-TrFE and PCL in osteogenic cultures, which underwent dynamic compression and perfusion only in bioreactor conditions at days 14 and 28. a $p<0.05$ significant difference between PCL and other groups in dynamic at day 14. b $p<0.05$ significant difference between PCL perfusion and other perfusion groups at day 14. c $p<0.05$ significant difference between PCL dynamic and other dynamic groups at day 28. d $p<0.05$ significant difference between PCL perfusion and other perfusion groups at day 28.

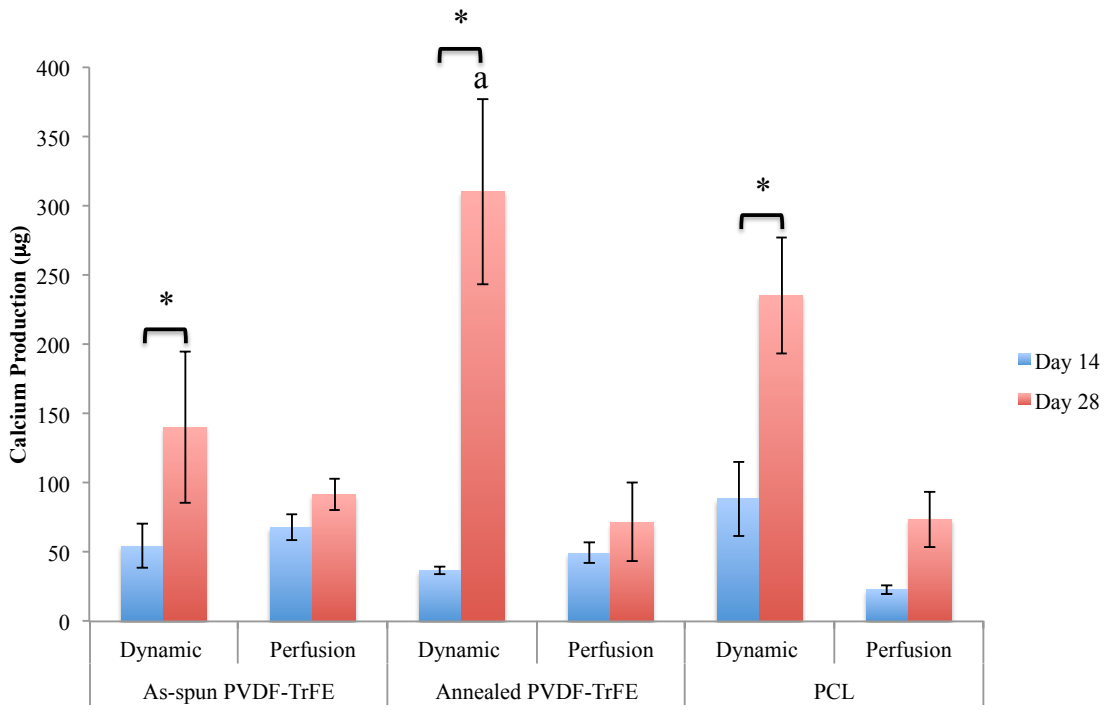

Figure B.3 Mineralization on scaffolds of as-spun PVDF-TrFE, annealed PVDF-TrFE and PCL in osteogenic cultures, which underwent dynamic compression and perfusion only in bioreactor conditions at days 14 and 28. *$p<0.05$ significant difference between day 14 and 28. a $p<0.05$ significant difference between annealed PVDF-TrFE and other groups in dynamic at day 28.

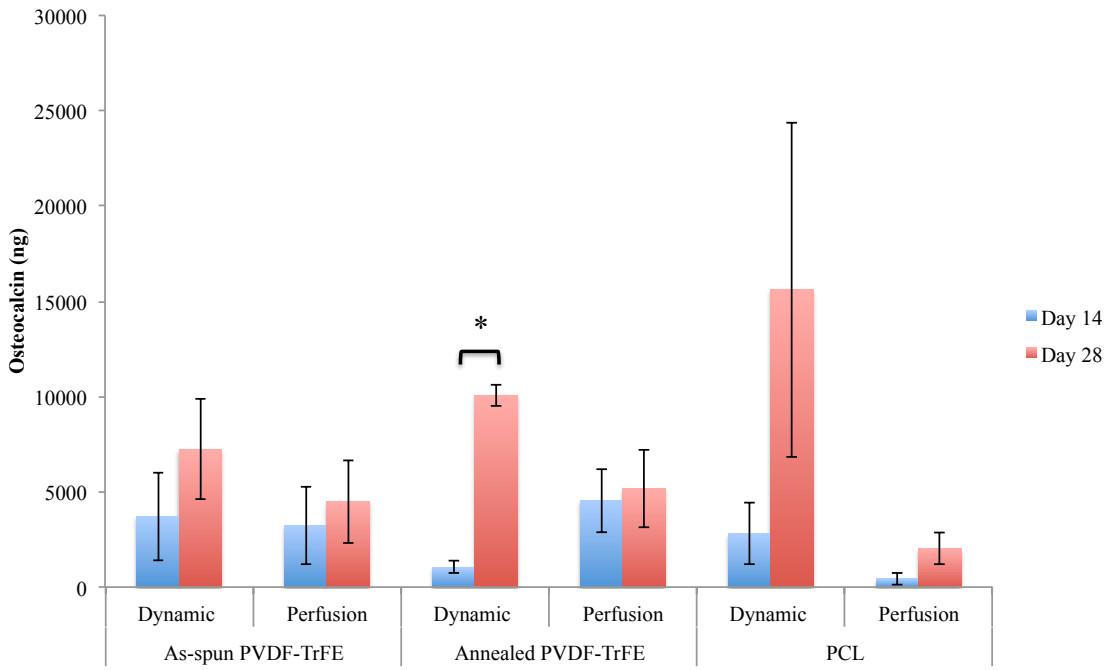

Figure B.4 Osteocalcin production on scaffolds of as-spun PVDF-TrFE, annealed PVDF-TrFE and PCL in osteogenic cultures, which underwent dynamic compression and perfusion only in bioreactor conditions at days 14 and 28. *$p<0.05$ significant difference between day 14 and 28.

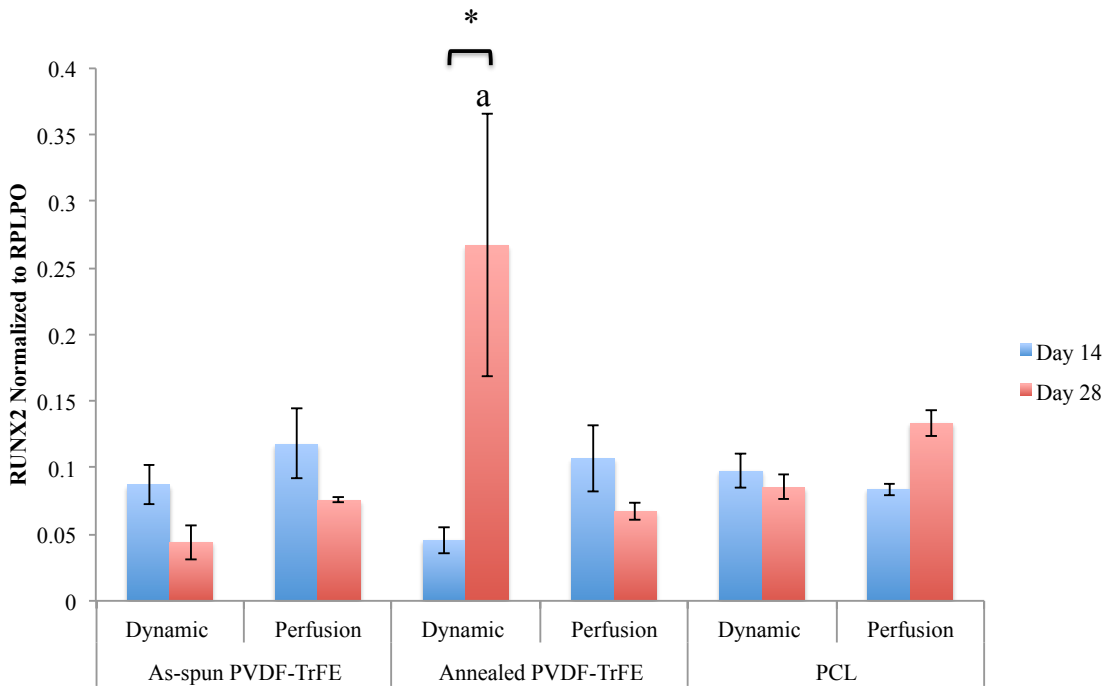

Figure B.5 RUNX2 gene expression normalized to RPLPO (housekeeping) on scaffolds of as-spun PVDF-TrFE, annealed PVDF-TrFE and PCL in osteogenic cultures, which underwent dynamic compression and perfusion only in bioreactor conditions at days 14 and 28. *$p<0.05$ significant difference between day 14 and 28. a $p<0.05$ significant difference between annealed PVDF-TrFE and other groups in dynamic at day 28.

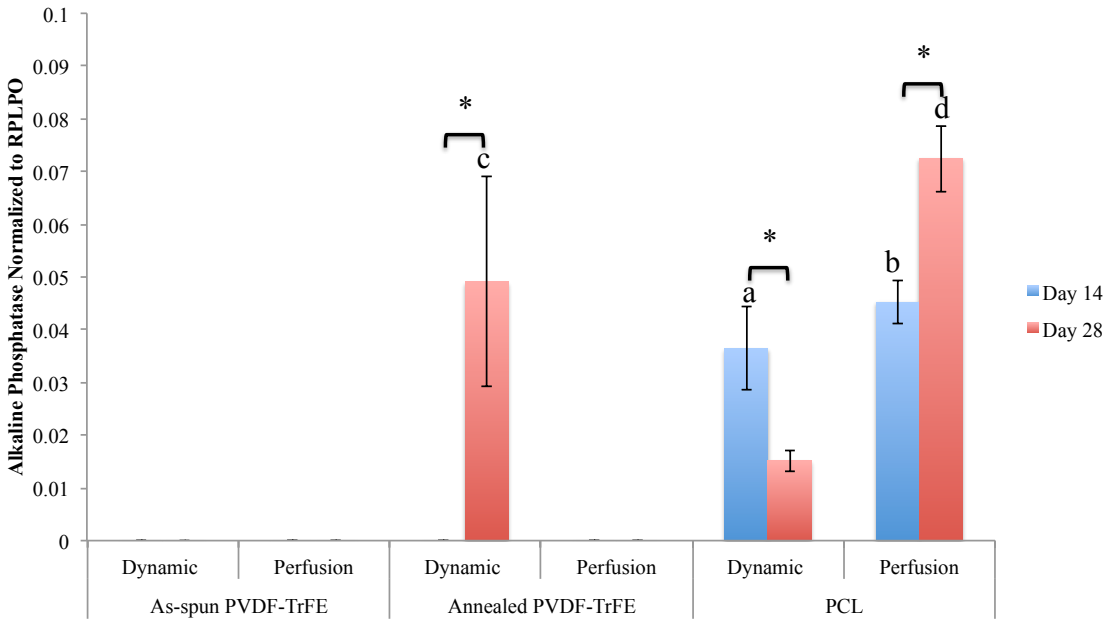

Figure B.6 Alkaline phosphatase gene expression normalized to RPLPO (housekeeping) on scaffolds of as-spun PVDF-TrFE, annealed PVDF-TrFE and PCL in osteogenic cultures, which underwent dynamic compression and perfusion only in bioreactor conditions at days 14 and 28. a $p<0.05$ significant difference between PCL and other groups in dynamic at day 14. b $p<0.05$ significant difference between PCL perfusion and other perfusion groups at day 14. c $p<0.05$ significant difference between annealed PVDF-TrFE dynamic and other dynamic groups at day 28. d $p<0.05$ significant difference between PCL perfusion and other perfusion groups at day 28.

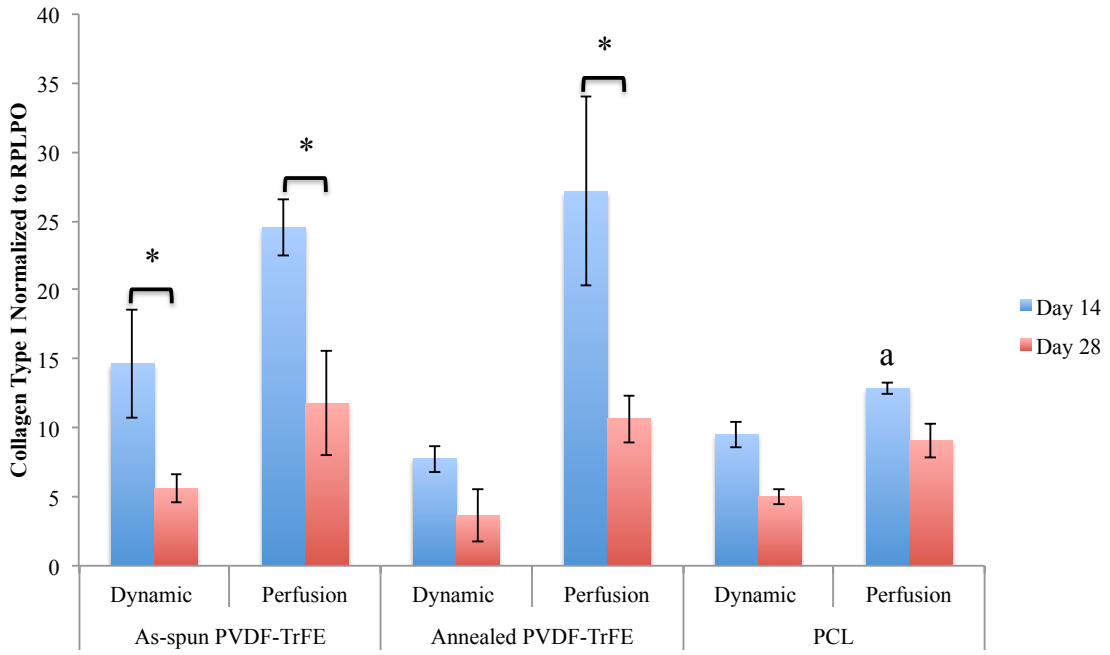

Figure B.7 Collagen type I gene expression normalized to RPLPO (housekeeping) on scaffolds of as-spun PVDF-TrFE, annealed PVDF-TrFE and PCL in osteogenic cultures, which underwent dynamic compression and perfusion only in bioreactor conditions at days 14 and 28. a $p<0.05$ significant difference between PCL perfusion and other groups in perfusion at day 14.

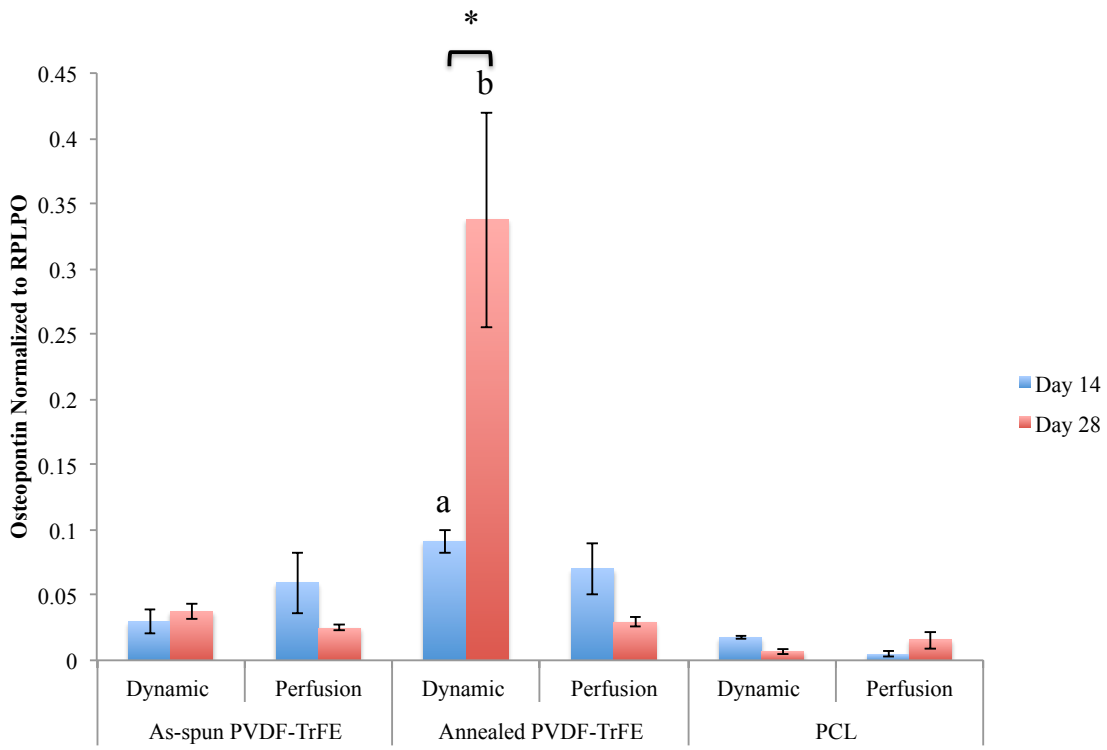

Figure B.8 Osteopontin gene expression normalized to RPLPO (housekeeping) on scaffolds of as-spun PVDF-TrFE, annealed PVDF-TrFE and PCL in osteogenic cultures, which underwent dynamic compression and perfusion only in bioreactor conditions at days 14 and 28. a $p<0.05$ significant difference between annealed PVDF-TrFE dynamic and other groups in dynamic at day 14. b $p<0.05$ significant difference between annealed PVDF-TrFE dynamic and other dynamic groups at day 28.

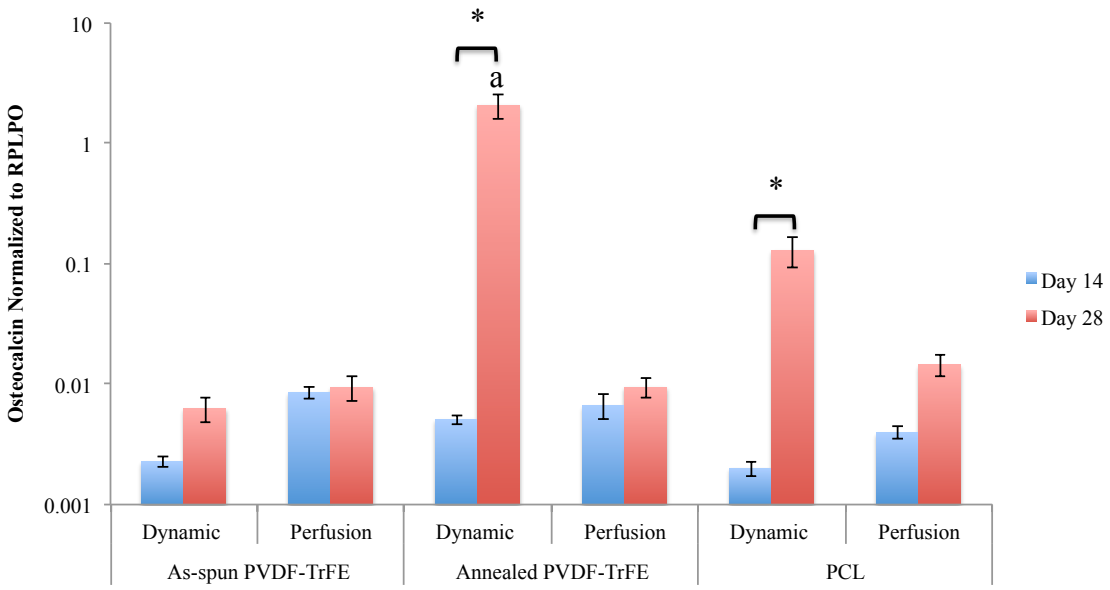

Figure B.9 Osteocalcin gene expression normalized to RPLPO (housekeeping) production on scaffolds of as-spun PVDF-TrFE, annealed PVDF-TrFE and PCL in osteogenic cultures, which underwent dynamic compression and perfusion only in bioreactor conditions at days 14 and 28. *$p<0.05$ significant difference between day 14 and 28. a $p<0.05$ significant difference between annealed PVDF-TrFE dynamic and other groups in dynamic at day 28.

REFERENCES

[1] Murphy L, Helmick CG. The impact of osteoarthritis in the United States: a population-health perspective: a population-based review of the fourth most common cause of hospitalization in U.S. adults. Orthopaedic Nursing 2012;31:85-91.

[2] Brady MA, Waldman SD, Ethier CR. The application of multiple biophysical cues to engineer functional neocartilage for treatment of osteoarthritis (part I: cellular response). Tissue Engineering Part B: Reviews 2014;21:1-19.

[3] Goldring S, Goldring M. Clinical aspects, pathology and pathophysiology of osteoarthritis. Journal of Musculoskeletal and Neuronal Interactions 2006;6:376-8.

[4] Burr DB, Gallant MA. Bone remodelling in osteoarthritis. Nature Reviews Rheumatology 2012;8:665-73.

[5] Nukavarapu SP, Dorcemus DL. Osteochondral tissue engineering: current strategies and challenges. Biotechnology advances 2013;31:706-21.

[6] Csaki C, Schneider PRA, Shakibaei M. Mesenchymal stem cells as a potential pool for cartilage tissue engineering. Annals of Anatomy - Anatomischer Anzeiger 2008;190:395-412.

[7] Mollon B, Kandel R, Chahal J, Theodoropoulos J. The clinical status of cartilage tissue regeneration in humans. Osteoarthritis and Cartilage 2013;21:1824-33.

[8] Demoor M, Ollitrault D, Gomez-Leduc T, Bouyoucef M, Hervieu M, Fabre H, et al. Cartilage tissue engineering: molecular control of chondrocyte differentiation for proper cartilage matrix reconstruction. Biochimica et Biophysica Acta (BBA)-General Subjects 2014;1840:2414-40.

[9] Schmidt-Rohlfing B, Schneider U, Goost H, Silny J. Mechanically induced electrical potentials of articular cartilage. Journal of Biomechanics 2002;35:475-82.

[10] Nooeaid P, Salih V, Beier JP, Boccaccini AR. Osteochondral tissue engineering: scaffolds, stem cells and applications. Journal of Cellular and Molecular Medicine 2012;16:2247-70.

[11] Mow VC, Guo XE. Mechano-electrochemical properties of articular cartilage: their inhomogeneities and anisotropies. Annual Review of Biomedical Engineering 2002;4:175-209.

[12] Bassett CAL, Pawluk RJ. Electrical behavior of cartilage during loading. Science 1972;178:982-3.

[13] Telega JJ, Wojnar R. Piezoelectric effects in biological tissues. Journal of Theoretical and Applied Mechanics 2002;40:723-60.

[14] Castañeda S, Roman-Blas JA, Largo R, Herrero-Beaumont G. Subchondral bone as a key target for osteoarthritis treatment. Biochemical Pharmacology 2012;83:315-23.

[15] Isaacson BM, Bloebaum RD. Bone bioelectricity: What have we learned in the past 160 years? Journal of Biomedical Materials Research Part A 2010;95:1270-9.

[16] Minary-Jolandan M, Yu M-F. Nanoscale characterization of isolated individual type I collagen fibrils: polarization and piezoelectricity. Nanotechnology 2009;20:1-6.

[17] Ahn AC, Grodzinsky AJ. Relevance of collagen piezoelectricity to "Wolff's Law": A critical review. Medical Engineering & Physics 2009;31:733-41.

[18] Shamos MH. Piezoelectricity as a fundamental property of biological tissues. Nature 1967;213:267-9.

[19] Griffin M, Bayat A. Electrical stimulation in bone healing: critical analysis by evaluating levels of evidence. Eplasty 2011;11:1-34.

[20] Mano J, Reis R. Osteochondral defects: present situation and tissue engineering approaches. Journal of Tissue Engineering and Regenerative Medicine 2007;1:261-73.

[21] Martin I, Miot S, Barbero A, Jakob M, Wendt D. Osteochondral tissue engineering. Journal of Biomechanics 2007;40:750-65.

[22] Bose S, Roy M, Bandyopadhyay A. Recent advances in bone tissue engineering scaffolds. Trends in Biotechnology 2012;30:546-54.

[23] Amini AR, Laurencin CT, Nukavarapu SP. Bone tissue engineering: recent advances and challenges. Critical Reviews™ in Biomedical Engineering 2012;40:363-408.

[24] Liu Y, Lim J, Teoh S-H. Review: development of clinically relevant scaffolds for vascularised bone tissue engineering. Biotechnology Advances 2013;31:688-705.

[25] Kock L, van Donkelaar CC, Ito K. Tissue engineering of functional articular cartilage: the current status. Cell and Tissue Research 2012;347:613-27.

[26] Mahmoudifar N, Doran PM. Chondrogenesis and cartilage tissue engineering: the longer road to technology development. Trends in Biotechnology 2012;30:166-76.

[27] Pelttari K, Steck E, Richter W. The use of mesenchymal stem cells for chondrogenesis. Injury 2008;39:58-65.

[28] Strioga M, Viswanathan S, Darinskas A, Slaby O, Michalek J. Same or not the same? Comparison of adipose tissue-derived versus bone marrow-derived mesenchymal stem and stromal cells. Stem Cells and Development 2012;21:2724-52.

[29] Stockmann P, Park J, von Wilmowsky C, Nkenke E, Felszeghy E, Dehner J-F, et al. Guided bone regeneration in pig calvarial bone defects using autologous mesenchymal stem/progenitor cells – A comparison of different tissue sources. Journal of Cranio-Maxillofacial Surgery 2012;40:310-20.

[30] Arthur A, Zannettino A, Gronthos S. The therapeutic applications of multipotential mesenchymal/stromal stem cells in skeletal tissue repair. Journal of Cellular Physiology 2009;218:237-45.

[31] Pittenger MF, Mackay AM, Beck SC, Jaiswal RK, Douglas R, Mosca JD, et al. Multilineage potential of adult human mesenchymal stem cells. Science 1999;284:143-7.

[32] Friedenstein A, Chailakhyan R, Gerasimov UV. Bone marrow osteogenic stem cells: *in vitro* cultivation and transplantation in diffusion chambers. Cell and Tissue Kinetics 1987;20:263-72.

[33] Haynesworth S, Baber M, Caplan A. Cell surface antigens on human marrow-derived mesenchymal stem cells are detected by monoclonal antibodies. Journal of Cellular Physiology 1992;138:8-16.

[34] Jaiswal N, Haynesworth SE, Caplan AI, Bruder SP. Osteogenic differentiation of purified, culture-expanded human mesenchymal stem cells *in vitro*. Journal of cellular biochemistry 1997;64:295-312.

[35] Kadiyala S, Jaiswal N, Bruder SP. Culture-expanded, bone marrow-derived mesenchymal stem cells can regenerate a critical-sized segmental bone defect. Tissue Engineering 1997;3:173-85.

[36] Rickard DJ, Sullivan TA, Shenker BJ, Leboy PS, Kazhdan I. Induction of rapid osteoblast differentiation in rat bone marrow stromal cell cultures by dexamethasone and BMP-2. Developmental Biology 1994;161:218-28.

[37] Chen L, Tredget EE, Liu C, Wu Y. Analysis of allogenicity of mesenchymal stem cells in engraftment and wound healing in mice. PloS One 2009;4:1-7.

[38] Arinzeh TL, Peter SJ, Archambault MP, Van Den Bos C, Gordon S, Krasus K, et al. Allogeneic mesenchymal stem cells regenerate bone in a critical-sized canine segmental defect. Journal of Bone and Joint Surgery, American 2003;85:1927-35.

[39] Xie H, Yang F, Deng L, Luo J, Qin T, Li X, et al. The performance of a bone-derived scaffold material in the repair of critical bone defects in a rhesus monkey model. Biomaterials 2007;28:3314-24.

[40] Freyria A-M, Mallein-Gerin F. Chondrocytes or adult stem cells for cartilage repair: the indisputable role of growth factors. Injury 2012;43:259-65.

[41] Lieberman JR, Daluiski A, Einhorn TA. The role of growth factors in the repair of bone. The Journal of Bone & Joint Surgery 2002;84:1032-44.

[42] Fortier LA, Barker JU, Strauss EJ, McCarrel TM, Cole BJ. The role of growth factors in cartilage repair. Clinical Orthopaedics and Related Research® 2011;469:2706-15.

[43] Danišovič Ľ, Varga I, Polák Š. Growth factors and chondrogenic differentiation of mesenchymal stem cells. Tissue and Cell 2012;44:69-73.

[44] Boden SD. Bioactive factors for bone tissue engineering. Clinical Orthopaedics and Related Research 1999;367:S84-S94.

[45] Kelly DJ, Jacobs CR. The role of mechanical signals in regulating chondrogenesis and osteogenesis of mesenchymal stem cells. Birth Defects Research Part C: Embryo Today: Reviews 2010;90:75-85.

[46] Rauh J, Milan F, Günther K-P, Stiehler M. Bioreactor systems for bone tissue engineering. Tissue Engineering Part B: Reviews 2011;17:263-80.

[47] Steward AJ, Kelly DJ. Mechanical regulation of mesenchymal stem cell differentiation. Journal of Anatomy 2014.

[48] Lee C, Grad S, Wimmer M, Alini M. The influence of mechanical stimuli on articular cartilage tissue engineering. Topics in tissue engineering 2005;2:1-32.

[49] Campbell JJ, Lee DA, Bader DL. Dynamic compressive strain influences chondrogenic gene expression in human mesenchymal stem cells. Biorheology 2006;43:455-70.

[50] Latham W, Lau JTC. Bone Stimulation: A Review of Its Use as an Adjunct. Techniques in Orthopaedics 2014;29:210-7.

[51] Brighton CT, Wang W, Seldes R, Zhang G, Pollack SR. Signal transduction in electrically stimulated bone cells. The Journal of Bone & Joint Surgery 2001;83:1514-23.

[52] Xu J, Wang W, Clark C, Brighton C. Signal transduction in electrically stimulated articular chondrocytes involves translocation of extracellular calcium through voltage-gated channels. Osteoarthritis and Cartilage 2009;17:397-405.

[53] Klinge U, Klosterhalfen B, Öttinger A, Junge K, Schumpelick V. PVDF as a new polymer for the construction of surgical meshes. Biomaterials 2002;23:3487-93.

[54] Lang S, Muensit S. Review of some lesser-known applications of piezoelectric and pyroelectric polymers. Applied Physics A 2006;85:125-34.

[55] Gimenes R, Zaghete MA, Bertolini M, Varela JA, Coelho LO, Silva Jr NF. Composites PVDF-TrFE/BT used as bioactive membranes for enhancing bone regeneration. Smart Structures and Materials 2004:539-47.

[56] Lee Y-S, Arinzeh TL. The influence of piezoelectric scaffolds on neural differentiation of human neural stem/progenitor cells. Tissue Engineering Part A 2012;18:2063-72.

[57] Sharma T, Aroom K, Naik S, Gill B, Zhang JX. Flexible thin-film PVDF-TrFE based pressure sensor for smart catheter applications. Annals of Biomedical Engineering 2013;41:744-51.

[58] Holzwarth JM, Ma PX. Biomimetic nanofibrous scaffolds for bone tissue engineering. Biomaterials 2011;32:9622-9.

[59] Holmes B, Castro NJ, Zhang LG, Zussman E. Electrospun fibrous scaffolds for bone and cartilage tissue generation: recent progress and future developments. Tissue Engineering Part B: Reviews 2012;18:478-86.

[60] Agarwal S, Wendorff JH, Greiner A. Use of electrospinning technique for biomedical applications. Polymer 2008;49:5603-21.

[61] Ribeiro C, Correia DM, Ribeiro S, Sencadas V, Botelho G, Lanceros‐Méndez S. Piezoelectric poly (vinylidene fluoride) microstructure and poling state in active tissue engineering. Engineering in Life Sciences 2015.

[62] Damaraju SM, Wu S, Jaffe M, Arinzeh TL. Structural changes in PVDF fibers due to electrospinning and its effect on biological function. Biomedical Materials 2013;8:1-11.

[63] Mao D, Gnade BE, Quevedo-Lopez MA. Ferroelectric Properties and Polarization Switching Kinetic of Poly (vinylidene fluoride-trifluoroethylene) Copolymer. Ferroelectrics - Physical Effects 2011:77-100.

[64] Chang J, Dommer M, Chang C, Lin L. Piezoelectric nanofibers for energy scavenging applications. Nano Energy 2012;1:356-71.

[65] Persano L, Dagdeviren C, Su Y, Zhang Y, Girardo S, Pisignano D, et al. High performance piezoelectric devices based on aligned arrays of nanofibers of poly (vinylidenefluoride-co-trifluoroethylene). Nature Communications 2013;4:1633.

[66] Lee Y-S, Collins G, Livingston Arinzeh T. Neurite extension of primary neurons on electrospun piezoelectric scaffolds. Acta Biomaterialia 2011;7:3877-86.

[67] Lopes HB, de S Santos T, de Oliveira FS, Freitas GP, de Almeida AL, Gimenes R, et al. Poly (vinylidene-trifluoroethylene)/barium titanate composite for *in vivo* support of bone formation. Journal of Biomaterials Applications 2014;29:104-12.

[68] Shanmugasundaram S, Chaudhry H, Arinzeh TL. Microscale versus nanoscale scaffold architecture for mesenchymal stem cell chondrogenesis. Tissue Engineering Part A 2010;17:831-40.

[69] Sell S, Barnes C, Simpson D, Bowlin G. Scaffold permeability as a means to determine fiber diameter and pore size of electrospun fibrinogen. Journal of Biomedical Materials Research Part A 2008;85A:115-26.

[70] Liu Y, Weiss DN, Li J. Rapid nanoimprinting and excellent piezoresponse of polymeric ferroelectric nanostructures. ACS nano 2009;4:83-90.

[71] Haynesworth S, Goshima J, Goldberg V, Caplan A. Characterization of cells with osteogenic potential from human marrow. Bone 1992;13:81-8.

[72] Schmittgen TD, Livak KJ. Analyzing real-time PCR data by the comparative CT method. Nature Protocols 2008;3:1101-8.

[73] Yoshimoto H, Shin Y, Terai H, Vacanti J. A biodegradable nanofiber scaffold by electrospinning and its potential for bone tissue engineering. Biomaterials 2003;24:2077-82.

[74] Lau K, Liu Y, Chen H, Withers R. Effect of annealing temperature on the morphology and piezoresponse characterisation of poly (vinylidene fluoride-trifluoroethylene) films via scanning probe microscopy. Advances in Condensed Matter Physics 2013;2013.

[75] Laxminarayana K, Jalili N. Functional nanotube-based textiles: pathway to next generation fabrics with enhanced sensing capabilities. Textile Research Journal 2005;75:670-80.

[76] Mandal D, Yoon S, Kim KJ. Origin of piezoelectricity in an electrospun poly (vinylidene fluoride‐trifluoroethylene) nanofiber web‐based nanogenerator and nano‐pressure sensor. Macromolecular Rapid Communications 2011;32:831-7.

[77] Huang Z-M, Zhang YZ, Kotaki M, Ramakrishna S. A review on polymer nanofibers by electrospinning and their applications in nanocomposites. Composites Science and Technology 2003;63:2223-53.

[78] Keun Kwon I, Kidoaki S, Matsuda T. Electrospun nano- to microfiber fabrics made of biodegradable copolyesters: structural characteristics, mechanical properties and cell adhesion potential. Biomaterials 2005;26:3929-39.

[79] Wong S-C, Baji A, Leng S. Effect of fiber diameter on tensile properties of electrospun poly(ε-caprolactone). Polymer 2008;49:4713-22.

[80] Puppi D, Chiellini F, Piras A, Chiellini E. Polymeric materials for bone and cartilage repair. Progress in Polymer Science 2010;35:403-40.

[81] Hutmacher DW, Schantz JT, Lam CXF, Tan KC, Lim TC. State of the art and future directions of scaffold‐based bone engineering from a biomaterials perspective. Journal of Tissue Engineering and Regenerative Medicine 2007;1:245-60.

[82] Zhou Y, Hutmacher DW, Varawan S-L, Lim TM. *In vitro* bone engineering based on polycaprolactone and polycaprolactone–tricalcium phosphate composites. Polymer International 2007;56:333-42.

[83] Tuli R, Tuli S, Nandi S, Huang X, Manner PA, Hozack WJ, et al. Transforming growth factor-β-mediated chondrogenesis of human mesenchymal progenitor cells involves N-cadherin and mitogen-activated protein kinase and Wnt signaling cross-talk. Journal of Biological Chemistry 2003;278:41227-36.

[84] Barry F, Boynton RE, Liu B, Murphy JM. Chondrogenic differentiation of mesenchymal stem cells from bone marrow: differentiation-dependent gene expression of matrix components. Experimental cell research 2001;268:189-200.

[85] Engler AJ, Sen S, Sweeney HL, Discher DE. Matrix elasticity directs stem cell lineage specification. Cell 2006;126:677-89.

[86] Wang N, Tolić-Nørrelykke IM, Chen J, Mijailovich SM, Butler JP, Fredberg JJ, et al. Cell prestress. I. Stiffness and prestress are closely associated in adherent contractile cells. American Journal of Physiology - Cell Physiology 2002;282:C606-C16.

[87] Singh P, Schwarzbauer JE. Fibronectin and stem cell differentiation–lessons from chondrogenesis. Journal of Cell Science 2012;125:3703-12.

[88] Li W-J, Jiang YJ, Tuan RS. Chondrocyte phenotype in engineered fibrous matrix is regulated by fiber size. Tissue Engineering 2006;12:1775-85.

[89] Kumar G, Tison CK, Chatterjee K, Pine PS, McDaniel JH, Salit ML, et al. The determination of stem cell fate by 3D scaffold structures through the control of cell shape. Biomaterials 2011;32:9188-96.

[90] Wang W, Wang Z, Zhang G, Clark CC, Brighton CT. Up-regulation of chondrocyte matrix genes and products by electric fields. Clinical Orthopaedics and Related Research 2004:S163-73.

[91] Hronik-Tupaj M, Rice W, Cronin-Golomb M, Kaplan D, Georgakoudi I. Osteoblastic differentiation and stress response of human mesenchymal stem cells exposed to alternating current electric fields. Biomedical Engineering Online 2011;10:9.

[92] Beloti MM, de Oliveira PT, Gimenes R, Zaghete MA, Bertolini MJ, Rosa AL. *In vitro* biocompatibility of a novel membrane of the composite poly (vinylidene - trifluoroethylene)/barium titanate. Journal of Biomedical Materials Research Part A 2006;79:282-8.

[93] Arinzeh TL, Peter SJ, Archambault MP, Van Den Bos C, Gordon S, Kraus K, et al. Allogeneic mesenchymal stem cells regenerate bone in a critical-sized canine segmental defect. The Journal of Bone & Joint Surgery 2003;85:1927-35.

[94] Livak KJ, Schmittgen TD. Analysis of Relative Gene Expression Data Using Real-Time Quantitative PCR and the $2^{-\Delta\Delta C}$T Method. Methods 2001;25:402-8.

[95] Krug D, Klinger M, Haller R, Hargus G, Büning J, Rohwedel J, et al. Minor cartilage collagens type IX and XI are expressed during embryonic stem cell-derived *in vitro* chondrogenesis. Annals of Anatomy-Anatomischer Anzeiger 2013;195:88-97.

[96] Jagodzinski M, Breitbart A, Wehmeier M, Hesse E, Haasper C, Krettek C, et al. Influence of perfusion and cyclic compression on proliferation and differentiation of bone marrow stromal cells in 3-dimensional culture. Journal of Biomechanics 2008;41:1885-91.

[97] Freed LE, Langer R, Martin I, Pellis NR, Vunjak-Novakovic G. Tissue engineering of cartilage in space. Proceedings of the National Academy of Sciences 1997;94:13885-90.

[98] Abrahamsson CK, Yang F, Park H, Brunger JM, Valonen PK, Langer R, et al. Chondrogenesis and mineralization during *in vitro* culture of human mesenchymal stem cells on three-dimensional woven scaffolds. Tissue Engineering Part A 2010;16:3709-18.

[99] Huang AH, Farrell MJ, Mauck RL. Mechanics and mechanobiology of mesenchymal stem cell-based engineered cartilage. Journal of Biomechanics 2010;43:128-36.

[100] Lima EG, Bian L, Ng KW, Mauck RL, Byers BA, Tuan RS, et al. The beneficial effect of delayed compressive loading on tissue-engineered cartilage constructs cultured with TGF-β3. Osteoarthritis and Cartilage 2007;15:1025-33.

[101] Bean AC, Tuan RS. Fiber diameter and seeding density influence chondrogenic differentiation of mesenchymal stem cells seeded on electrospun poly (ε-caprolactone) scaffolds. Biomedical Materials 2015;10:1-15.

[102] Guo H-F, Li Z-S, Dong S-W, Chen W-J, Deng L, Wang Y-F, et al. Piezoelectric PU/PVDF electrospun scaffolds for wound healing applications. Colloids and Surfaces B: Biointerfaces 2012;96:29-36.

[103] Low YK MN, Niphadkar ND, Boey FY, and Ng KW. α- and β-poly(vinylidene fluoride) evoke different cellular behaviours. Journal of Biomaterial Science 2011;22:1651-67.

[104] Ribeiro C, Moreira S, Correia V, Sencadas V, Rocha JG, Gama FM, et al. Enhanced proliferation of pre-osteoblastic cells by dynamic piezoelectric stimulation. RSC Advances 2012;2:11504-9.

[105] Ribeiro C, Pärssinen J, Sencadas V, Correia V, Miettinen S, Hytönen VP, et al. Dynamic piezoelectric stimulation enhances osteogenic differentiation of human adipose stem cells. Journal of Biomedical Materials Research Part A 2014.

[106] Beringer LT, Xu X, Shih W, Shih W-H, Habas R, Schauer CL. An electrospun PVDF-TrFE fiber sensor platform for biological applications. Sensors and Actuators A: Physical 2015;222:293-300.

[107] Titushkin IA, Rao VS, Cho MR. Mode-and cell-type dependent calcium responses induced by electrical stimulus. Plasma Science, IEEE Transactions on 2004;32:1614-9.

[108] McCullen SD, McQuilling JP, Grossfeld RM, Lubischer JL, Clarke LI, Loboa EG. Application of low-frequency alternating current electric fields via interdigitated electrodes: effects on cellular viability, cytoplasmic calcium, and osteogenic differentiation of human adipose-derived stem cells. Tissue Engineering Part C: Methods 2010;16:1377-86.

[109] Sun S, Liu Y, Lipsky S, Cho M. Physical manipulation of calcium oscillations facilitates osteodifferentiation of human mesenchymal stem cells. The FASEB Journal 2007;21:1472-80.

[110] Fitzsimmons RJ, Strong DD, Mohan S, Baylink DJ. Low-amplitude, low-frequency electric field-stimulated bone cell proliferation may in part be mediated by increased IGF-II release. Journal of Cellular Physiology 1992;150:84-9.

[111] Illingworth CM, Barker A. Measurement of electrical currents emerging during the regeneration of amputated finger tips in children. Clinical Physics and Physiological Measurement 1980;1:87.

[112] Nogami H, Aoki H, Okagawa T, Mimatsu K. Effects of electric current on chondrogenesis i*n vitro*. Clinical Orthopaedics and Related Research 1982;163:243-7.

[113] Akanji O, Lee D, Bader D. The effects of direct current stimulation on isolated chondrocytes seeded in 3D agarose constructs. Biorheology 2008;45:229-43.

[114] Hu JC, Athanasiou KA. A self-assembling process in articular cartilage tissue engineering. Tissue engineering 2006;12:969-79.

[115] Murdoch AD, Hardingham TE. Clonally derived human bone marrow mesenchymal cells show differential collagen II/collagen X expression in chondrogenic culture. Trans Orthop Res 2008;33:91.

[116] Pelttari K, Winter A, Steck E, Goetzke K, Hennig T, Ochs BG, et al. Premature induction of hypertrophy during *in vitro* chondrogenesis of human mesenchymal stem cells correlates with calcification and vascular invasion after ectopic transplantation in SCID mice. Arthritis & Rheumatism 2006;54:3254-66.

[117] Sladkova M, de Peppo GM. Bioreactor systems for human bone tissue engineering. Processes 2014;2:494-525.

[118] Matta C, Zákány R. Calcium signalling in chondrogenesis: implications for cartilage repair. Frontiers in Bioscience 2013;5:305-24.

[119] Mauck R, Wang C-B, Oswald E, Ateshian G, Hung C. The role of cell seeding density and nutrient supply for articular cartilage tissue engineering with deformational loading. Osteoarthritis and cartilage 2003;11:879-90.

[120] Mauck R, Yuan X, Tuan R. Chondrogenic differentiation and functional maturation of bovine mesenchymal stem cells in long-term agarose culture. Osteoarthritis and cartilage 2006;14:179-89.

[121] Bhumiratana S, Eton RE, Oungoulian SR, Wan LQ, Ateshian GA, Vunjak-Novakovic G. Large, stratified, and mechanically functional human cartilage grown *in vitro* by mesenchymal condensation. Proceedings of the National Academy of Sciences 2014;111:6940-5.

[122] Byers B, Mauck R, Chiang I, Tuan R. Temporal exposure of TGF-beta3 under serum-free conditions enhances biomechanical and biochemical maturation of tissue-engineered cartilage. Trans Orthop Res Soc 2006;31:43.

[123] Cartmell SH, Porter BD, García AJ, Guldberg RE. Effects of medium perfusion rate on cell-seeded three-dimensional bone constructs *in vitro*. Tissue engineering 2003;9:1197-203.